ABSTRACT

Title of Dissertation: META-TRANSCRIPTOMIC PROFILING OF HUMAN CUTANEOUS LEISHMANIASIS

Stephen M. Christensen, Doctor of Philosophy, 2018

Dissertation directed by: Dr. David M. Mosser, Professor
Department of Cell Biology & Molecular Genetics

Our understanding of the spectral nature of the neglected tropical disease leishmaniasis, and of host-parasite interactions in general, remains incomplete. In this work, we used high throughput RNA-sequencing (RNA-seq) to analyze human host and *Leishmania* gene expression in cutaneous leishmaniasis patients. Skin biopsies were taken from a total of 25 localized cutaneous leishmaniasis (LCL), 6 diffuse cutaneous leishmaniasis (DCL), and 10 healthy patients. LCL separated into groups that lacked detectable parasite transcripts in lesions (PT^{Neg}) and a group in which parasite transcripts were readily detected (PT^{Pos}). These groups exhibited substantial differences in host responses to infection, including B lymphocyte presence, B and T cell activation, and immunoglobulin production. Analysis of DCL lesions revealed distinct differences in host responses relative to LCL, including atypical B lymphocyte accumulation, diminished cytotoxic T lymphocyte responses, and an altered macrophage activation state. Surprisingly, neither localized nor diffuse forms of the disease could be correlated with any indication of a Th2 immune response that had previously been implicated in

mouse models of *L. major* susceptibility. The presence of low levels of parasite transcripts in the majority of LCL patients made it difficult to obtain a comprehensive analysis of the parasite transcriptome in LCL. However, high levels of parasite transcripts in DCL afforded a unique opportunity to examine parasite gene expression in this disease. Despite differences in age, gender, and illness duration, there was a remarkable uniformity in parasite gene expression in all 6 DCL patients. We identified transcripts that were highly expressed by all 6 DCL patients, and then curated a subset of conserved genes highly expressed in multiple *Leishmania* species. These subsets of genes emerge as targets for further research on host-pathogen interactions and a better understanding of *Leishmania* infection.. In summary, RNA-seq allowed us to fully examine host and parasite transcriptomes, characterize host responses in localized and diffuse cutaneous leishmaniasis lesions, and determine factors that define the variations in disease manifestation. New approaches to modify host immune responses in this disease and new parasite targets for drug development may emerge from this work.

META-TRANSCRIPTOMIC PROFILING OF HUMAN CUTANEOUS LEISHMANIASIS

By

Stephen M. Christensen

Dissertation submitted to the Faculty of the Graduate School of the
University of Maryland, College Park, in partial fulfillment
of the requirements for the degree of Doctor of Philosophy
2018

Advisory Committee:

Professor David M. Mosser, Chair

Professor Volker Briken

Professor Najib El-Sayed

Professor Kevin McIver

Professor Xiaoping Zhu, Dean's Representative

© Copyright by

Stephen M. Christensen

2018

Foreword

This dissertation includes original work that has been published in 2 peer-reviewed papers. The first of these papers is: Christensen SM, Dillon LA, Carvalho LP, Passos S, Novais FO, Hughitt VK, Beiting DP, Carvalho EM, Scott P, El-Sayed NM, and Mosser DM. (2016) Meta-transcriptome Profiling of the Human-*Leishmania braziliensis* Cutaneous Lesion. *PLoS Negl Trop Dis*. 10(9): e0004992.. The candidate is the first author on this work and took the lead on essentially all the analyses provided in the paper. He wrote the first draft of the paper and developed all the figures. He received assistance with the writing from (co-authors Mosser and El-Sayed). He received assistance with the bioinformatics from (co-authors) Dillon and Hughitt. The patient samples were provided by (co-authors) Carvalho, Passos, Novais and Scott. The second paper is: Hamidzadeh K, Christensen SM, Dalby E, Chandrasekaran P, Mosser DM (2017) Macrophages and the Recovery from Acute and Chronic Inflammation. *Annu Rev Physiol* 79:567–592. The candidate is listed as the second author. He prepared sections of this review that are used in this paper with the help of co-authors Hamidzadeh, Dalby, Chandrasekaran, and Mosser.

Acknowledgements

So far, my science "career" has been a whirlwind. I would not be where I am today without the opportunities my parents have provided me over the years. I have had their unrelenting support from the first day I became interested in how things work to taking apart electronics to my undergraduate education and beyond. Little did they know I would end up working on a microscopic level. For all that they put up with and all the support I received, I thank them wholeheartedly.

When I decided to embark on this journey, I was living in Boston and dating a woman I met less than a year before. Over the past 5 years, that incredible person has become my wife and I would not be here today without her undying love and support. She has been there for me through every struggle and success during my PhD journey and I am honored to call her my wife. There is no one I'd rather come home to after a long day at the lab than her and our dog, Lunchbox.

I would also like to thank the members of the Mosser Lab that have contributed to my sanity, my successes, and my happiness as I've completed this program. To Dr. Prabha Chandrasekaran, thank you for your immense patience and knowledge as you've helped guide me and other graduate students through the process of becoming independent scientists, all while continuing to excel in your studies and your research. To Kajal Hamidzadeh, you've been a phenomenal fellow graduate student and friend. It's been a pleasure going through the ups and downs up a PhD program with you.

Lastly, I would like to thank David Mosser for his guidance through this process and for taking a chance on a young scientist, eager to learn. Your guidance and teaching has helped mold me into a successful and independent-thinking scientist. For that, I will always be grateful.

Table of Contents

LIST OF TABLES

LIST OF FIGURES

List of Abbreviations

AIM2	Absent in melanoma 2
ALR	AIM2-like receptor
APC	Antigen presenting cell
AMP	antimicrobial peptide
ATP	adenosine triphosphate
BCR	B cell receptor
cAMP	cyclic adenosine monophosphate
CD	cluster of differentiation
CL	Cutaneous leishmaniasis
CR	Complement receptor
CTL	Cytotoxic T-lymphocytes
DAMP	Danger associated Molecular Pattern
DC	Dendritic cells
DL	Disseminated Leishmaniasis
DNA	Deoxyribonucleic acid
DTH	Delayed-type hypersensitivity
FcR	Fc (fragment crystallizable) receptor
GPCR	G-protein-coupled receptor
HIV	Human immunodeficiency virus
IFN	Interferon
Ig	Immunoglobulin
IL-10	Interleukin 10

IL-1β	Interleukin 1 beta
IL-12	Interleukin 12
ILC	Innate lymphoid cell
iNOS	Inducible nitric oxide synthase
IRF	Interferon regulatory factor
JNK	c-Jun N-terminal kinase
LCL	Localized cutaneous leishmaniasis
LPG	Lipophosphoglycan
LOS	Lipooligosaccharide
LPS	Lipopolysaccharide
MAPK	mitogen-activated protein kinase
MCL	Mucocutaneous leishmaniasis
MHC	Major histocompatibility complex
MMP	Matrix metalloproteinase
MR	Mannose receptor
MyD88	Myeloid differentiation primary response gene 88
NF-κB	Nuclear factor-κ B
NK Cell	Natural killer cell
NLR	Nod-like receptor
NOD	nucleotide-binding oligomerization domain
NTD	Neglected tropical disease
PAMP	Pathogen associated molecular pattern
PBMC	Peripheral blood mononuclear cell

PCA	Principal component analysis
PCR	Polymerase chain reaction
PRR	Pattern recognition receptor
RIG-I	Retinoic acid-inducible gene I
RLR	RIG-I-like receptor
RNA	ribonucleic acid
RNA-seq	RNA sequencing
SNP	Single nucleotide polymorphism
STAT	Signal transducers and activators of transcription
TCR	T-cell Receptor
TGFβ	Transforming growth factor β
Th	T-helper lymphocyte
TLR	Toll-like receptor
TNF	Tumor necrosis factor
Treg	Regulatory T-cell
Th1	T helper cell 1
Th2	T helper cell 2
Th17	T helper cell 17
WGCNA	Whole genome coexpression network analysis

Chapter 1: Introduction

1.1 Innate Immunity

Innate immunity is comprised of physical barriers, humoral factors, and specific immune cells that developed over millions of years. It is most often described as the first line of defense used by organisms in the presence of infection, injury, or damage. At its most basic level, human innate immunity employs physical barriers like the skin and mucosal surfaces to stop or trap debris and microbes, preventing contact with epithelial layers and sensitive areas that require protection in order to maintain homeostasis. As immunity continued to evolve, innate responses developed various non-specific factors to immediately respond to the presence of foreign material. For example, antimicrobial peptides (AMPs) recognize and kill harmful microbes residing on the skin, in the gut, and in bodily fluids through the recognition of differences between human and microbial lipid layers. Coagulation factors, another non-specific development by the immune system, prevent microbial access to injured tissue and quickly arrest bleeding after vascular injury. The even more complicated complement system in the blood can bind foreign pathogens, leading to uptake by professional phagocytes, production of inflammatory signals, and downstream formation of membrane attack complexes. This occurs through a cascade of convertase formation and protease activity involving many different complement proteins working in consort. The evolution and development of these aspects of innate immunity help form a complex system that prevents and responds to infection, injury, and tissue damage.

Within the construct of innate immunity, cells employ receptors that enable the detection and differentiation between self and foreign molecular patterns. The seminal

work by Le Maître and Hoffman first uncovered toll-like receptors (TLRs), demonstrating the susceptibility of the fruitfly to fungal infection when lacking the TLR1 gene (1). We now know that this and many other pattern recognition receptors (PRRs) (2) exist: toll-like receptors (TLRs), retinoid acid-inducible gene I (RIG-I)-like receptors (RLRs), AIM2-like receptors (ALRs), and nucleotide-binding oligomerization domain (NOD)-like receptors (NLRs). These all recognize pathogen associated molecular patterns (PAMPs) or damage associated molecular patterns (DAMPs), inducing quick and effective neutralization of pathogens or damaging circumstances. Downstream signaling cascades initiated by PRR ligation typically lead to cellular production of cytokines and chemokines and also initiate downstream pathways involved in pathogen uptake and killing.

The signaling pathways downstream of PAMP and DAMP receptor ligation of PRRs swiftly induce inflammatory responses and contribute to the initiation of adaptive immunity (3). In a well-studied example, bacterial lipopolysaccharide (LPS), signaling through TLR4, causes the rapid production of inflammatory cytokines such as tumor necrosis factor (TNF) by macrophages. This production is due to the activation of basal state positioning of RNA polymerase II on the gene's promoter (4). PRR ligation also leads to stabilization of major histocompatibility complex (MHC) antigen presentation and upregulation of costimulatory molecules necessary for T cell activation (discussed later). The early inflammatory response induced by PRRs consists of downstream cytokine and chemokine production while simultaneously preparing contributions to adaptive immunity.

It is vital that homeostasis is restored after initial inflammatory responses via immunoregulatory pathways to prevent immune-driven pathology. Endogenous regulators such as adenosine, prostaglandin, resolvins, and lipoxins can help to promote the resolution of inflammation (5). Adenosine triphosphate (ATP) is produced during inflammation as a result of metabolic switching and released from macrophages (6). Once outside the cell, ATP is catabolized to adenosine by the CD39 and CD73 ectoenzymes (7, 8). Our lab has shown that adenosine then acts as a secondary signal that decreases production of TNF and inflammatory interleukin 12 (IL-12) while simultaneously increasing anti-inflammatory interleukin 10 (IL-10) production (9). Prostaglandins and prostanoids, signaling through G-protein coupled receptors (GPCRs), stimulate the release of cyclic adenosine monophosphate (cAMP). Coupling cAMP release with TLR signaling decreases macrophage production of inflammatory IL-12 and TNF while increasing IL-10 release (10, 11). Resolvins and lipoxins are also produced during inflammation and act as negative feedback to decrease inflammatory signaling. They also discourage further infiltration of polymorphonuclear cells and encourage uptake of dying or necrotic cells (5, 12). These endogenous regulators act through a variety of pathways toward the same goal of restoring homeostasis after inflammation.

The immune system can also react to exogenous inhibition of inflammation. Glucocorticoids are one well-studied exogenous inhibitor of inflammation. Ligation of glucocorticoid receptors decreases inflammatory cytokine production, antigen presentation, and mRNA stability while increasing the phagocytosis of apoptotic cells. This occurs via downstream inhibition of nuclear factor kappa-B (NF-κB) nuclear translocation (13–18). The potency of this exogenous regulation has led to use of

glucocorticoids in treatments of MS, rheumatoid arthritis, psoriasis, and other autoimmune diseases (15). Other exogenous regulators of inflammation signal through specific receptors like CD47, CD200R, TREM2, TAM receptors, and phosphatidylcholine receptors in mucosal layers (5, 19). Whether to reestablish homeostasis or prevent initial activation, the signaling cascades initiated by exogenous mediators aim to subdue the inflammatory response and reduce the production of inflammatory cytokines and superoxides.

Our knowledge of which cell types are most important to innate immunity continues to evolve. Macrophages, dendritic cells, neutrophils, and natural killer (NK) cells have always been considered part of innate immunity, contributing to removal and destruction of foreign material, rapid infiltration of damaged tissue, coordination of immune responses via cytokine and chemokine production, and targeted cell killing to eliminate infected cells. However, growing knowledge has also uncovered subsets of T and B lymphocytes that contribute to innate immunity through a restricted set of antigen receptors. In early immune responses, these cells can do much of the same processes as the aforementioned cells as well as produce a repertoire of natural antibodies (B cells). Research continues to uncover entire subgroups of lymphoid cells that contribute to innate immunity. The discovery of these so-called innate lymphoid cells (ILCs) have expanded our understanding of the complex innate immune system.

Despite the complexities of innate immunity, pathogens have evolved numerous paths to avoid or manipulate innate immunity meant for pathogen killing or neutralization. Formation of capsules by bacteria prevents PRR access to bacterial membranes. *Leishmania* spp. (the focus of this work) can interfere with mitogen activated

protein kinase (MAPK) signaling to decrease inflammatory IL-12 production and promote anti-inflammatory IL-10 production (20). *M. tuberculosis* relies on an inhibition of inflammatory interferon-gamma (IFN-γ) and promotion of IL-10 production to survive and replicate in macrophages (21). Intestinal and urogenital bacteria such as *Lactobacillus rhamnosus* can also promote anti-inflammatory responses from macrophages. The commensal bacteria's secretome is able to induce granulocyte colony-stimulating factor (G-CSF) production by macrophages, leading to activation of signal transducers and activators of transcription 3 (STAT3), c-Jun N-terminal kinase (JNK) inactivation, and inflammatory TNF suppression in LPS or *E. coli*-activated macrophages (22). As immune systems have evolved to defend against pathogens, so too have pathogens evolved to manipulate immune systems.

1.2 Adaptive Immunity

While innate immunity responds in a similar manner every time it encounters the same antigen or trigger, the adaptive immune system provides a learned, specific memory used to prevent reinfection by the same pathogen. The initiation of an adaptive immune response typically starts with antigen presenting cells (APCs) and professional phagocytes like dendritic cells and macrophages. These professional phagocytes engulf and kill pathogens, in the process breaking down peptides that are subsequently presented to T cells using MHCs. Presentation of peptide from exogenous sources in MHC II interacts with $CD4^+$ T cells, while presentation of peptide from endogenous sources in MHC I interacts with $CD8^+$ T cells. These interactions will lead to either T helper cell proliferation ($CD4^+$) necessary for downstream B cell activation or CTL proliferation ($CD8^+$) necessary for targeted killing of infected cells. In both cases, cytokine production

directs responses as well. Alongside MHC-peptide complex presentation to T cells, signaling via PRRs is needed to upregulate costimulatory molecules CD80 (B7.1) and CD86 (B7.2) that interact with CD28 on T cells, eliciting T cell activation. Without the presentation of antigenic peptide by APCs, adaptive immunity lacks the signals required for activation.

T cells use the T cell receptor (TCR) to achieve diverse repertoires that recognize short peptides presented in MHC. The T cell receptor forms through DNA recombination during maturation and does not undergo further mutations after encountering antigen. Most T cell function is determined by the expression of either CD4 or CD8, forming T helper (Th) cells or cytotoxic T lymphocytes (CTL), respectively. Helper T cells play a prominent role in B cell activation, producing cytokines that will bias immune responses. These can be inflammatory (Th1), anti-inflammatory (Th2), or a mixture of the two. Cytotoxic responses are either inflammatory or cytolytic. Recent discoveries of numerous other T cell subsets have revealed regulatory T cells (Treg), γδ T cells, and NK T cells. Research continues to uncover new T lymphocyte functions, but some of the most basic include cytokine responses, immune regulation, targeted cell killing, and B cell activation.

In B lymphocytes, diversity is also accomplished through a diverse repertoire of receptors created through DNA recombination events during cell maturation that enable each cell to recognize a specific antigen. Each B cell produces clonal B cell receptors (BCRs) unique to that cell that can bind antigen and send proliferative signals with the help of the CD79A/CD79B (Igα/Igβ) signaling proteins. The gene encoding for the BCR can also produce a secreted form known as antibody that plays a role in pathogen

opsonization and uptake, neutralization, and killing. Exposure to antigens drives B cell proliferation and leads to somatic hypermutation and affinity maturation of BCRs and antibody to allow for stronger binding of antigen and more rapid future responses. After antigen recognition, B cells proliferate into plasma and memory cells, poised to produce large amounts of antibody, neutralize the current infection and produce robust immune memory for any subsequent encounters with the same antigen.

During infection, B cells typically respond via T cell-dependent pathways. B cell receptors (IgM or IgD) may recognize surface or soluble antigen produced by pathogens. However, the recognition of antigen does not induce most B cell proliferation effectively without T cell help. This process occurs mainly through T cell production of cytokines and ligation of CD40 on B cells, inducing B cell proliferation and determining immunoglobulin isotype class switching, the irreversible DNA splicing of constant regions in the immunoglobulin sequence to produce IgG, IgA, or IgE. Determinants of most B cell proliferation and class switching events depend highly on the signals present in the microenvironment, cytokines, and signals from helper T cells.

The isotype of immunoglobulin produced by each B cell directly influences B cell function. Production of IgM either on the surface or in a soluble pentameric form can occur in immature or mature B cells. The IgM isotype is the most effective isotype for complement activation. Production of IgA typically arises in or near mucosal membranes due to its ability to permeate mucosal surfaces and “neutralize” potential pathogens. The IgE isotype relates to allergic responses, binding to fragment crystallizable (Fc) epsilon-receptors on mast cells. Subsequent binding of IgE to allergens en masse causes the release of histamines and leukotrienes. Even within the higher affinity IgG isotype, the

role of specific IgGs varies. In humans, four types of IgG (IgG1, IgG2, IgG3, IgG4) differ in structure, their abilities to bind specific molecules (proteins, polysaccharides, allergens, complement C1q protein), and their affinity for various Fc receptors. While IgG1 and IgG3 usually induce strong effector reactions, IgG2 and IgG4 usually promote more subtle responses (23). The various functions of immunoglobulin isotypes drives B cell function throughout the entire human body.

While the complex nature of the adaptive immune response allows for highly specific and powerful responses to pathogenic invasion, many pathogens rely on avoidance or manipulation of the immune system for their survival (24). As a first level of defense, many bacterial pathogens avoid detection through the previously mentioned formation of capsules, preventing antibody or complement binding. Other pathogens use antigenic variation to avoid detection by B and T memory cells, altering surface proteins like the highly conserved bacterial LPS or more specific lipooligosaccharide (LOS) on *Neisseria* spp. (25). Trypanosomes, close relatives of the *Leishmania* genus, possess variant surface glycoproteins (VSGs) and replenish this dense protein coat to prevent antibody detection and complement activation (26). Probably the most well-known example of pathogenic evasion of immune memory is antigenic switching by the influenza virus. Slight changes in the genes coding for viral surface proteins are enough to avoid detection by memory antibody from previous flu infections.

Evasion of immune responses is not the only way pathogens survive in host environments. We also know that pathogens manipulate adaptive immune responses by actively interfering with signaling cascades to promote favorable conditions for survival. Various nematodes and helminths can powerfully regulate the immune response,

decreasing inflammatory Th1/Th17 responses and promoting Th2 response environments (27). A toxin produced by *Helicobacter pylori* disrupts T cell proliferation by inhibiting IL-2 signaling (28). The Opa protein on *Neisseria gonorrhoeae* binds the host protein CEACAM1, dampening CD4 T cell activation and proliferation (29). Probably the most well-known example of adaptive immune modulation is used by human immunodeficiency virus (HIV) when the gp120 envelope glycoprotein expressed on the virion surface aides viral binding to and entry into $CD4^+$ T cells (30–32). Pathogens are continuously finding ways to avoid and manipulate our adaptive immune system despite its complexity and diversity.

1.3 Skin Immunity and Wound Healing

There are many cellular immune responses involved in skin immunity besides the structural aspect acting as a physical barrier. Within this construct, there are tissue-resident cells that act as first-responders to pathogens or damage, recruiting and working in concert with infiltrating immune cells. Keratinocytes produce AMPs (antimicrobial peptides) in response to PRR ligation or cytokine signaling (33). Additionally, keratinocytes contribute substantially to early cytokine and chemokine production necessary for leukocyte recruitment (34). Various dendritic cell (DC) types like Langerhans cells also contribute to skin immune responses by promoting tolerance to natural skin flora (35). Research has also show that this specific subset of DCs is quite effective at suppressing immune responses by either inducing T cell deletion (36) or activating regulatory T cells (37). Other DC subtype functions include capturing dead cells and being the the first cells to process and present antigen (33). In *Leishmania* infection, dermal dendritic cells are the first to present antigen are important for

successful T cell activation (38). Recent discoveries of innate lymphoid cells (ILCs) in skin have suggested their contribution to inflammation and immune suppression, specifically by the ILC2 subtype characterized by GATA3, IL-4, and IL-13 expression (39). Lastly, tissue-resident T cells that do not leave the skin can either possess the common αβ TCR or the less diverse and less common γδ TCR. Particularly after previous infection, αβ T cells remain in the skin to provide immune memory and prevent future infection. As for γδ T cells, their function appears to lie in the realm of monitoring epidermal stress and contributing to wound healing (40).

Immune cells not only protect against pathogen invasion and damage, but contribute to the resolution of damage through wound healing. This process occurs in three stages: inflammation, proliferation, and remodeling (41). During the beginning of inflammation, infiltrating neutrophils function to both prevent pathogenic infection and activate keratinocytes, fibroblasts, and other immune cells (42–44). Infiltrating macrophages produce growth factors, matrix metalloproteinases (MMPs), VEGF, and TGFβ, all of which promote re-epithelialization, fibroblast growth, angiogenesis, and extracellular matrix remodeling (45–47). In *Leishmania* infection, constitutive expression of inflammatory and cytotoxic cytokines prevents this process in a manner similar to the skin inflammatory disease psoriasis (48). Eventual re-epithelialization, proliferation of fibroblasts, and activation of keratinocytes in the wound area promote the remodeling stage of wound healing, contributing to the structural rebuilding by upregulated production of extracellular matrix components like fibronectin and collagen (42). The process of wound healing begins as soon as the response to infection or damage begins.

1.4 Macrophage Roles in Immunity

Whether in the liver (Kuppfer cells), central nervous system (microglia), bone (osteoclasts), lung (alveolar) or other tissues, macrophages play an important role in homeostatic maintenance and immune responses. They contribute extensively to innate immunity, and serve as a key connection between innate and adaptive immunity. In addition to these roles, macrophages can promote cell growth and tissue repair, regulate metabolic responses, and scavenge for cellular debris. Macrophages reside in many tissues throughout the body and each tissue-specific classification has phenotypic and functional properties that differentiate them from those in other tissues. In addition, the type and strength of response to stimuli depends strongly on local microenvironmental signals, resulting in myriad activation states. Despite these differences, there are various general functions that macrophages employ in all tissues.

1.4.1 Macrophages in Innate Immunity

The role of macrophages in innate immunity is of particular importance to this research, specifically the phagocytosis and killing of pathogens. Initiation of phagocytosis occurs via receptors designed to help cells recognize foreign materials. Macrophages express a wide variety of receptors for this purpose including Fc receptors, complement receptors (CR), mannose receptors (MR), and scavenger receptors. Ligation of these receptors leads to the polymerization of actin and subsequent ingestion of the pathogen into phagosomes (49). Coordination between this actin-mediated event and microtubule trafficking within the cell is important for the subsequent processing of the phagosome which depends highly on the receptor and environmental signals.

The phagosome can mature into the phagolysosome, designed for intracellular pathogen killing, through a series of fusion and fission events. Lysosomes use proton pumps to decrease internal pH and after fusion with phagosomes, the acidic environment initiates enzyme degradation of phagocytized material. Promotion of this process occurs via signaling events like interferon-γ signaling through STAT1 and interferon regulatory factor 1 (IRF-1) and TLR ligation and subsequent myeloid differentiation primary response 88 (MyD88) and MAPK pathways. This leads to translocation of transcription factors like NFκB and AP-1 to the nucleus. The increased presence of these transcription factors in the nucleus induces pro-inflammatory pathways that kill intracellular pathogens (50), a specialized ability that highlights the integral role of macrophages in innate immunity.

Macrophages employ multiple strategies for killing pathogens alongside enzymatic degradation of pathogenic material in the phagolysosome. Macrophage stimulation with inflammatory cytokines (IFNγ, TNF) or TLR ligation can lead to production of reactive nitrogen and oxygen intermediates (51). The protein NOS2 generates NO that diffuses into the phagolysosome due to its production location in the cytosol. Stimulation with IFN-γ also recruits the protein NOX2 to the phagolysosome where it produces reactive oxygen intermediates such as superoxide anions, hydrogen peroxide, and hydroxyl radicals (52). In the phagosome, the reactive nitrogen and oxygen intermediates can spontaneously react to form molecules that efficiently kill pathogens: nitrogen dioxide, peroxynitrite, dinitrogen trioxide, and more (42, 53). These can cause the destruction of membrane lipids, DNA, and thiol and tyrosine residues (51). Additionally, macrophages limit the resources available to the pathogen. NOS2 and

indoleamine 2,3-dioxygenase 1 (IDO1) catabolize the essential amino acids arginine and tryptophan, respectively. Using a combination of these pathways enables macrophages to successfully kill intracellular pathogens.

1.4.2 Macrophages in Adaptive Immunity

While macrophages contribute significantly to innate immune responses, they also act as a key connection between innate and adaptive immunity via antigen presentation. After phagolysosomal killing, macrophages degrade foreign proteins and present the degraded short peptides in MHC to T cells (discussed earlier). Activation of macrophages via PRRs upregulates MHC, costimulatory molecule, and cytokine production, all necessary for T cell activation. MHC processing and presentation is extremely important for initiation of adaptive immune responses, as individuals with mutations in MHC processing proteins are susceptible to various infections (54). Macrophage antigen presentation, cytokine production, and costimulation emphasize the vital contributions macrophages make to adaptive immunity.

1.4.3 Macrophage Regulation of Inflammation

Despite the benefits of inflammatory responses to host immunity, they must be regulated to avoid immunopathologies such as those associated with autoimmune diseases. Macrophages support homeostasis through metabolic influences, scavenging for cell debris, promotion of angiogenesis, and induction of immune tolerance, helping to downregulate and prevent excess inflammation. However, the resolution of inflammatory responses by macrophages is not simply dependent on turning off inflammatory signal production but also by increasing the production of anti-inflammatory mediators. The most common of these mediators are IL-10 and transforming growth factor beta (TGF-β).

These immunoregulatory cytokines exist to keep innate immune responses in check and, during later stages, to limit adaptive immunity.

IL-10 is a potent anti-inflammatory cytokine that signals through the IL-10 receptor on macrophages, inhibiting inflammatory cytokine production, antigen presentation, and frequently decreasing the killing of intracellular pathogens (55). Many cells produce IL-10, and genetic alterations that result in a failure to produce this cytokine are invariably associated with inflammatory immunopathology (56). However, the potent immunoregulatory activity of IL-10 has generally not led to the utilization of recombinant IL-10 to treat autoimmunity. Unfortunately, the administration of recombinant IL-10 has been largely unsuccessful at achieving a sustained reversal of inflammatory pathology in patients suffering with autoimmunity, including psoriasis and Crohn's disease (57). One reason may be that IL-10 is frequently diverted to the many different cells that have receptors for IL-10, preventing its delivery to inflamed areas. Localized induction of IL-10 may be more effective in regulating inflammation.

Whether produced by macrophages or other cell types, IL-10 release depends on the strength of stimulation (57). In macrophages, increased signaling through a combination of stimuli results in high levels of IL-10 production. For example, the addition of LPS in combination with the ligation of macrophage Fc-γ receptors by high-density immune complexes can not only induce high levels of IL-10 production but also potently downregulate IL-12 production (58). This reciprocal alteration in these two key cytokines results in a macrophage population that can mitigate inflammation and provide protection against acute endotoxicity (59). These macrophages also exhibit increased susceptibility to intracellular pathogens (60). The physiological relevance of this

phenotypic alteration was demonstrated in an infectious disease model in which the intracellular parasite *Leishmania* uses this pathway to induce macrophage IL-10 to promote its survival within macrophages (60).

Although TGF-β exhibits a wider range of roles in cellular processes when compared to IL-10, its ability to modulate inflammation and influence disease progression renders it an extremely important immune modulator. The abundance and activity of TGF-β ligands, the presence of SMAD cofactors, and epigenetic modifications all contribute to the intensity and type of signal created from TGF-β signaling (61). SMAD proteins, activated via the TGF-β receptor, form complexes with each other and with other cofactors to activate or inhibit gene transcription. The addition of exogenous TGF-β to LPS-stimulated macrophages decreased the release of proinflammatory cytokines, suggesting paracrine functions of the signaling (62). In mouse models, TGF-β treatment prevented disease in collagen-induced arthritis and prevented relapse in rheumatoid arthritis, consistent with its anti-inflammatory activity (63). Use of TGF-β as a therapeutic in mouse models for multiple sclerosis showed improved clinical status and decreased nervous system damage, indicating its promise (64). However, the multifaceted effect of TGF-β production is illustrated by its contribution to fibrotic diseases, showing the need to continue studying this complex pathway (65).

The previous paragraphs detailing IL-10 and TGF-β were adapted from the previously published work: Hamidzadeh K, Christensen SM, Dalby E, Chandrasekaran P, Mosser DM (2017) Macrophages and the Recovery from Acute and Chronic Inflammation. *Annu Rev Physiol* 79:567–592.

1.4.4 Macrophage Activation and Classification

Classification of macrophage activation states has evolved over the years as we continue to uncover the complexities of macrophage plasticity. Originally, macrophages were categorized as either classically activated (M1) or alternatively activated (M2) (66). The classical activation (M1) characterization is widely accepted, utilizes IFNγ/LPS stimulation, and translates well to human models. "Classically activated" macrophages secrete inflammatory cytokines and recruiting chemokines and produce high levels of superoxides designed to kill engulfed pathogens in the phagolysosome (13). However, growing knowledge indicates that the spectrum of macrophage activation is much more complex, involving more than 2 activation states, and this oversimplification can lead to confusion. Activation via IL-4 or IL-13 (M2a), known to promote Th2 responses and contribute to wound healing through angiogenic and fibrotic factors, is well classified in the murine system (13, 67–70). However, markers of M2 murine macrophages do not translate well into human systems, and research has struggled to identify markers of human M2a macrophages (70, 71). The so-called regulatory macrophages, also called M2b (69), have been generated via stimulation with TLR ligands in conjunction with immune complexes, prostaglandin, adenosine, or apoptotic bodies. These macrophages potently downregulate IL-12, upregulate IL-10, and secrete growth and angiogenic factors. Our lab has begun to identify markers of human regulatory macrophages and apply them to the disease model leishmaniasis in this work.

1.5 Leishmaniasis

Infections from *Leishmania* species present in a wide range of clinical characterizations and we still lack a full understanding of the host-pathogen interactions and pathology of the disease. Endemic to tropical and subtropical regions, leishmaniasis

manifests as either cutaneous infections in the skin or visceral infections that are systemic and potentially fatal (72). This work pertains to cutaneous leishmaniasis, an infection that, while rarely fatal, can cause disfiguration and a significant reduction in quality of life. Following the bite of an infected female phlebotomine sandfly, disease manifestation relies strongly on the species of parasite present, a panel of over 20 known species throughout the globe. More than 90% of cutaneous leishmaniasis cases occur in only twelve countries: Afghanistan, Algeria, Brazil, Colombia, Iran, Iraq, Morocco, Peru, Saudi Arabia, Sudan, Syrian Arab Republic, and Tunisia (73). Patients of Old World cutaneous disease (mainly eastern hemisphere) do not usually require treatment due to the spontaneous, self-healing nature of the lesions. However, treatment of New World cutaneous leishmaniasis is recommended and usually involves administration of antimonials, despite the many adverse side-effects of these toxic drugs. Leishmaniasis is classified as a "neglected tropical disease" (NTD) by the WHO due to struggles in vaccine and therapeutic advancements to effective clinical stages, stressing the need for further research.

Cutaneous lesions can be split into four types of disease: localized cutaneous (LCL), diffuse cutaneous (DCL), disseminated (DL), and mucocutaneous (MCL). The four main cutaneous clinical classifications reside on a spectrum of pathology, ranging from hyposensitive to hypersensitive (Figure 1) (74). At the hyposensitive end, DCL patients show no delayed-type hypersensitivity (DTH) response, exhibit large numbers of parasites in lesions, and produce little to no IFNγ or TNF in response to the infection.

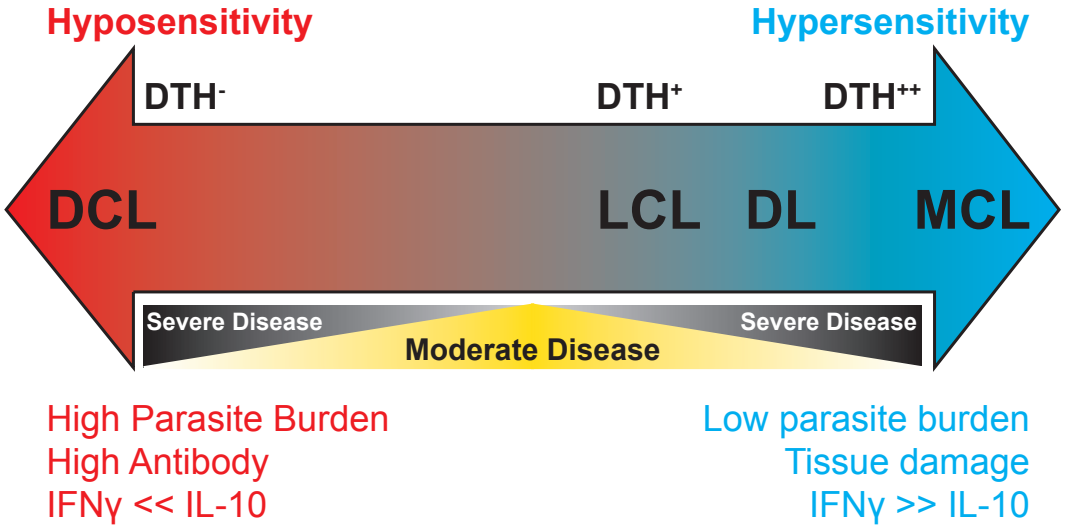

Figure 1. Spectral nature of leishmaniasis Representation of the spectral nature of leishmaniasis infections. Severe disease resides at each end of the spectrum in diffuse cutaneous lesions (DCL) or mucocutaneous lesions (MCL). Hyposensitive DCL patients are typically DTH negative, indicative of failure to produce cell-mediated immunity and Th1 cells. DCL contains high numbers of parasite in lesions, high IL-10 in lesions, and increased serum antibody. Hypersensitive mucocutaneous lesions are characterized by increased IFNγ, low parasite numbers, and immense tissue damage. Localized and disseminated leishmaniasis spontaneously self-heal and are considered moderate disease. Localized disease manifests as a single nodule that can progress to an ulcerated lesion, while disseminated disease manifests as multiple acneiform and papular lesions. LCL and DL patients do have a DTH positive response. Localized disease is the most common manifestation; DCL, DL, and MCL are considered rare. Figure adapted from Scorza et al. (74).

At the other end of the spectrum, MCL pathology is mainly immune-mediated with an intense DTH response, high levels of IFNγ, low parasite numbers, and tissue damage that can lead to disfiguring disease. Less hypersensitive than MCL, lesions in DL and LCL patients are still on the hypersensitive end of the spectrum, with uncontrolled Th1 responses sometimes associated with ulcerated lesions.

The *Leishmania* life cycle consists of mammalian hosts and the sandfly vector. Parasites become metacyclic and highly infective in the gut of the sandfly, allowing for rapid infection of host macrophages and dendritic cells after the blood meal is taken. Once in macrophages, the parasites survive and replicate as amastigotes in the phagolysosome, inhibiting macrophage killing. The phagolysosome eventually bursts and the *Leishmania* are taken up by neighboring phagocytes, perpetuating the cycle and spreading the parasite through the tissue. Parasites return to the sandfly vector when it takes a blood meal from an infected individual.

1.5.1 Immune responses in leishmaniasis

Dating back 30 years, murine models have helped to characterize resistant and susceptible species of mice based on the prevalence of a Th1 or Th2 immune response, respectively (75, 76). Activated professional phagocytes will migrate to lymph nodes where they present antigen to T cells. The activation state of CD4+ helper T cells in murine models relies heavily on the cytokines IL-12 (Th1) or IL-4 (Th2). Th1 cells produce IFNγ and TNF, molecules that classically activate macrophages to kill the intracellular parasite (77–79). “Improper” Th2 responses, generated via the production of IL-4 and IL-13 signaling through IL-4 receptor-alpha result in alternative macrophage activation (M2a), defective macrophage-mediated killing, and survival of parasites in

susceptible mice (80). Additionally, susceptibility has not surprisingly been tied to anti-inflammatory IL-10 production as well. Mice deficient in IL-10 are highly resistant to infection from multiple species (81–83).

Despite this seemingly simple dichotomy, timing and strength of signal can also play an important role in determining protection and susceptibility. Resistant mice actually produce small amounts of IL-4 during the early response to infection but it does not appear to be sufficient to affect the Th1 outcome (84). Treatment of susceptible mice with IL-12 plus anti-IL-4 antibody at one month after infection shifted responses toward Th1 and decreased parasite burden and lesion size (85). Conversely, treatment of susceptible mice with IL-4 within hours of infection can lead to protective and Th1 responses in dendritic cells (DCs) (86). These complexities that are observed in inbred strains of mice emphasize the need for further study, especially in human models.

In human *Leishmania* infection, aspects of Th1 resistance and Th2 susceptibility have been uncovered but controversy remains. Both Th1 and Th2 cytokines have previously been observed in LCL, MCL, and DCL (87, 88). Santos et al. have highlighted the role of IFNγ production by Th1 cells in parasite clearance (89). Although high levels of IFNγ and TNF correlate well to decreased parasite burden, uncontrolled Th1 cytokine production drives immunopathology in localized and mucocutaneous infections from *L. braziliensis* (90, 91). Inferences of IL-4 contributions to susceptibility or parasite persistence via peripheral blood, lesions, and cultured cells has been observed in some cases (92–96), but not others (91, 97, 98). Research has shown the presence of IL-13, but not IL-4, in response to *Leishmania* antigen after healing (99). In *ex vivo* studies, monoclonal antibody blocking of IL-4 did not restore IFNγ production capabilities to

peripheral blood mononuclear cells (PBMCs) but IL-10 antibody or IL-12 protein did (100). Indeed, human cutaneous leishmaniasis lesions contain high levels of IL-10 and TGFβ (87, 94, 101, 102). These combined findings suggest that perhaps IL-4 is not as large a contributor as originally believed and human susceptibility relies more on the balance between IL-12/IFNγ and IL-10/TGFβ.

In addition to studies on T helper cell contributions to human cutaneous lesions, other studies have shown contributions of CD8 T cells in the healing process and resistance to *Leishmania* infection (103, 104). Conversely, cytotoxic T cell production of granzymes can lead to extensive tissue damage (89). The exact role of these cells in resolution or pathology seems to depend on production of either IFNγ or cytolytic molecules, but further analyses are required (72).

The majority of leishmaniasis research has focused on phagocytic cell killing of parasites as well as T cell influences on infection. The focus on these cells is warranted, yet research has increasingly shown the importance of other cells in the control or persistence of disease. Infiltration of T cells, macrophages, B cells, NK cells, and granulocytes into lesions has previously been shown but until recently some of these cell types were not extensively studied (105). Contemporary research shows early neutrophil responses acting as a Trojan horse to protect parasites during initial infection (106). An increasingly wide range of T cell populations have been implicated in infection resolution and pathology and T cell anergy has been shown to promote parasite survival (103, 107–110). Vaccine research has focused on the stimulation of NK cell cytotoxicity in preventing infection (111). Even still, the contributions of keratinocytes to immune activation have also been uncovered (112). Lastly, infiltration of B cells in lesions is

known (60, 113, 114), but studies on B cell subsets and their contribution to parasite persistence or killing are still in early stages.

The role of B cells and immunoglobulin production is especially pertinent to this work and previous works have pointed to complex and varied roles for immunoglobulin contributions to *Leishmania* infection. Uptake of *Leishmania* by phagocytes can occur through FcR-mediated phagocytosis (115), a process known to induce IL-10 production in macrophages (58, 116). In fact, Fc receptors and IgG exacerbated disease and are needed to establish infection in mice (60, 113, 117–120). In humans, levels of serum IgG vary depending on parasite species and clinical manifestation. High levels of IgG are tied to *L. amazonensis* in DCL patients and also in visceral leishmaniasis (60, 121–123). Although IgG has been shown to be protective against intracellular pathogens (124), this does not seem to be the case for *Leishmania*. However, it has been suggested that IgG2a in mice may contribute to lesion resolution (117) and vaccine development has focused on inducing IgG2a in mice and dogs to curate a Th1 bias that promotes healing (125–128).

1.5.2 Immune Evasion by *Leishmania*

Leishmania sp. have developed numerous methods to avoid killing and promote survival within host macrophages and dendritic cells. During initial infection after the sandfly bite, parasites are able to avoid complement activation using the glycoprotein GP63, which cleaves the complement protein C3 into its inactive C3bi form. This not only prevents the formation of the membrane attack complex (129), but also serves as an opsonin that directs phagocytes to engulf the pathogen (130, 131). Once inside the cell, *Leishmania* can also interfere with TLR signaling, produce antioxidants, regulate host

arginase, and inhibit inflammatory signals such as phagolysosome maturation and costimulatory molecule production (132–134). At the same time, induction of IL-10, IL-4, IL-5, PGE2, and TGF-β also have been shown during infection (135). While the specifics are known for some manipulations, a complete framework of the host-pathogen interaction is lacking.

Research has identified some of the various proteins and pathways that *Leishmania* use to evade and even harness the immune response for their advantage. One of the most commonly known virulence factors is glycoprotein 63 (GP63). This protein has been shown to be multifunctional in parasite virulence, not just in cleaving C3 as described earlier. GP63 can cleave PKC substrates necessary for oxidative bursts (136). Cleavage of RelA subunits by GP63 and other cysteine peptidases induces chemokines that aid parasite survival (137, 138). GP63 can also cleave c-Jun and c-Fos to prevent the transcription factor AP-1 from inducing intracellular killing (139) and cleave mTOR to promote parasite survival (140). The surface protein lipophosphoglycan (LPG) is another virulence factor that has been shown to facilitate binding to multiple proteins on macrophage membranes (135) to encourage phagocytosis of the parasite. Once inside the cell, *Leishmania* LPG can inhibit endosome maturation (141) and phagosome acidification (142) and "quench" superoxide radials (143). LPG can also inhibit the induction of the monocyte chemoattractant CCL2 (144). *Leishmania* require iron for growth and counteract host iron efflux from the phagosome through the parasite iron transporter protein LIT1 (145). While these virulence factors are known, full annotation of parasite genomes is still lacking. Our investigation of the parasite transcriptome in human infections is another step toward an extensive understanding of these pathogens.

1.6 Summary

The complexities of the immune system allow organisms, from flies to humans, to defend against pathogens, recover from injury, maintain homeostasis, and much more. Divided into two branches, the immune system is poised to react to acute injury or infection (innate immunity) while also providing immune memory (adaptive immunity). Myriad cell types, signaling cascades, and checks and balances contribute to the efficacy of innate and adaptive immune responses. While the complexities of the immune system demonstrate its ability to defend against a plethora of pathogens, it also provides numerous ways for pathogens to evade and even control responses for their benefit. One of these, the tropical parasite *Leishmania*, infects millions of people each year who suffer from a spectrum of disfiguring and fatal disease. Effective vaccines are not available and safe therapeutics remain in developmental stages of production. In order to further understand leishmaniasis microenvironments and host-pathogen interactions, I describe the host and parasite transcriptomes in two forms of the disease: localized cutaneous leishmaniasis in *L. braziliensis*-infected patients and diffuse cutaneous leishmaniasis in *L. amazonensis*-infected patients. In-depth characterization of host and parasite gene expression could elucidate biomarkers or targets for effective vaccines and therapeutics, both of which are desperately needed for this neglected tropical disease.

Chapter 2: Materials and Methods

2.1 RNA Sequencing and Transcriptomics

2.1.1 Background Methods to examine the transcriptome have advanced in recent years, from hybridization to sequence-based techniques. Custom-made microarrays are high-throughput and less expensive, relying on hybridization of fluorescently-labeled cDNA to gene-specific constructs that allows for relative gene expression comparisons. However, this technology is deficient in numerous ways: being restricted to a subset of gene probes, limited on distinguishing low or high expression levels, and difficult to compare across experiments. Rapidly improving sequence-based technologies like RNA-seq remedy these limitations and provide a deeper understanding of the transcriptome. RNA-seq methods can map reads to an entire genome, not just a subset, and can even be used for de novo assembly of previously unsequenced genomes. This technology is not limited to probes and allows for single base pair resolution that illuminates exactly where transcription starts, ends, skips (introns and exons) (146), and even varies (SNPs) (147). On one end, there is little to no background noise in RNA-seq output that permits inclusion of lowly expressed genes, while on the other end, there is no upper limit to the quantity of reads mapping to any single region. Additionally, comparisons across experiments requires less strenuous normalization methods. The most important aspect of RNA-seq applicable to this work is the ability to simultaneously analyze the transcriptomes of multiple species. Using RNA isolated from infected human tissue, we can simultaneously map reads to human and pathogen genomes.

2.1.2 Experimental Application The goal of this research was to better understand the underpinnings of the human-Leishmania infection by analyzing the transcriptomes of

both species during infection. Previous work by our collaborators used microarray technology to examine LCL lesions in *L. braziliensis*-infected patients, characterizing a general signature of immunopathology and identifying enriched pathways, citing commonalities between LCL and psoriasis lesions (48). To expand upon these results and develop a better understanding of the host and parasite transcriptome, we performed RNA-seq on the LCL biopsies and mapped reads to the human and parasite genomes. We further acquired biopsies from DCL patients and performed RNA-seq on these samples as well, enabling us to compare and contrast two different manifestations of cutaneous disease from the human and parasite perspectives. The results are detailed in the subsequent chapters of this dissertation.

2.1.3 RNA isolation and cDNA library preparation. Samples were placed in RNAlater and homogenized using a rotor-stator. Total RNA was isolated using the RNeasy Plus Kit from Qiagen (Hilden, Germany). RNA integrity was assessed using an Agilent 2100 bioanalyzer. Poly(A)$^+$-enriched cDNA libraries were generated using the Illumina TruSeq Sample Preparation kit (San Diego, CA) and checked for quality and quantity using the bioanalyzer and quantitative polymerase chain reaction (qPCR) (KAPA Biosystems).

2.1.4 RNA-seq data generation, pre-processing, and quality trimming. Paired end reads (~100 bp) were obtained using the Illumina HiSeq 1500 platform. Trimmomatic (148) was used to remove any remaining Illumina adapter sequences from reads and to trim bases off the start or the end of a read when the quality score fell below a threshold of 20. Sequence quality metrics were assessed using FastQC [http://www.bioinformatics.babraham.ac.uk/projects/fastqc/].

2.1.5 Mapping cDNA fragments to the reference genome, abundance estimation, and data normalization. TopHat (v 2.0.13) (149) was used to align reads to the applicable genome(s) with each genome alignment performed independently. Reads from healthy, LCL, and DCL skin samples were aligned to the human genome (v. hg19/GRCh37) obtained from the UCSC genome browser (http://genome.ucsc.edu). Reads from LCL and DCL infection samples were additionally aligned to the *L. braziliensis* (v. MHOM/BR/75M2904, Sanger Institute) or *L. mexicana* (v. MHOM/GT/2001/U1103) genomes respectively, obtained from the TriTrypDB database (www.tritrypdb.org). Two mismatches per read were permitted (default TopHat parameter) and reads were allowed to map only to a single locus (TopHat option –g 1). Additionally, gene model annotations were provided for the mapping (TopHat option –G) with limitations on the identification of novel splice junctions (TopHat option –no-novel-juncs). The abundance of reads mapping to each gene feature in the aligned genome was determined using HTSeq (150). Each resulting count table was restricted to protein-coding genes: 20,956 genes for human, 8,556 genes for *L. braziliensis*, 8,336 for *L. amazonensis*. Non-expressed and weakly expressed genes, defined as having less than 1 read per million in n of the samples, where n is the size of the smallest group of replicates (151) (here n=8 for human and *L. braziliensis*, n=6 for *L. amazonensis*), were removed prior to subsequent analyses, resulting in count tables of 15,256 (human), 8,556 (*L. braziliensis*), and 8,336 genes (*L. amazonensis*).

2.1.6 Global data assessment, visualization and differential expression analysis. Quantile normalization was applied to all samples (152) and data were $\log_2$-transformed. Multiple approaches were used to evaluate replicates and to visualize the relationships

between samples, including Pearson correlation and Principal Component Analysis (PCA). Limma (a Bioconductor package) was used to conduct differential expression analyses (153). The voom module was used to transform the data based on observational level weights derived from the mean-variance relationship prior to statistical modeling (154). Pairwise contrasts were done within limma to identify differentially expressed (DE) genes between conditions. Genes with a Benjamini-Hochberg (BH) multiple-testing adjusted *P* value of < 0.05 were defined as differentially expressed. Components of our statistical pipeline, named cbcbSEQ, can be accessed on GitHub (https://github.com/kokrah/cbcbSEQ/).

2.1.7 Immunoglobulin sequencing analysis Using filtered and trimmed sequences from the aforementioned pre-processing, reads were aligned and filtered using miXCR and pRESTO (155, 156). After preparation, sequences were collapsed and submitted to the ImMunoGeneTics database (IMGT) HighV-QUEST web server for gene annotation and analysis (157, 158). IMGT output was analyzed using in house scripts and bcREP (159).

2.2 Ethics Statement

These studies were conducted according to the principles specified in the Declaration of Helsinki and under local ethical guidelines and this study was approved by the Ethics Committees of the Federal University of Bahia (Salvador,Bahia, Brazil)(010/10), University of Maryland (College Park)(925281-2) and the University of Pennsylvania IRB (Philadelphia, Pa)(813390). All patients provided written informed consent for the collection of samples and subsequent analysis.

2.3 Patients and Procedures

All localized cutaneous leishmaniasis (LCL) patients were seen at the health post in Corte de Pedra, Bahia, Brazil, an area endemic to *L. braziliensis*. Diagnosis consisted of visual confirmation of a lesion characteristic of LCL and parasite DNA detection and/or a positive delayed-type hypersensitivity response to *Leishmania* antigen. Biopsies were collected at the border of the lesions using a 4 mm punch before therapy. Patients consisted of 15 males and 10 females with illness duration ranging from 15 to 90 days and lesion sizes ranging from 4-960 mm^2 (Table 1). Healthy (uninfected) skin samples were taken from volunteers living in a non-endemic area without a history of leishmaniasis, as described (48). All diffuse cutaneous leishmaniasis (DCL) patients were seen at Institute Evandro Chagas, Professor Ralph Lainson Laboratory of Leishmaniasis, Ananindeua, Para Brazil. Biopsies were collected at the border of the lesions using a 4 mm punch. Patients consisted of 5 males and 1 female with illness duration ranging from 14 to 35 years and age ranging from 15-50 (Table 2).

Table 1. Patient metadata for healthy skin and LCL biopsies

Sample	Infection status	Lesion Size (mm^2)	Illness duration at time of biopsy (days)	Patient age (years)	Gender
N1	Uninfected	NA	NA	NA	NA
N2	Uninfected	NA	NA	NA	NA
N3	Uninfected	NA	NA	NA	NA
N4	Uninfected	NA	NA	NA	NA
N5	Uninfected	NA	NA	NA	NA
N6	Uninfected	NA	NA	NA	NA
N7	Uninfected	NA	NA	NA	NA
N8	Uninfected	NA	NA	NA	NA
N9	Uninfected	NA	NA	NA	NA
N10	Uninfected	NA	NA	NA	NA
E1	Early infection	36	21	44	F
E2	Early infection	40	21	24	M
E3	Early infection	56	15	31	F
E4	Early infection	12	20	25	F
E5	Early infection	80	20	33	M
E6	Early infection	120	15	25	F
E7	Early infection	25	30	30	F
E8	Early infection	4	15	40	M
L1	Late infection	100	30	25	M
L2	Late infection	440	37	28	M
L3	Late infection	100	90	19	M
L4	Late infection	560	90	33	F
L5	Late infection	180	60	18	M
L6	Late infection	252	30	27	M
L7	Late infection	100	30	45	F
L8	Late infection	48	30	21	M
L9	Late infection	550	30	37	M
L10	Late infection	380	60	25	M
L11	Late infection	250	30	30	M
L12	Late infection	100	35	33	F
L13	Late infection	440	40	25	M
L14	Late infection	192	25	19	F
L15	Late infection	400	30	40	M
L16	Late infection	48	45	26	F
L17	Late infection	960	30	19	M

Table 2. Patient metadata for DCL biopsies

Patient	Patient age (years)	Gender	Illness duration at time of biopsy (years)
DCL.1	50	F	22
DCL.2	42	M	35
DCL.3	43	M	20
DCL.4	37	M	34
DCL.5	30	M	27
DCL.6	15	M	14

Chapter 3: Meta-transcriptome profiling of the human-*Leishmania braziliensis* localized cutaneous lesion

Adapted from previous publication: Christensen SM, Dillon LAL, Carvalho LP, Passos S, Novais FO, Hughitt VK, Beiting DP, Carvalho EM, Scott P, El-Sayed NM, Mosser, DM. Meta-transcriptome Profiling of the Human-*Leishmania braziliensis* Cutaneous Lesion. PLoS Negl Trop Dis. 2016.

ABSTRACT

Host and parasite gene expression in skin biopsies from *Leishmania braziliensis*-infected patients were simultaneously analyzed using high throughput RNA-sequencing. Biopsies were taken from 8 patients with early cutaneous leishmaniasis, 17 patients with late cutaneous leishmaniasis, and 10 healthy volunteers. Although parasite DNA was found in all patient lesions at the time of biopsy, the patients could be stratified into a group that lacked detectable parasite transcripts (PT^{Neg}) in lesions and another group in which parasite transcripts were readily detected (PT^{Pos}). These groups exhibited substantial differences in host responses to infection. PT^{Pos} biopsies contained an unexpected increase in B lymphocyte-specific and immunoglobulin transcripts in the lesions, and an upregulation of inflammatory and immune inhibitory molecules. Biopsies without detectable parasite transcripts showed decreased evidence for B cell activation, but increased expression of antimicrobial genes and genes encoding skin barrier functions. The composition and abundance of *L. braziliensis* transcripts in PT^{Pos} lesions were surprisingly conserved among all six patients, with no differences between lesions from patients with early and late cutaneous leishmaniasis. Some of the most highly expressed *in vivo* transcripts encoded amastin-like proteins, hypothetical genes, putative parasite

virulence factors, as well as histones and tubulin. We compared parasite gene expression to previously sequenced data of *in vitro* macrophage infections. Despite some similarities, overall parasite expression differed between the lesion and laboratory environments, suggesting a varied parasite response due to immune stress. In summary, RNA-seq allowed us to simultaneously analyze human and *L. braziliensis* transcriptomes in lesions of infected patients, and identify unexpected differences in host immune responses correlated with active transcription of parasite genes.

INTRODUCTION

Leishmaniasis is characterized as a spectral disease, with clinical presentations ranging from a self-healing cutaneous form of the disease to a visceral form associated with high morbidity and mortality. The immune response to the various species is also spectral in nature, with *L. donovani* inducing minimal immune responses or actually inhibiting inflammation and immunity (160), and *L. braziliensis* inducing immune activation and immune-mediated pathology (103). *L. braziliensis* is the causative agent of tegumentary leishmaniasis in South America. Approximately 3-5% of patients infected with *L. braziliensis* will eventually develop mucocutaneous disease, a disfiguring manifestation involving the nasal and oropharyngeal mucosa (161). *L. braziliensis* infections are typically associated with a strong Th1 response and a positive skin test response to soluble leishmanial antigens characterized by high levels of TNF and IFN-γ (90).

'Early' *L. braziliensis* lesions frequently present as a small papule that can eventually progress to larger 'late' ulcerative lesions, typically containing small numbers of parasites. The more severe mucocutaneous forms of the disease are associated with

increased cytokine responses and increased T cell proliferation responses to parasite antigens (90). The robust immune response to this organism despite low or undetectable numbers of parasites in lesions, and the increased immune responses in mucocutaneous forms of the disease have led to the suggestion that exaggerated Th1 host immune responses contribute to the pathological tissue damage associated with *L. braziliensis* infections (162). Recent studies suggest that a major factor in the development of disease caused by *L. braziliensis* is the recruitment of cytolytic CD8+ T cells that promote increased inflammation (89, 107).

Immune responses in the skin of infected patients may not be accurately reflected by the type and magnitude of host responses in peripheral blood. Previous studies using immunohistochemistry have described the infiltration of T cells, macrophages, B cells, NK cells, and granulocytes into lesions (105, 163, 164). Some research has implicated CCR2-positive monocytes in parasite killing (165, 166), while other studies have described the contribution of the skin micro-environment to the local immune response (167–170). For these reasons, a meta-transcriptomic profiling of lesions may provide a more complete picture of host and parasite responses during infection.

A microarray-based transcriptomic profiling of skin lesions from patients infected with *L. braziliensis* was recently reported (48). This work showed an association between chemokines and cytotoxic T cell responses and disease-associated pathology. We extended this work using RNA-seq to simultaneously analyze host and parasite transcripts in these lesions. This approach allowed the detection of parasite transcripts expressed in the skin of infected patients, and revealed unexpected differences in the host response associated with the detectability of parasite transcripts in lesions. It also

revealed *L. braziliensis* transcripts most abundantly produced in human lesions of localized cutaneous leishmaniasis.

RESULTS

Global data assessment, visualization and differential expression analysis. Samples were classified as PT^{Pos} and PT^{Neg} based on the percentage of reads mapping to the *L. braziliensis* genome. Parasite detectable-positive samples were defined as those with more than 0.5% of reads mapping to the parasite genome. In the six PT^{pos} samples, the average proportion of reads that mapped to the parasite genome was 0.98%, for an average of 867,489 parasite reads per tissue sample sequenced to an average depth of 88 million reads. The 10 PT^{Neg} samples were defined as those with fewer than 0.01% reads mapping to the parasite; the proportion of reads in the PT^{Neg} samples that mapped to the parasite genome was not different than the 10 healthy controls. We designated nine additional samples as PT^{Int} because they expressed low levels of transcripts (between 0.01-0.2% of total reads) that could only tentatively be assigned to the parasite. The number of parasite reads in this group was too low to provide a meaningful analysis of parasite gene expression and therefore they were excluded from the PT^{Pos} group.

The human host transcriptome in lesions of *L. braziliensis* infected patients. RNA-seq analysis was performed on biopsies from 10 healthy and 25 *L. braziliensis* infected patients. Principal Component Analysis (PCA) (Figure 2A) and hierarchical clustering (Figure 3A) of the human transcriptome data revealed distinct differences between healthy skin and lesions from infected patients, as expected. Lesions are clinically defined as either ‘early’ (small papule, no ulceration, ≤ 30 days illness duration) or ‘late’ (ulcerated lesions, ≥ 30 days illness duration) (Table 1).

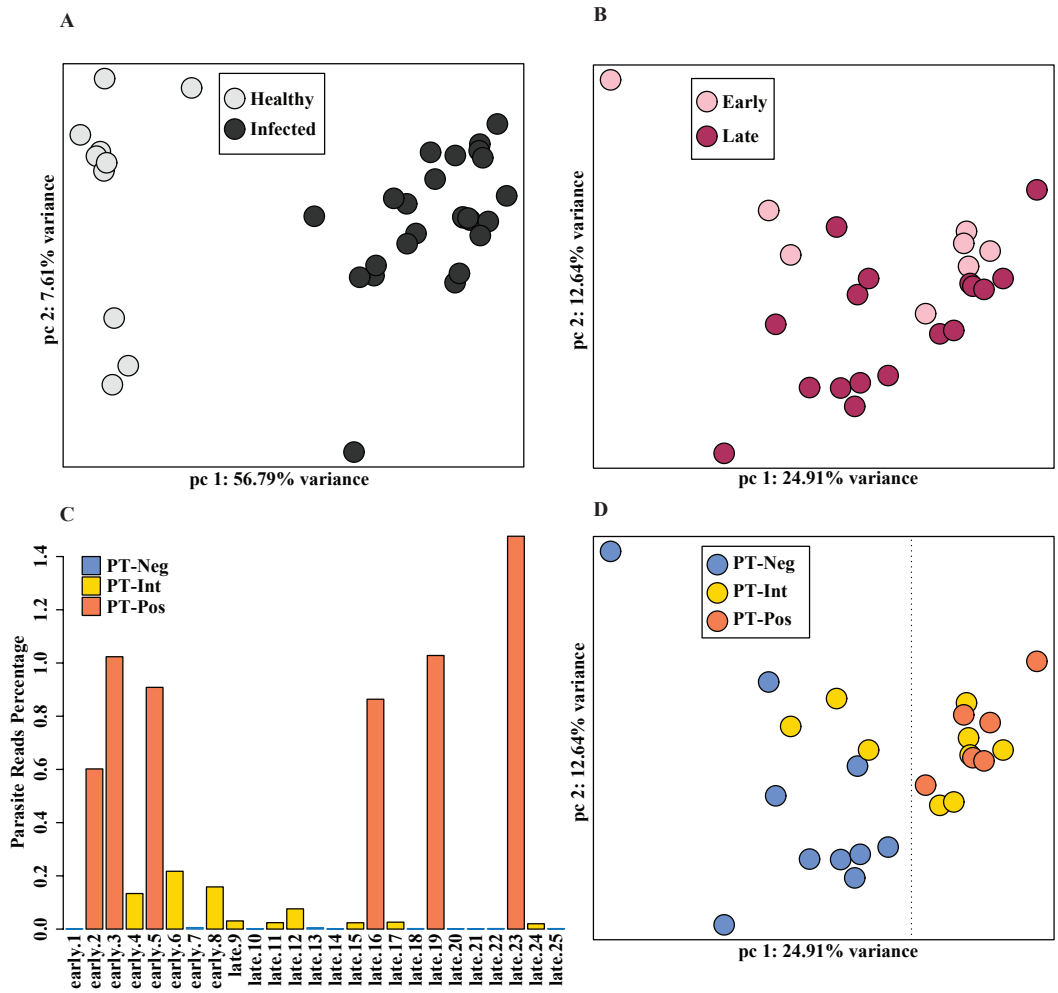

Figure 2. Human and parasite transcriptomes in lesions of *L. braziliensis* infected patients. (A) Principal component analysis (PCA) of human transcriptomes from 10 healthy volunteers (light gray) and 25 *L. braziliensis*-infected patients (dark gray) is shown. The first two principal components (PC) are displayed on each axis along with the variance (56.79% and 7.61%). **(B)** Principal component analysis (PCA) plot of human transcriptomes from 8 early-stage (pink), and 17 late-stage (maroon) leishmaniasis patients. The first two principal components (PC) are displayed on each axis along with the variance (24.91% and 12.64%). **(C)** The percentage of total reads that mapped to the *Leishmania braziliensis* genome from each of the 25 infected patient samples are plotted as bars. The samples containing > 0.5% reads are labeled as parasite transcript positive (PT^{Pos}, orange), 0.01-0.5% reads as parasite transcript intermediate (PT^{Int}, yellow), and the rest < 0.01% reads as parasite transcript negative (PT^{Neg}, blue). **(D)** PCA plot of patient samples grouped according to parasite transcript levels: PT^{Neg} (blue), PT^{Int} (yellow), and PT^{Pos} (orange). The first two principal components (PC) are displayed on each axis along with the variance (24.91% and 12.64%).

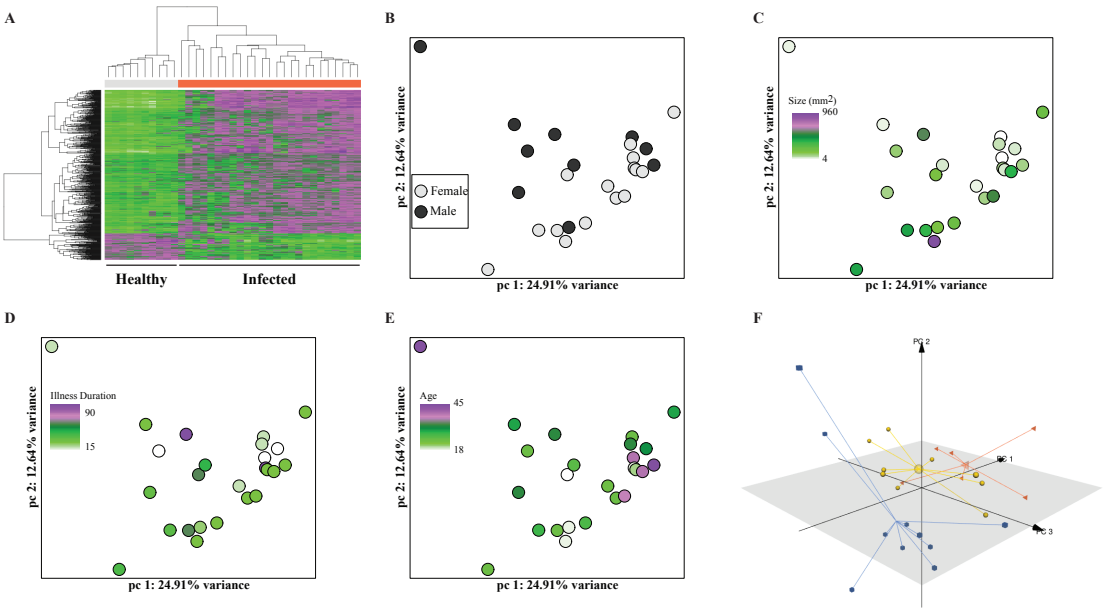

Figure 3. Comparisons of *L. braziliensis* lesions (3A) Panel A shows a heatmap enriched pathways (using GSEA) comparing healthy controls (gray line, top) and leishmaniasis patients (orange line). 680 pathways showed ≥2 fold differences that were clustered hierarchically. (3B) Principal component analysis (PCA) plot of human transcriptomes from 15 female (light gray), and 10 male (dark gray) leishmaniasis patients. The first two principal components (PC) are displayed on each axis along with the variance (24.91% and 12.64%). (3C) Principal component analysis (PCA) plot of human transcriptomes from 25 leishmaniasis patients, colored by lesion size. The first two principal components (PC) are displayed on each axis along with the variance (24.91% and 12.64%). (3D) Principal component analysis (PCA) plot of human transcriptomes from 25 leishmaniasis patients, colored by illness duration. The first two principal components (PC) are displayed on each axis along with the variance (24.91% and 12.64%). (3E) Principal component analysis (PCA) plot of human transcriptomes from 25 leishmaniasis patients, colored by patient age. The first two principal components (PC) are displayed on each axis along with the variance (24.91% and 12.64%). (3F) 3-D Principal component analysis (PCA) plot of human transcriptomes from 25 leishmaniasis patients, colored by parasite transcript displayed on each axis (PC1: 24.91%, PC2: 12.64%, PC3: 11.89%).

Within the group of biopsies from the 25 infected individuals, there were minimal appreciable differences in host responses between patients with early and late cutaneous leishmaniasis (Figure 2B, Table 3), as previously reported (48). There was also no separation in host responses as a function of sex (Figure 3B), lesion size (Figure 3C), illness duration (Figure 3D), or age (Figure 3E).

RNA-seq allows the simultaneous analysis of both host and parasite transcriptomes, and we sought to determine whether the presence or absence of detectable parasite transcripts in lesions could impact host responses. Lesions from six of the patients were considered parasite transcript positive (PT^{Pos}) when greater than 0.5% of the total reads mapped to the parasite genome (Figure 2C, orange). Ten lesions were considered parasite transcript negative (PT^{Neg}) because less than 0.01% of the total reads mapped to the parasite (Figure 2C, blue). This is the same proportion of parasite reads that map non-specifically to highly conserved homologous sequences in the human genome. Nine lesions were considered parasite transcript intermediate (PT^{Int}) when percent reads ranged from 0.01-0.2 (Figure 2C, yellow). The number of parasite reads in this group was too low to provide a meaningful analysis of parasite gene expression, and therefore they were excluded from the PT^{Pos} group. By PCA, there was a clear separation in host responses of the PT^{Pos} (Figure 2D, orange) and PT^{Neg} groups (Figure 2D, blue, note dashed line separating blue and orange), with the PT^{Int} group (Figure 2D, yellow) falling in between these two. This separation between groups becomes even more obvious with the addition of the third principal component, accounting for 11.89% of the variance (Figure 3F).

Table 3. Differential expression between early and late cutaneous *L. braziliensis* lesions

ID	Symbol	logFC	adj.P.Val
ENSG00000137857	DUOX1	1.101722038	0.040
ENSG00000180921	FAM83H	1.048863823	0.047
ENSG00000119514	GALNT12	-1.313526975	0.036
ENSG00000137869	CYP19A1	-1.402417898	0.049
ENSG00000143867	OSR1	-1.566920662	0.046
ENSG00000105825	TFPI2	-2.306474341	0.015
ENSG00000124212	PTGIS	-2.392557657	0.014
ENSG00000116690	PRG4	-2.724259154	0.015
ENSG00000188257	PLA2G2A	-3.212912709	0.015
ENSG00000004799	PDK4	-3.237094127	0.015
ENSG00000170323	FABP4	-3.633646574	0.023
ENSG00000000005	TNMD	-3.790990591	9.53E-05
ENSG00000196616	ADH1B	-4.004318602	0.016

Thus, there is a surprising separation of host responses, depending on the presence or absence of detectable parasite transcripts in lesions, allowing us to correlate host responses with parasite elimination or persistence.

Host transcriptomic responses in PT^{Pos} and PT^{Neg} samples. We found large differences in host transcripts between healthy controls and infected patients, as expected, with 4579 host genes being differentially expressed in lesions relative to normal skin using a cutoff fold change > 2 and *P* value < 0.05. A total of 3884 differentially expressed genes were common to PT^{Neg} and PT^{Pos}, but there was a total of 477 differentially expressed genes unique to PT^{Pos} lesions (Figure 4A, orange circle) and 241 differentially expressed genes unique to PT^{Neg} lesions (Figure 4A, blue circle), relative to healthy controls.

The intermediate (PT^{Int}) samples shared 3817 differentially expressed genes with PT^{Neg} and PT^{Pos}, as well as an additional 987 genes with PT^{Pos} and 214 genes with PT^{Neg}. A total of 238 genes showed differential expression unique to the PT^{Int} group (Figure 4A, yellow circle). Tables 4 and 5 show some of the direct comparison between gene expression in PT^{Pos} and PT^{Neg} lesions. Twenty-five of the top 30 upregulated genes in PT^{Pos} lesions relative to PT^{Neg} lesions encoded immunoglobulin fragments, including 9 of the top 10 genes (Figure 4B, black bars). This group also included CXCL8 (granulocyte migration), IL-21 (B cell proliferation), and granulysin (cellular cytotoxicity). The genes most highly expressed in PT^{Neg} lesions relative to PT^{Pos} lesions included genes involved in skin defenses and epidermal cell development. The top 10 genes in this category included loricrin, filaggrin-1, filaggrin-2, and hornerin, all involved in skin development (Figure 4B, light gray bars).

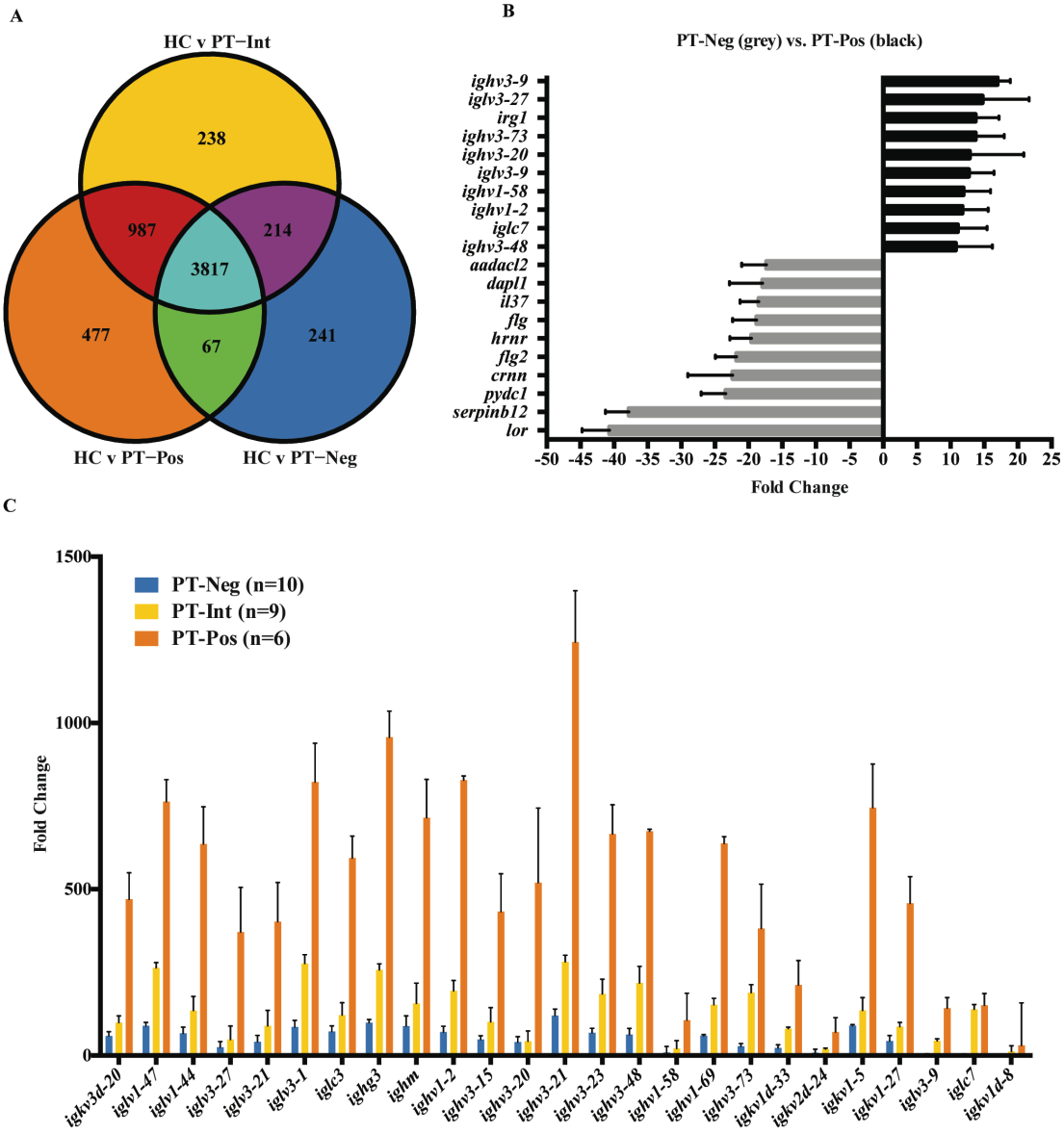

Figure 4. Comparison of human host transcriptomes in lesions with parasite detectable-positive transcripts (PT^{Pos}) versus parasite detectable-negative (PT^{Neg}) transcripts. (A) Venn diagram showing differentially expressed genes in three patient populations compared to healthy controls (HC): PT^{Pos} (orange circle), PT^{Neg} (blue circle), PT^{Int} (yellow circle). **(B).** The top ten significantly upregulated (black) and downregulated (light gray) genes when comparing PT^{Pos} to PT^{Neg} (mean plus SEM). **(C)** Shown are the 25 immunoglobulin genes exhibiting the highest differential expression between PT^{Neg} and PT^{Pos} samples. Bars depict the fold change in expression in PT^{Neg} (blue), PT^{Int} (yellow), and PT^{Pos} (orange) samples relative to healthy controls (mean plus SEM).

Table 4. Top 50 upregulated genes in PT^{Pos} compared to PT^{Neg}

Symbol	Description	logFC
IGHV3-9	immunoglobulin heavy variable 3-9	4.08
IGLV3-27	immunoglobulin lambda variable 3-27	3.88
IRG1	immunoresponsive 1 homolog	3.77
IGHV3-73	immunoglobulin heavy variable 3-73	3.77
IGHV3-20	immunoglobulin heavy variable 3-20	3.68
IGLV3-9	immunoglobulin lambda variable 3-9	3.67
IGHV1-58	immunoglobulin heavy variable 1-58	3.57
IGHV1-2	immunoglobulin heavy variable 1-2	3.55
IGLC7	immunoglobulin lambda constant 7	3.47
IGHV3-48	immunoglobulin heavy variable 3-48	3.43
IGHV1-69	immunoglobulin heavy variable 1-69	3.42
IGKV1-27	immunoglobulin kappa variable 1-27	3.39
IGHV3-21	immunoglobulin heavy variable 3-21	3.38
IGKJ5	immunoglobulin kappa joining 5	3.36
IGHV1-8	immunoglobulin heavy variable 1-8	3.31
IGHV3-23	immunoglobulin heavy variable 3-23	3.29
IGHG3	immunoglobulin heavy constant gamma 3 (G3m marker)	3.28
IGLV3-21	immunoglobulin lambda variable 3-21	3.28
IGLV3-1	immunoglobulin lambda variable 3-1	3.26
IGLV1-44	immunoglobulin lambda variable 1-44	3.25
IGKV1D-8	immunoglobulin kappa variable 1D-8	3.23
IGKV1D-33	immunoglobulin kappa variable 1D-33	3.21
LAG3	lymphocyte-activation gene 3	3.17
IGHV3-15	immunoglobulin heavy variable 3-15	3.17
IGLV1-47	immunoglobulin lambda variable 1-47	3.10
CXCL8	chemokine (C-X-C motif) ligand 8	3.09
IL21	interleukin 21	3.06
IGKV1-5	immunoglobulin kappa variable 1-5	3.06
GNLY	granulysin	3.05
IGLC3	immunoglobulin lambda constant 3 (Kern-Oz+ marker)	3.04
IGKV2D-24	immunoglobulin kappa variable 2D-24 (non-functional)	3.04
IGHM	immunoglobulin heavy constant mu	3.01
IGKV3D-20	immunoglobulin kappa variable 3D-20	2.99
IGKV3D-15	immunoglobulin kappa variable 3D-15 (gene/pseudogene)	2.98
IGLV3-16	immunoglobulin lambda variable 3-16	2.95
KIR2DL4	killer cell Ig-like receptor two domains long cytoplasmic tail 4	2.93
IGLV7-43	immunoglobulin lambda variable 7-43	2.93
IGKV1-33	immunoglobulin kappa variable 1-33	2.87
IGHJ5	immunoglobulin heavy joining 5	2.86

IGLV4-69	immunoglobulin lambda variable 4-69	2.85
CCL7	chemokine (C-C motif) ligand 7	2.84
GZMB	granzyme B	2.80
POU2AF1	POU class 2 associating factor 1	2.76
IGLV6-57	immunoglobulin lambda variable 6-57	2.75
FCRL2	Fc receptor-like 2	2.75
IGHJ6	immunoglobulin heavy joining 6	2.72
IGLV2-11	immunoglobulin lambda variable 2-11	2.71
BHLHA15	basic helix-loop-helix family member a15	2.71
PTHLH	parathyroid hormone-like hormone	2.69
CNGA3	cyclic nucleotide gated channel alpha 3	2.67

Table 5. Top 50 genes downregulated genes in PT^{Pos} compared to PT^{Neg}

Symbol	Description	logFC
LOR	loricrin	-5.35
SERPINB12	serpin peptidase inhibitor clade B (ovalbumin) member	-5.24
PYDC1	PYD (pyrin domain) containing 1	-4.55
CRNN	cornulin	-4.48
FLG2	filaggrin family member 2	-4.45
HRNR	hornerin	-4.29
FLG	filaggrin	-4.23
IL37	interleukin 37	-4.21
DAPL1	death associated protein-like 1	-4.16
AADACL2	arylacetamide deacetylase-like 2	-4.12
LCE1E	late cornified envelope 1E	-3.97
ARG1	arginase 1	-3.94
UGT1A7	UDP glucuronosyltransferase 1 family polypeptide A7	-3.74
LCE1D	late cornified envelope 1D	-3.70
LCE2B	late cornified envelope 2B	-3.68
LCE1B	late cornified envelope 1B	-3.56
SLURP1	secreted LY6/PLAUR domain containing 1	-3.55
CLEC2A	C-type lectin domain family 2 member A	-3.53
CHRNA9	cholinergic receptor nicotinic alpha 9 (neuronal)	-3.46
ELMOD1	ELMO/CED-12 domain containing 1	-3.39
LCE1C	late cornified envelope 1C	-3.39
PSORS1C2	psoriasis susceptibility 1 candidate 2	-3.31
HS3ST6	heparan sulfate (glucosamine) 3-O-sulfotransferase 6	-3.30
LCE2D	late cornified envelope 2D	-3.29
CHP2	calcineurin-like EF-hand protein 2	-3.28
LCE1F	late cornified envelope 1F	-3.27
ANXA9	annexin A9	-3.22
SERPINA12	serpin peptidase inhibitor clade A member 12	-3.22
AQP5	aquaporin 5	-3.20
KRT1	keratin 1 type II	-3.20
LCE2C	late cornified envelope 2C	-3.20
LCE1A	late cornified envelope 1A	-3.18
LCE6A	late cornified envelope 6A	-3.11
STMN2	stathmin 2	-3.10
IL20RA	interleukin 20 receptor alpha	-3.09
CORIN	corin serine peptidase	-3.08
F13A1	coagulation factor XIII A1 polypeptide	-3.08
HAL	histidine ammonia-lyase	-3.05
SLC1A6	solute carrier family 1 (high affinity aspartate/glutamate transporter) member 6	-3.03

KRT2	keratin 2 type II	-3.03
ASPRV1	aspartic peptidase retroviral-like 1	-3.01
ALDH3A1	aldehyde dehydrogenase 3 family member A1	-2.99
KRT10	keratin 10 type I	-2.97
GSTA3	glutathione S-transferase alpha 3	-2.96
APOB	apolipoprotein B	-2.95
LCE2A	late cornified envelope 2A	-2.94
GPX2	glutathione peroxidase 2	-2.94
WFDC12	WAP four-disulfide core domain 12	-2.93
KPRP	keratinocyte proline-rich protein	-2.92
IL36B	interleukin 36 beta	-2.90

Although immunoglobulin gene expression in PT^{Neg} lesions increased slightly relative to uninfected healthy skin (Figure 4C, blue), immunoglobulin gene expression in PT^{Pos} lesions was substantially higher (367 fold $\pm$ 261 compared to 56 fold $\pm$ 32) (Figure 4C, orange). The level of immunoglobulin transcripts in the PT^{Int} group (Figure 4B, yellow) fell between the PT^{Pos} and PT^{Neg} groups (122 fold $\pm$ 75). Thus, high Ig levels in lesions may portend a poor prognosis in this disease, as previously suggested (23).

Immune response signatures of PT^{Pos} and PT^{Neg} patients. An assessment of transcripts encoding cell-specific markers pointed to an increase in B cells and their products in the PT^{Pos} lesions. B cell transcripts encoding CD79A, CD19, and CD20, were upregulated in PT^{Pos} lesions, relative to healthy controls (Figure 5A) and relative to PT^{Neg} lesions (indicated by a # symbol). Transcript levels in the PT^{Int} group fell in between PT^{Pos} and PT^{Neg} (Figure 5A, yellow). Increases in transcripts encoding B cell markers were not observed when comparing lesions from early and late cutaneous leishmaniasis (Figure 6A). T cell markers (CD3e, CD4, and CD8a) demonstrated no significant differences between PT^{Pos}, intermediate and PT^{Neg} lesions (Figure 5A). As expected, no significant differences in T cell markers were detected between early and late cutaneous lesions (Figure 6A). Transcripts for inflammatory molecules (IFN-γ, TNF, IL-1β and FASLG), inhibitory molecules (IL-10, CTLA4, PD1, PDL1, and LAG3), and activation markers (CD80 and CD38) were all higher in PT^{Pos} lesions compared to PT^{Neg} lesions (Figure 4B), with PT^{Int} lesions exhibiting intermediate transcript levels (Figure 5B). In contrast to the differences observed between PT^{Pos} and PT^{Neg} lesions, we saw no significant difference in the levels of transcripts for cytokines in early versus late lesions (Figure 6B).

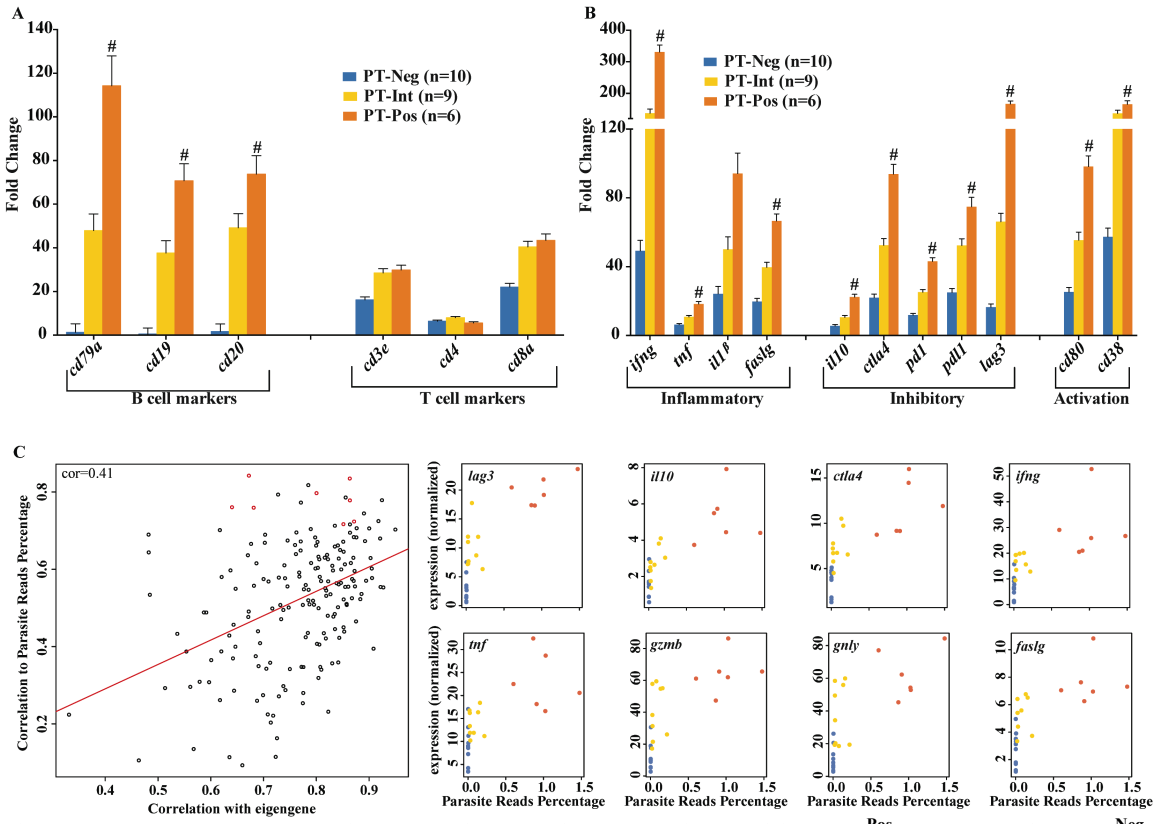

Figure 5. Immune response signatures in parasite transcript positive (PT^{Pos}) and negative (PT^{Neg}) lesions. (A) Bars represent the fold change of RNA expression of cell-specific markers in PT^{Neg} (blue), PT^{Int} (yellow), and PT^{Pos} (orange) samples, each compared to healthy controls (mean plus SEM). Statistically significant differentially expressed genes, when comparing PT^{Pos} to PT^{Neg} are identified with a # symbol ($p<0.05$) **(B)** Transcripts encoding inflammatory cytokines (*ifnγ, tnf, IL12p40, IL-10, faslg*), anti-inflammatory and inhibitory signals (*il10, ctla4, pdcd1, cd274, lag3*), and activation markers (*cd80, cd38*) in lesions of all three classifications compared to healthy controls (mean plus SEM). Statistically significant differentially expressed genes when comparing PT^{Pos} to PT^{Neg} are identified with a # symbol ($p<0.05$). **(C).** The top module (by p-value, see * in Supplemental Figure 3A) and representative genes from within the module correlated to percent parasite reads using WGCNA analysis. The left plot demonstrates correlation to the module eigengene versus correlation to parasite percent reads for each gene. On the right, plots demonstrate normalized expression (rpkm) versus parasite percent reads for selected genes from within the module (highlighted in red in the left plot).

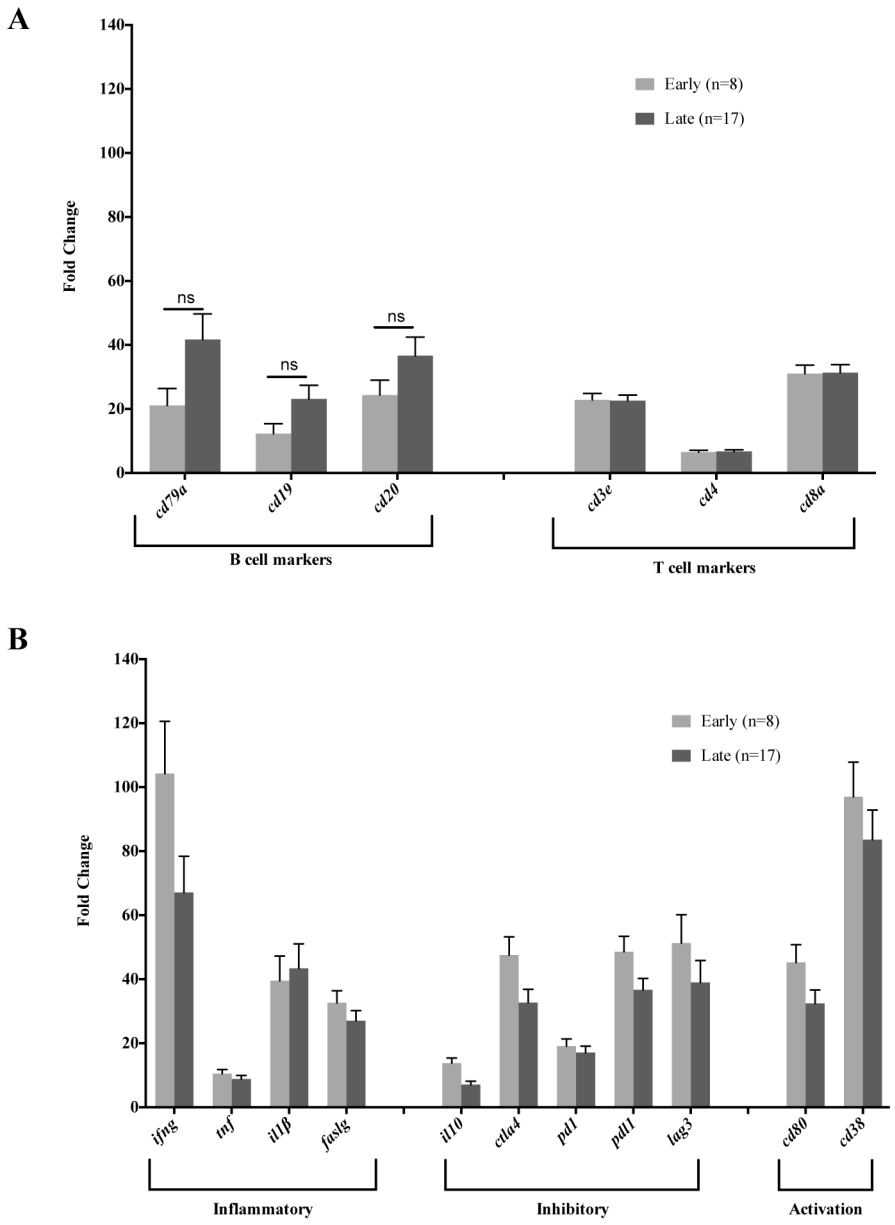

Figure 6. Immune response signatures in early and late cutaneous L. braziliensis lesions. Bars represent the fold change (mean plus SEM) of RNA expression of cell-specific markers in early (light grey) and late (dark grey) cutaneous samples,, each compared to healthy patients, showing **(A)** infiltration of B cell (cd79a, cd19, cd20) and T cell (cd3e, cd4, cd8a) biomarkers, and **(B)** increased inflammatory (ifnγ, tnf, IL12p40, IL-10, faslg), anti-inflammatory and inhibitory signals (il10, ctla4, pdcd1, cd274, lag3), and activation markers (cd80, cd38) in lesions with no difference observed between early and late (NS = not significant).

The weighted gene co-expression network analysis program (WGCNA) was used to cluster human host gene expression through comparison of gene expression profiles using pairwise correlations. Cluster profiles were then assessed as a function of parasite transcript abundance. This analysis yielded three modules of genes (among a total of 51 modules in the network) whose expression exhibited a significant correlation with parasite transcript abundance (Figure 5B, Figure 7). The most highly correlated module (see * in Figure 7A) contained 100 genes (Figure 7C, left). Eight of the top 14 genes and their normalized expression versus parasite transcript number are shown in Figure 7C, right. These host genes included IL-10, IFN-γ, TNF, granzyme B and fas ligand. All of the genes in this module exhibited a higher expression in PT^{pos} lesions (Figure 5C, orange dots). The two additional modules that also showed a significant correlation between host gene expression and parasite transcript numbers contained immunoglobulin transcripts, chemokine genes, cytokines and growth factors (Figure 7B).

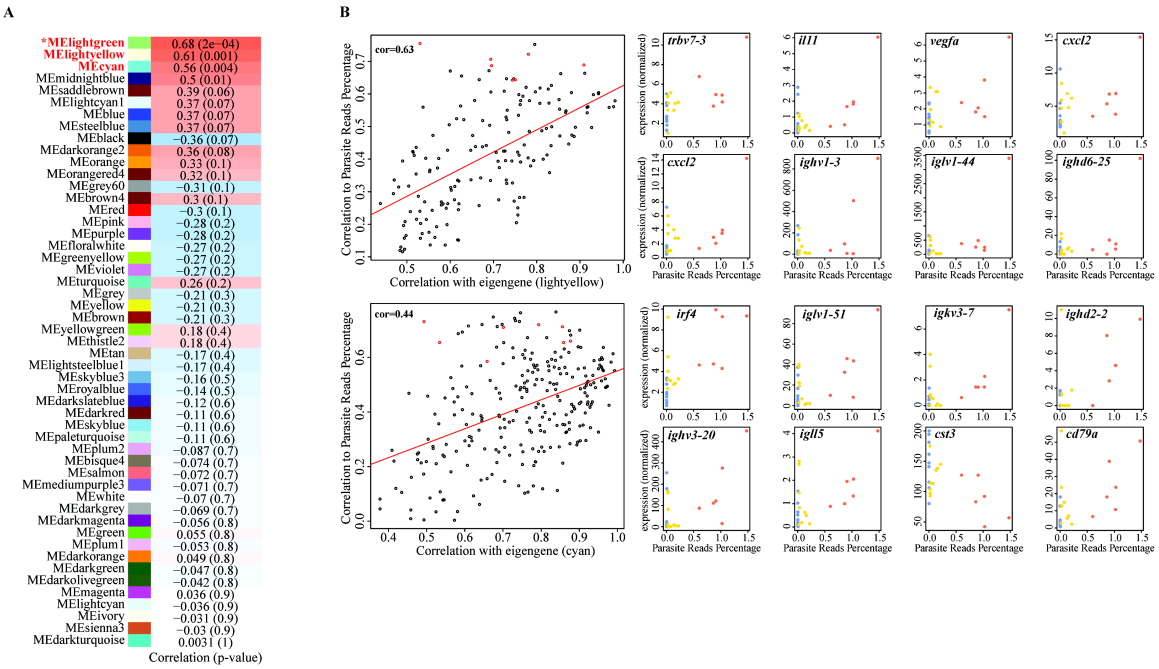

Figure 7. Weighted gene co-expression network analysis as a function of parasite transcript reads. **(A)** Heatmap comparing the module eigengene relationship to the trait of percent parasite reads. Heatmap color indicates correlations of -1 (blue) to +1 (red) and p-values are shown in parentheses. Modules are sorted top to bottom by significance and a different color block represents each module. The three most significant modules are indicated in red type with the most significant module, indicated by a *, which is explored further in Figure 5C. **(B)** The second (light yellow, top) and third (cyan, bottom) module (by p-value) and representative genes from within the module correlated to percent parasite reads using WGCNA analysis. The left plots demonstrate module membership versus correlation to parasite percent reads for each gene. On the right, plots demonstrate normalized expression (rpkm) versus parasite percent reads for selected genes from within the modules (highlighted in red in the left plots).

Functional interactions and distinct clustering among differentially expressed genes. The Reactome FI plugin for Cytoscape was used to observe known interactions between the 719 genes that were differentially expressed between PT^{Neg} and PT^{Pos}. An additional 149 linker genes, known to influence or connect multiple genes in the gene set, were included in this analysis. A network of 558 genes generated numerous clusters showing a dense interaction of genes differentially expressed between PT^{Neg} and PT^{Pos}. When clustering genes by functional interactions from the Reactome database, the top three clusters highlight specific immune and cellular pathways (Figure 8). The largest cluster (Figure 8, blue nodes) consists of 137 genes associated with immune cell activation, costimulation, and cytokine and chemokine signaling, including TNF, IL-10, and multiple C-C motif chemokines (Figure 9A). Gene regulation in this category is associated with NF-κβ, CREB/STAT3, JUN, and SP1 signaling. The second largest cluster (Figure 8, red nodes) includes 103 genes involved in B and T cell activation and inhibition, regulated by SYK, SRC, FYN, PLCG1 and 2, and PTPN11 (Figure 9B). Cluster 3 (Figure 8, yellow nodes) includes 72 genes associated with cell growth and proliferation signals (Figure 9C). The transcriptomic differences between PT^{Pos} and PT^{Neg} patients demonstrate the potential of these clusters to lead to the identification of new drug targets for treating cutaneous leishmaniasis.

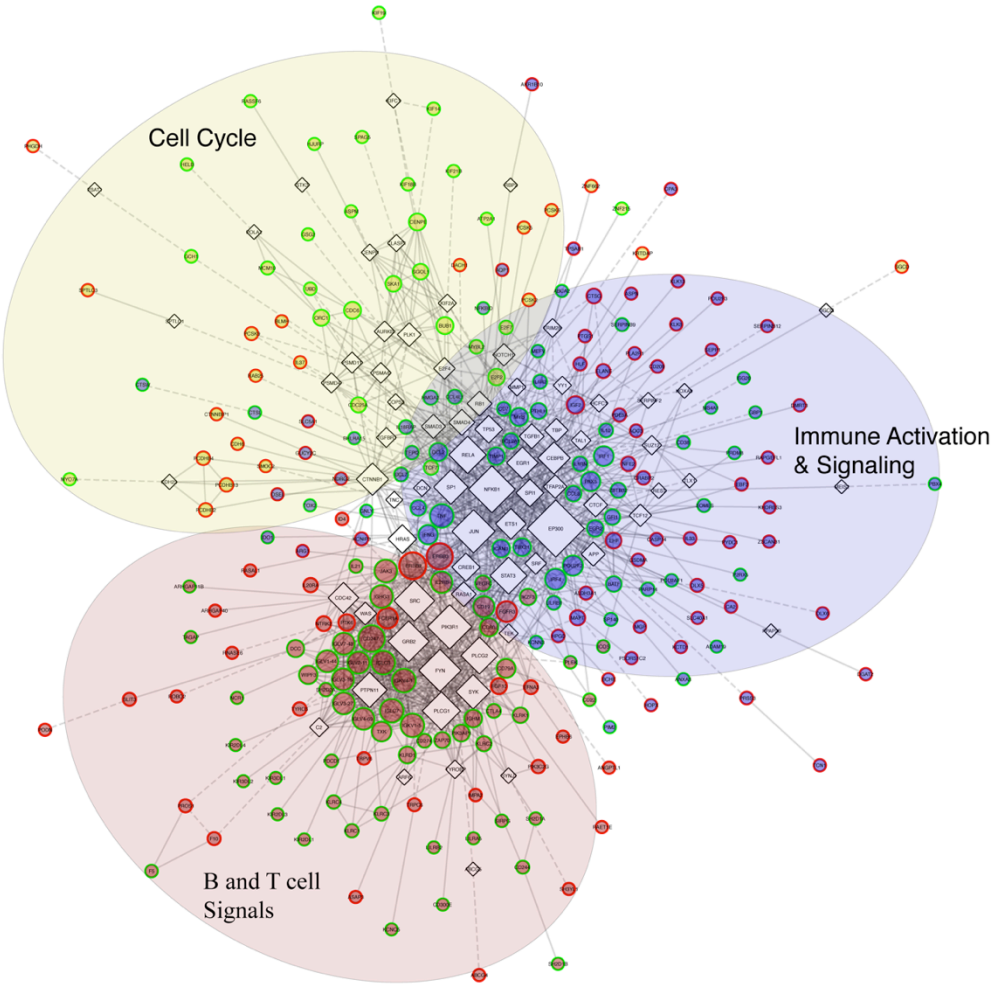

Figure 8. Functional interactions among differentially expressed genes. A group of 237 of the 719 differentially expressed genes between PT^{Neg} and PT^{Pos} (circular nodes) along with 75 associated linker genes (diamond nodes, black border) show numerous functional interactions (edges). Node size is relative to the number of interactions. The three largest gene clusters are depicted by color (blue, red, and yellow), and direction of differential expression of genes within the clusters is depicted by node border, with green borders designating upregulated and red borders designating downregulated genes.

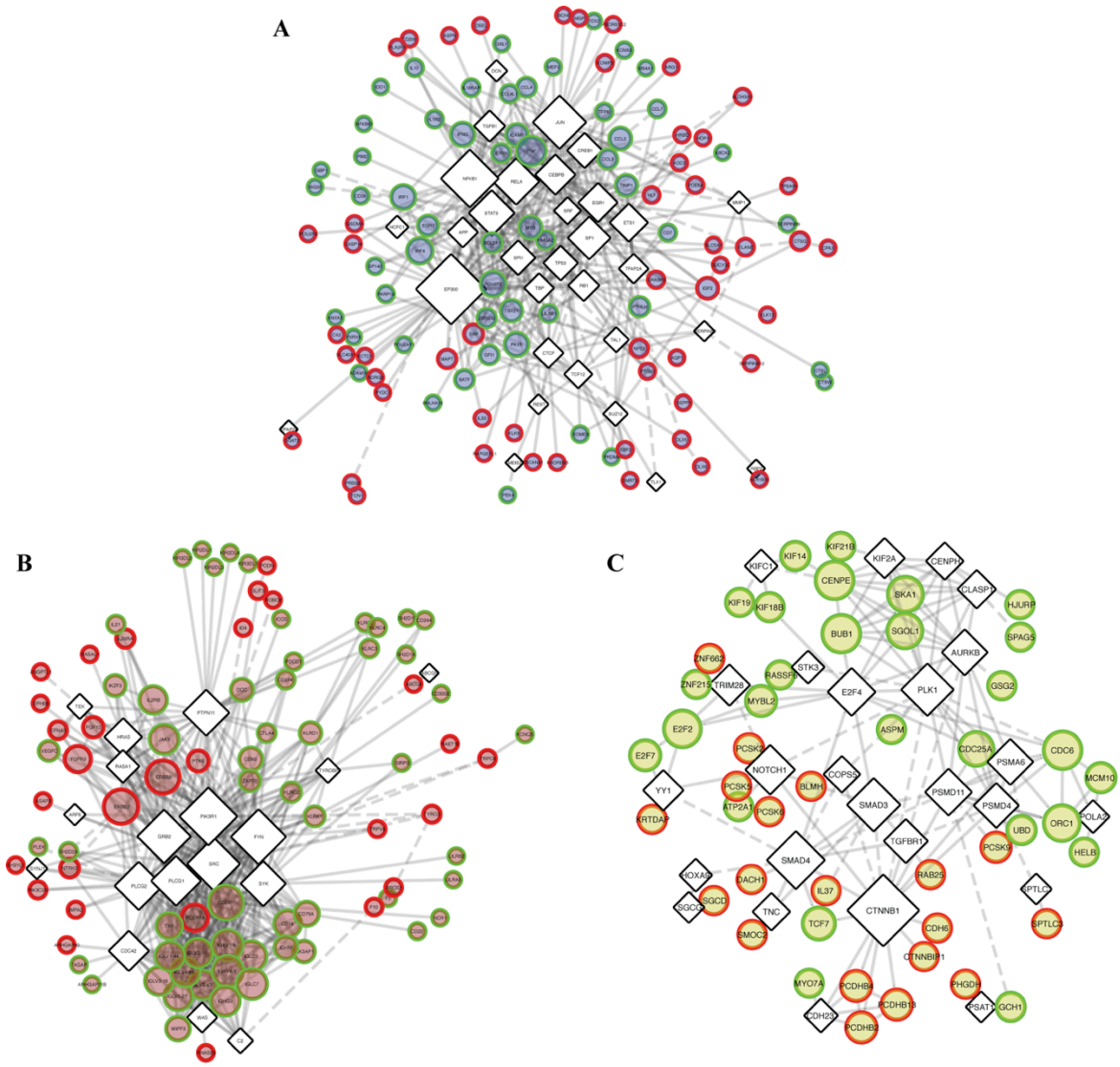

Figure 9. Three largest functional interaction groups in PT-pos DE genes. The largest three clusters consisting of 137 (A), 103 (B), and 72 (C) genes show numerous functional interactions (edges). Gene clusters are depicted by color and direction of differential expression is depicted by node border, with green borders designating upregulated and red borders designating downregulated genes. Node size indicates the number of interactions. **(A)** Network of genes associated with immune cell activation, costimulation, and cytokine and chemokine signaling, including TNF, IL-10, and multiple C-C motif chemokines regulated by NFκβ, CREB/STAT3, JUN, and SP1 signaling. **(B)** Network of 103 genes involved in B and T cell activation and inhibition, regulated by SYK, SRC, FYN, PLCG1 and 2, and PTPN11. **(C)** Interaction of 72 genes associated with cell growth and proliferation signals.

Identification of *L. braziliensis* transcripts in lesions. We analyzed parasite gene expression in the six PT^{Pos} patient samples and despite substantial differences in lesion size and duration (three early and three late cutaneous PT^{Pos} lesions), there was uniformity in *L. braziliensis* transcript expression in all six patient lesions. Pearson correlation analysis of the top 50 parasite genes in each sample quantitatively demonstrated the similarity between samples, and ranged from 0.83 to 0.92 (Figure 10A). The 40 most highly-expressed parasite transcripts by average RPKM, listed in Table 6, were fairly randomly dispersed across the different parasite chromosomes (Figure 11). Six of these chromosomes are illustrated in Figure 10B and the parasite gene expression (in RPKM) is shown by vertical lines in the 6 patients (each patient designated by a different color intensity). Again, there is remarkable uniformity in parasite gene expression from patient to patient. Within these six chromosomes, 12 of the top 20 parasite genes (by RPKM) are noted, including cysteine peptidases, cysteine synthase, a proteasome subunit, and various hydrolase-like and hypothetical proteins.

All 20 of the most highly expressed parasite genes were expressed in all six patients, regardless of whether the lesions were early or late (Figure 11). The top parasite transcripts (Table 6) consisted of a cysteine peptidase, a phosphodiesterase, as well as kinases and transport proteins. The presence of hypothetical proteins in this list illustrates our lack of understanding of parasite gene expression during natural infections. Several amastin family genes and known virulence factors, including GP63, heat-shock proteins 70 and 83, and cysteine peptidases, appear in the top 100 observed transcripts.

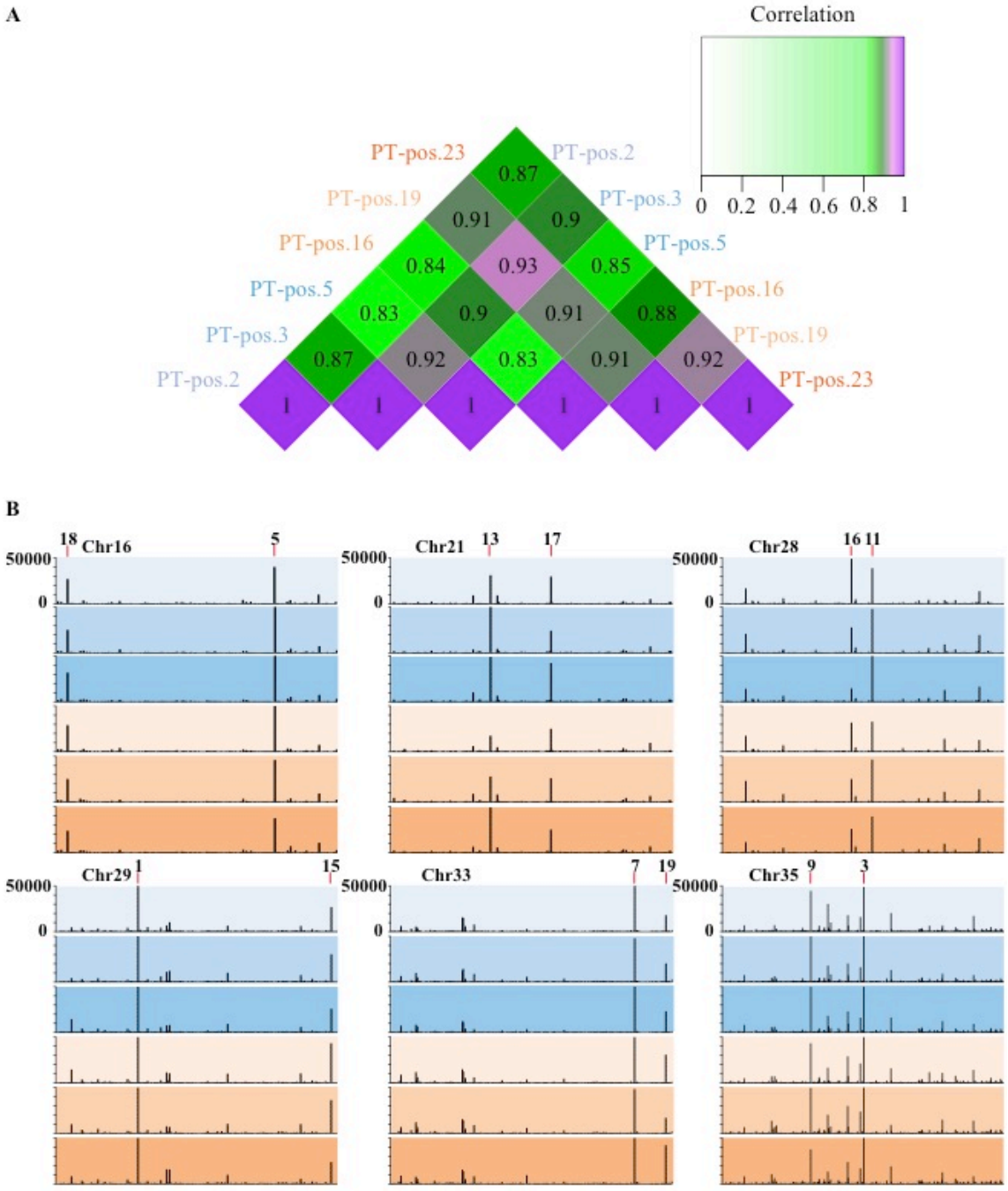

Figure 10. *L. braziliensis* gene expression in human lesions. RPKM values of all samples were scaled to the sample with the highest total normalized reads. **(A)** Pearson correlation of parasite gene expression of the top 50 parasite genes in the six PT^{Pos} samples. **(B)** Representation of six parasite chromosomes (16, 21, 28, 29, 33, 35) showing the RPKM levels for each PT^{Pos} patient, early patients depicted in pink hues, late patients in purple hues. RPKM is depicted on the y axis (0 to 50,000), and genes that appear in the 20 most-highly expressed parasite genes are labeled.

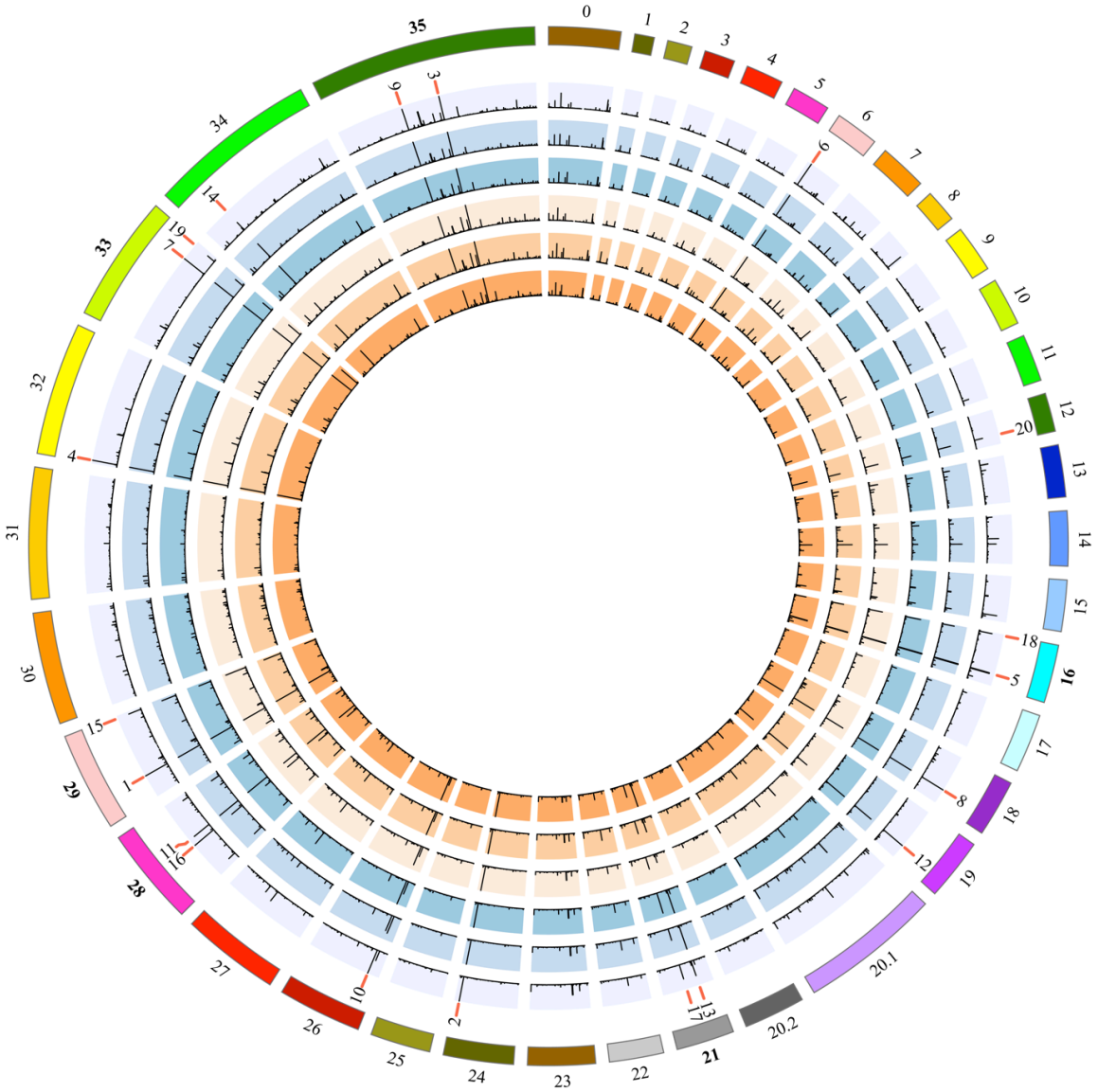

Figure 11. Circos plot of *L. braziliensis* genome. Representation of the *L. braziliensis* genome with the outermost ring (labeled 1–35) showing each individual chromosome. The subsequent concentric circles represent each of the six Vertical lines designate the relative expression levels of *L. braziliensis* gene expression in RPKM with the top 20 most highly-expressed genes marked by a red line, and numbered from 1–20. Chromosomes labeled in bold are viewed closer in Figure 10.

Table 6. Top 40 *L. braziliensis* genes expressed in detectable-positive lesions

ID	Description	*L. braziliensis* RPKM
LbrM.08.1060	amastin-like protein	38297
LbrM.08.0300	amastin-like surface protein, putative	12211
LbrM.08.1130	amastin-like surface protein, putative	11338
LbrM.18.0460	amastin-like surface protein	7271
LbrM.08.0310	amastin-like surface protein, putative	7125
LbrM.08.0290	amastin-like surface protein, putative	6529
LbrM.09.1400	histone H2B	6390
LbrM.08.1100	amastin-like protein	6164
LbrM.20.4300	amastin-like surface protein, putative	5869
LbrM.20.1090	kinesin, putative (pseudogene)	5014
LbrM.08.1030	amastin-like protein	3868
LbrM.18.1510	histone H1	3827
LbrM.20.0790	amastin-like surface protein, putative	3779
LbrM.20.3230	hypothetical protein, conserved	3753
LbrM.08.0670	amastin-like protein	3727
LbrM.28.2990	heat-shock protein hsp70, putative	3676
LbrM.21.2150	beta tubulin	3620
LbrM.18.0470	amastin-like surface protein	3567
LbrM.21.1140	histone H2A	3342
LbrM.20.1080	amastin-like surface protein, putative	3321
LbrM.21.1160	histone H2A, putative	3192
LbrM.27.1290	histone H1, putative	3145
LbrM.28.2980	heat-shock protein hsp70, putative (fragment)	3136
LbrM.10.0970	histone H3	2784
LbrM.20.4290	amastin-like surface protein, putative	2739
LbrM.20.4320	amastin-like surface protein, putative	2722
LbrM.30.0980	surface protein amastin, putative	2703
LbrM.28.2970	heat-shock protein hsp70, putative	2693
LbrM.13.0200	alpha tubulin	2645
LbrM.20.2410	amastin-like surface protein, putative	2634
LbrM.35.3090	40S ribosomal protein S24e	2616
LbrM.08.1120	amastin-like surface protein, putative	2528
LbrM.34.0280	60S ribosomal protein L30	2522
LbrM.20.1060	amastin-like surface protein, putative	2507
LbrM.02.0020	histone H4	2464
LbrM.16.1210	60S ribosomal protein L39, putative	2434
LbrM.13.0190	alpha tubulin	2415
LbrM.20.1070	amastin-like surface protein, putative	2414
LbrM.21.1150	histone H2A, putative	2236
LbrM.13.0270	ALBA-domain protein 1	2225

Recent work by our lab demonstrated the benefits of dual-transcriptomic analyses, using *in vitro* infection of macrophages with *L. major* and *L. amazonensis* to observe expression pattern changes in the host cell and parasite gene expression, ranging from 4 to 72 hours (171). To determine whether the *L. braziliensis* transcripts identified in lesions were the most highly expressed parasite genes expressed *in vitro*, we compared the top 10% of *L. braziliensis* transcripts identified in lesions (ranked by RPKM) to single reciprocal orthologous genes expressed by *L. amazonensis* or *L. major* 72 hours after an *in vitro* infection of human macrophages, as previously described by our lab (Figure 12). A direct comparison to *L. braziliensis* genes expressed *in vitro* was not possible because RNA-seq analysis of *L. braziliensis* transcripts following *in vitro* infection of human macrophages has not been performed.

A comparison of single reciprocal orthologs showed that of the most highly expressed (top 10%) *L. braziliensis* genes *in vivo* (Figure 12A, blue), roughly 35% (155) did not match the most highly expressed parasite genes in cultivated macrophages following *in vitro* infection with *L. amazonensis* (Figure 12A, red) or *L. major* (Figure 12A, green). In contrast, 35% (155) of the top genes expressed by *L. braziliensis* during *in vivo* infections matched the top *L. major* and *L. amazonensis* genes expressed *in vitro*. The remaining 30% of top genes expressed by *L. braziliensis* during *in vivo* infections were shared relatively evenly between either *L. major* (64) or *L. amazonensis* (57). Among all single reciprocal orthologs (6707), pearson correlation between samples ranged from 0.61 to 0.98 and samples hierarchically clustered into their respective groups (Figure 12B).

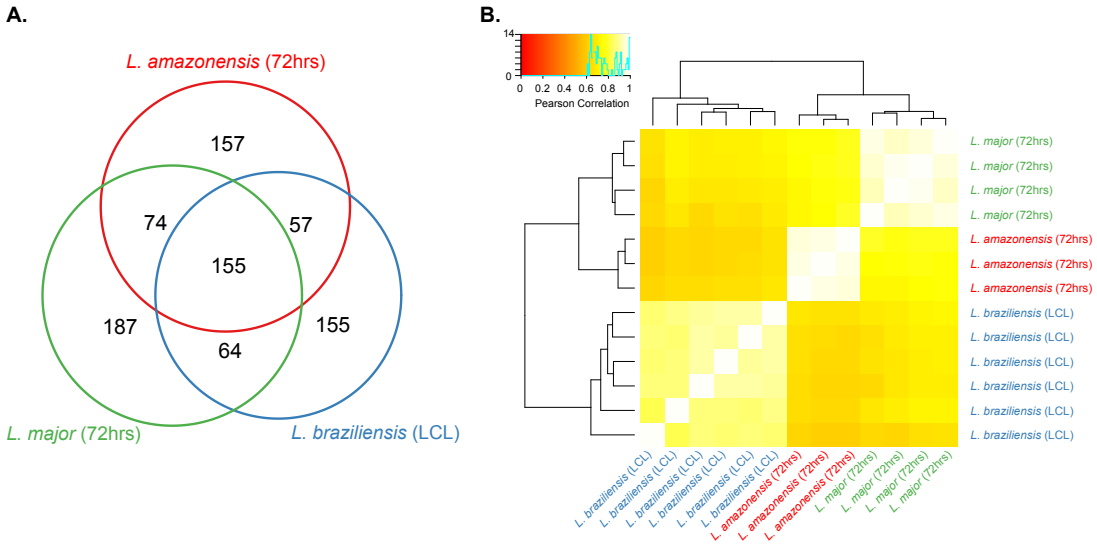

Figure 12. Parasite ortholog comparisons reveal similarities and differences (A) A Venn diagram compares the single reciprocal orthologs expressed in the top 10% (by average RPKM) of *L. braziliensis* in patients (blue circle), *L. major* in macrophages (green circle), and *L. amazonensis* in macrophages (red circle). **(B)** Pearson correlations between samples of *L. braziliensis* in patients (blue), *L. major* in macrophages (green), and *L. amazonensis* in macrophages (red) ranges from 0.62 to 0.98. Hierarchical clustering is demonstrated by dendrograms.

DISCUSSION

By applying RNA-seq technology to skin biopsy material, we were able to capture in detail the transcriptomes of both the parasite and the human host during *L. braziliensis* localized cutaneous infection. This analysis allowed us to examine host responses as a function of parasite persistence. *L. braziliensis* infections have often been described as having low parasite numbers in lesions (172). This is consistent with our observation that lesions from 10 of the 25 patients had no detectable parasite transcripts in them at the time of biopsy. This lack of detectable transcripts is consistent with an active elimination of parasites by the host. In contrast, six of the 25 patients had ample evidence of high confidence parasite transcripts in lesions (averaging nearly 1M parasite reads/sample). The presence of these transcripts indicates that viable parasites were persisting in lesions, and continuing to produce transcripts that could contribute to their survival. Therefore, we compared host immune responses in lesions where parasites were producing detectable transcripts (PT^{Pos}) to those where parasite transcripts were undetectable (PT^{Neg}).

The progression of *L. braziliensis* disease has been well-studied, and the small nodules of early tegumentary leishmaniasis typically progress to the larger sometimes necrotic lesions associated with late cutaneous leishmaniasis (173). Studies have examined the differences in immune responses between these two groups (174), and comparisons with regard to treatment efficacy between early and late disease have also been made (108, 172). A surprising result from the previous transcriptomic comparison between early and late *L. braziliensis* lesions was that the host immune response was initiated early during infection and persisted throughout the course of the disease (48).

Our RNA-seq confirms this previous observation. We could not separate the host response during early and late tegumentary leishmaniasis by Principal Component Analysis (Figure 2). However, when these responses were stratified by the presence or absence of parasite transcripts, a clear separation could be achieved between the host responses in lesions where parasite transcripts were detectable (PT^{pos}) versus those where they were not detectable (PT^{neg}). We chose to contrast those two groups with an eye to understanding host responses that may be associated with parasite persistence or parasite elimination.

One of the surprising observations from this work was the degree to which B cell transcripts were associated with lesions containing detectable levels of parasite transcripts. Of the top 100 genes that were differentially upregulated in PT^{Pos} lesions relative to healthy controls, 80 encoded immunoglobulin-related transcripts. Lesions in which parasite transcripts were not detectable (PT^{Neg}) also showed some evidence of B cell activation, but not to the same extent. The quantity of immunoglobulin transcripts in PT^{Pos} lesions was higher than PT^{Neg} lesions (Figure 3C), as were the number of B cells as judged by transcripts encoding CD79A, CD19, and CD20 (Figure 4A). We previously reported that in human visceral leishmaniasis, high levels of IgG were associated with ongoing disease, and that IgG levels decreased as cell mediated immunity developed following treatment (60). Furthermore, addition of parasite-specific IgG to *L. major*-infected J_H mice exacerbated disease, increasing lesion size and inducing IL-10 production (60). These previously published observations, along with the present association of high immunoglobulin transcripts in PT^{Pos} lesions, suggest that B cells and host IgG may be strong contributors to parasite persistence.

We and others previously demonstrated that IL-10 could contribute to parasite survival, and a correlation between IgG levels and IL-10 production was identified in visceral leishmaniasis (60, 175). The present studies extend this correlation to American tegumentary leishmaniasis, and demonstrate that PT^{pos} lesions had higher levels of IL-10 than PT^{Neg} lesions (Figure 4B). The association between parasite survival and cytokine production may be more complex than originally perceived, however, since PT^{Pos} lesions also expressed higher levels of IFN-γ and TNF, two cytokines that have well-established roles in classical macrophage activation and parasite elimination.

We also observed a correlation between the prevalence of parasite transcripts in the lesion and the expression of a subset of host immune response genes. Using the weighted gene co-expression network analysis program (WGCNA), we identified several key host response genes whose expression increased in lesions containing high levels of parasite transcripts (Figure 4C). IL-10 has been previously associated with disease progression, so perhaps its inclusion in this category may not have been unexpected. However, the association of TNF, granzyme B, and IFN-γ with parasite persistence was not expected. These observations may indicate that immunopathology is a driving factor in *L. braziliensis* infections. The second and third most significant modules (Figure 8B) correlate with several genes involved in B cell responses, immunoglobulin production and T cell interactions with parasite transcriptional activity. These observations are consistent with the hypothesis that B cells and IgG production may contribute to parasite survival.

In addition to an in depth look at the host response, RNA-seq also provides a picture of the parasite transcriptome during infection. Viewing parasite gene expression

within the lesion provided some interesting surprises. First and foremost, the uniformity of parasite gene expression across all six patients was not expected, given the differences in lesion size, duration, and degree of necrosis among the six patients analyzed. It is possible that the most highly expressed parasite genes in lesions have the potential to contribute to parasite persistence. The identification of these gene products may lead to new candidates for vaccine development or new targets for diagnosis. In addition to the presence of known virulence factors expressed at a high level, 4 of the 100 most highly expressed parasite genes encode "hypothetical proteins" of unknown function. The identification and characterization of these proteins may shed new light on how this parasite establishes infection, persists within mammalian cells, or escapes these cells to spread disease. We tested whether the parasite transcripts detected *in vivo* were a reflection of the most abundant transcripts expressed by amastigotes growing in human macrophages *in vitro*. Whole transcriptome gene expression by average RPKM was relatively highly correlated between species and conditions (Figure 12B). However, the top 10% of transcripts detected in lesions were different from the top 10% transcripts expressed *in vitro*, exhibiting just a 35% overlap between *L. braziliensis* gene expression in lesions and *L. major* and *L. amazonensis* gene expression in cultivated macrophages (Figure 12A). Although the parasite species and time post-infection may confound these findings, we believe that a contrast of the *Leishmania* genes expressed *in vivo* versus *in vitro* provides a useful baseline for future comparisons. This suggests that the transcripts identified in *L. braziliensis* lesions were not simply the most highly expressed leishmanial genes, but rather might be transcripts specific to parasite survival under immune pressure in the lesion microenvironment.

Chapter 4: Meta-transcriptome profiling of the anergic diffuse cutaneous human-*Leishmania amazonensis* lesion

ABSTRACT

Diffuse cutaneous leishmaniasis (DCL) is a rare form of cutaneous leishmaniasis where parasites grow uncontrolled in diffuse lesions across the skin. We used high throughput RNA-seq to simultaneously analyze human and parasite gene expression in *Leishmania amazonensis*-infected patients with diffuse cutaneous leishmaniasis. Transcripts in biopsies from six patients with DCL were sequenced, and results were compared to previously analyzed biopsies taken from localized cutaneous leishmaniasis (LCL). Meta-transcriptomic analysis demonstrated an increased infiltration of atypical B cells producing high levels of immunoglobulin transcripts including a preponderance of the IgG4 isotype, and variable region gene patterns consistent with an oligoclonal antibody response. DCL lesions contained a reduced number of CD8+ T cells and a marked reduction in transcripts encoding perforin, granzyme, and granulysin. The commonly used designation of 'anergic DCL' that is sometimes associated with this disease was not manifested in reduced CD4 T cell numbers nor in an upregulation of markers of T cell anergy. The number of pan-macrophage transcripts in DCL was similar to those observed in the more common localized cutaneous leishmaniasis (LCL), but alterations in macrophage activation state markers were observed in DCL. Whereas classically activated macrophages dominated localized disease, exhibiting high levels of M1 transcripts for IDO1, iNOS, CXCL9, CXCL10, CXCL11, IL6, TNFα, macrophages in DCL exhibited a regulatory phenotype with reduced levels of the M1-associated transcripts and higher levels of ABCB5, DC-STAMP, SPP1, and MMP19. Neither

localized or diffuse disease exhibited signs of Th2 responses or alternative macrophage activation. The high levels of parasite transcripts in DCL afforded a unique opportunity to study parasite gene expression in diffuse disease. Parasite transcription displayed remarkable uniformity among the six patients despite differences in infection duration and patient age. We identified the transcripts most highly expressed in DCL and utilized published datasets to uncover subsets of highly expressed genes common to multiple *Leishmania* species. Over half of these genes were hypothetical proteins, emphasizing the need for further research to annotate the parasite genomes. In summary, RNA-seq allowed us to fully examine host and parasite responses in diffuse cutaneous leishmaniasis lesions and determine factors that define the variation in disease manifestation of leishmaniasis.

INTRODUCTION

As previously discussed, parasitic *Leishmania spp* cause the spectral disease leishmaniasis, ranging from self-healing cutaneous lesions to a visceral and highly fatal form of disease (72, 74). Manifestations of cutaneous leishmaniasis depend highly on parasite species and host immune responses. Tegumentary leishmaniasis caused by *Leishmania braziliensis* infections typically result in a single dermal lesion, with small numbers of parasites and a strong host delayed-type hypersensitivity (DTH) response (90, 103). Roughly 3-5% of these infections can progress to a disfiguring mucocutaneous disease (161). The *L. amazonensis* species can also cause cutaneous disease, but in contrast to *L. braziliensis*, can manifest as diffuse cutaneous leishmaniasis (DCL). In this rare form of the disease, parasites grow uncontrolled in non-ulcerative lesions diffuse across the skin. Patients with DCL lack a DTH response (121) and are generally

refractory to chemotherapy (176). While the morphology and pathology of diffuse cutaneous lesions has been studied, the underlying causes are not as well understood.

Leishmaniasis can be considered a macrophage-mediated disease because macrophages act as the primary host cells in which the parasites reside and replicate. During infection, murine macrophages undergo transcriptional and morphological changes that allow for parasite survival, including inhibited iNOS, TNF-α, and IL-12 in concert with increases in IL-10, Arginase I, PGE2, and TGF-β expression (135). Research in mice demonstrates a clear role for Th1 responses, and implicates IFN-γ, TNF-α, and iNOS in parasite clearance. Conversely, Th2 responses (IL-4, IL-13) are associated with parasite persistence and disease exacerbation in the mouse (177, 178). A similar dichotomy has not been observed in humans. Whereas inflammatory Th1 markers have been associated with a restriction of parasite replication (72), the search for Th2 and specifically downstream alternative macrophage activation markers has been less successful (71). Our previous research (179) and that of our colleagues (48) observed a significant Th1 response in localized American tegumentary leishmaniasis. In this work, we aim to expand this knowledge and assess host and parasite responses in the diffuse form of the disease.

Diffuse cutaneous leishmaniasis was first catalogued in the mid-20th century characterized as lesions disseminated over the body, high parasite burden, negative skin tests, and unresponsiveness to antimony therapies (180). The causative parasite in Brazil is *L. amazonensis* (121, 181) and lesion infiltrates have previously been identified as mostly macrophage, with limited and rare lymphocyte or plasma cell presence (182–185). The ratio of IL-4 to IFNγ in previous studies was reported to be high, suggesting a Th2

dominant response in lesions (121). High levels of serum IgG specific to *Leishmania* have also been observed (122, 123), but whether they were simply a result of high parasite burden or actively contributed to disease pathology could not be determined. DCL has been termed "anergic" DCL, primarily due to the lack of DTH^+ responses in DCL patients (186).

In the previous chapter, data from human LCL lesions highlighted specific cell populations and activation states within lesions. (179). We hypothesize that the host immune response in localized lesions resides at the opposite end of the leishmaniasis disease spectrum (74), highlighting the need for in-depth analyses of diffuse cutaneous lesions. Incorporating previous analyses, we sequenced and analyzed the host and parasite transcriptomes in *L. amazonensis*-infected DCL patients and report dramatic similarities and differences between these diverging manifestations.

RESULTS

The human host transcriptome in *L. amazonensis*-infected DCL patients. RNA-seq was performed on biopsies from six DCL patients infected with *Leishmania amazonensis*. The age of the five male and 1 female patients ranged from 15 to 50, and the duration of illness ranged from 14 to 35 years (Table 2). Host responses to the infection were similar among all 6 patients and markedly different from LCL infections (Figure 13A, D, E), with Pearson Correlations generally being 0.70 or higher between all but one of the DCL patients (Patient #5, Figure 13B) despite substantial differences in age (Figure 13C) and illness duration (Figure 13D).

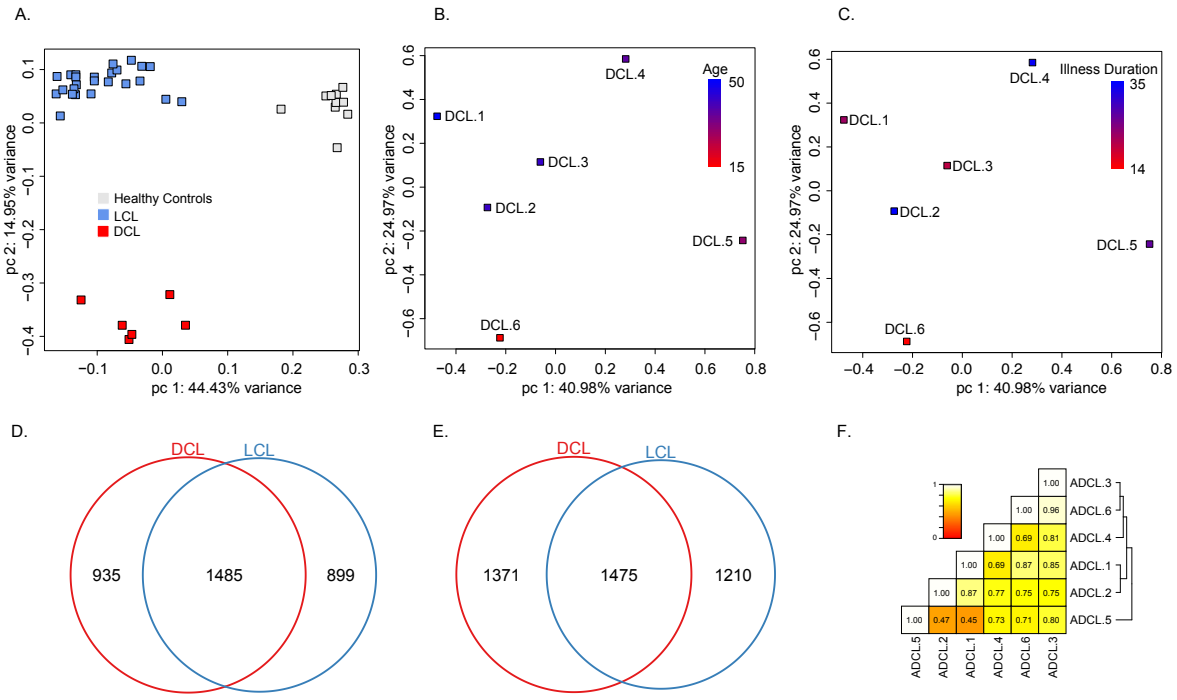

Figure 13. The human host transcriptome in *L. amazonensis*-infected DCL patients (A) A principle component analysis plot demonstrates whole-transcriptome differences between healthy (grey), LCL (blue), and DCL (red). **(B)** PCA analysis shows the age of the DCL patients on a color scale (red to blue). Principal component 1 represents 40.98% of the variance and principle component 2 represents 24.97%. **(C)** PCA analysis shows the illness duration of the DCL patients on a color scale (red to blue). Principal component 1 represents 40.98% of the variance and principle component 2 represents 24.97%. **(D-E)** Venn diagrams show up (E) and downregulated (F) genes in DCL (red) and LCL (blue) circles compared to healthy skin. **(F)** Pearson correlation between DCL patients demonstrates uniformity in host responses.

Differential expression comparisons with healthy patients (fold change > 2, p-value < 0.05) revealed 2420 host genes upregulated (Figure 13E) and 2846 genes downregulated (Figure 13F) (fold change > 2, p-value < 0.05) as compared to healthy skin. Previously sequenced LCL patients showed an upregulation of 2384 genes and a downregulation of 2685 genes (Figure 13E-F). DCL and LCL differential expression shared 1485 upregulated and 1475 downregulated genes.

An examination of host transcripts in the lesion pointed to two unusual aspects of the host immune response to this intracellular parasite. The first was the high level of transcripts encoding immunoglobulin fragments and the second was the paucity of transcripts that would likely be expressed by cytotoxic T cells. Compared to healthy skin, the top 10 most highly upregulated host transcripts in all six patient biopsies encoded immunoglobulin fragments (Figure 14A). In fact 90 of the top 100 most highly upregulated transcripts in lesions were immunoglobulin transcripts, and four of the other top 100 transcripts were related to B cells. This enrichment of Ig transcripts was common to all six patients, and there was a high degree of consensus among the individual Ig RPKMs (Figure 14A, triangles). Due to the mass upregulation of immunoglobulin transcripts, we subsequently analyzed immunoglobulin isotype gene usage and noted significant differences in Ig levels in DCL patient lesions relative to healthy controls and LCL lesions (Figure 14B). DCL patients expressed high levels of IgG1, IgG2, IgG3 and IgG4 with IgG4 unexpectedly accounting for an average of 40% of the immunoglobulin repertoire (Figure 14B). LCL patients exhibited lower levels of all immunoglobulin isotypes, and as expected IgG1 was the most highly expressed isotype transcript (Figure 14B).

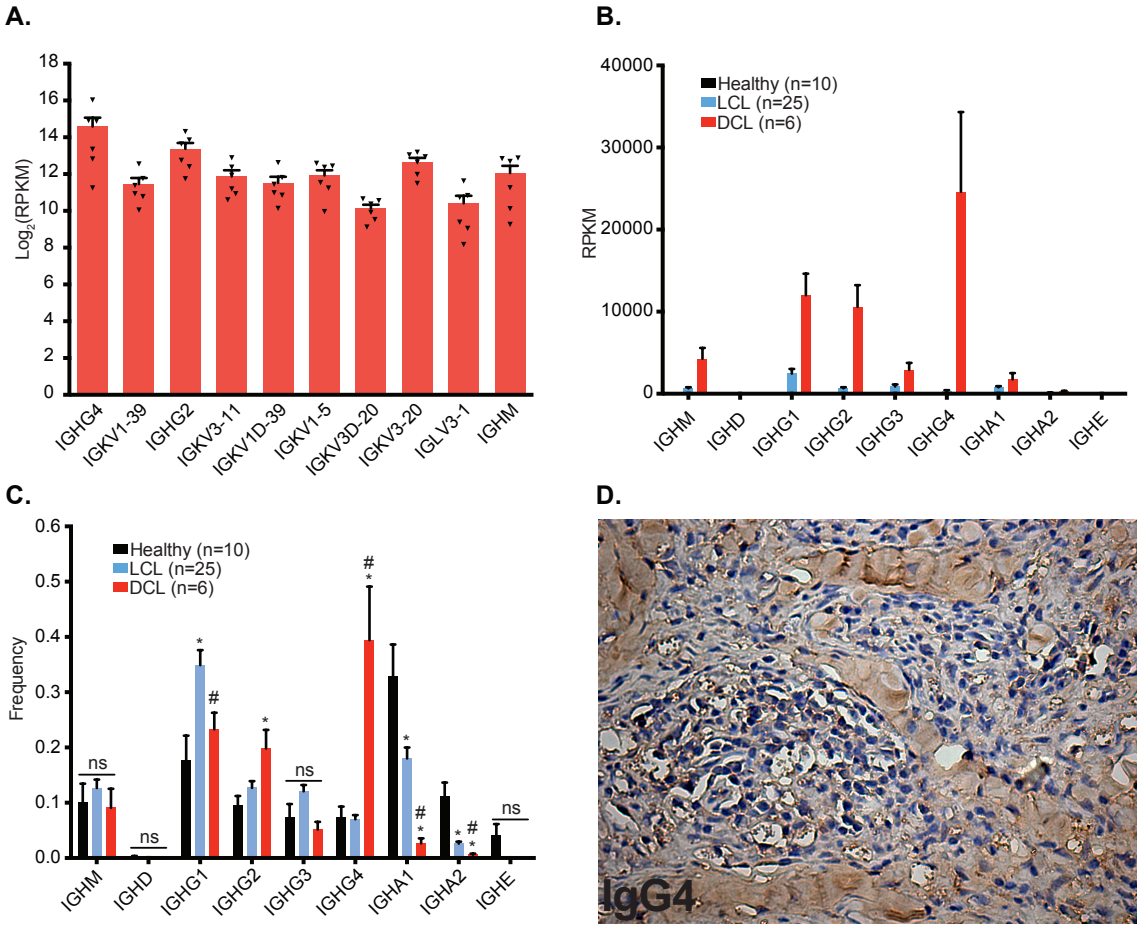

Figure 14. IgG4 transcripts are significantly upregulated in DCL lesions (A) Bars show the mean RPKM for the top ten upregulated genes (mean plus SEM), with each individual sample represented by a black triangle. **(B)** Bars represent the expression (RPKM mean plus SEM) for each immunoglobulin isotype in healthy skin (black), LCL lesions (blue), and DCL lesions (red). **(C)** Immunoglobulin isotype frequency analysis of healthy skin (black bars), LCL (blue bars) and DCL (red bars) is shown as mean plus SEM. Significant differences compared to healthy skin are marked with a * while significant differences between LCL and DCL are marked with a # ($p < 0.05$). **(D)** Staining of IgG4 in DCL lesions.

IgG4 levels in LCL were not different from uninfected controls. Analysis of isotype frequency emphasized the dominance of IgG4 in DCL lesions (Figure 14C). Subsequent staining of DCL lesions with IgG4 antibody revealed high levels of this isotype (Figure 14D).

In addition to upregulated immunoglobulin transcripts, a marked increase in B cell-related transcripts was observed in DCL lesions compared to both healthy skin and LCL lesions. The upregulation of B cell-related markers, including MZB1, CD79A, TNFRSF17, CD22, CD27, CD19, CD79b, BAFF, and APRIL, were observed in lesions from DCL patients (Figure 15A). Histology from diffuse lesions confirm these findings, with B cells expressing CD19 (Figure 15B) in DCL.

Using MiXCR and the bioconductor package bcRep, we observed an enrichment of specific V-J combinations and V gene usage demonstrative of an oligoclonal response in DCL patient lesions. A chord diagram of average heavy chain V-J combination frequency in DCL patients demonstrated a specific immunoglobulin gene selection response limited to 25% of IGHV genes used at a frequency greater than 1% (Figure 16).

We also observed differences in V gene usage between DCL and LCL lesions. The prominent heavy V gene subgroups present in DCL and LCL patients were IGHV1, IGHV3 and IGHV4 (Figure 17A). However, each of these V gene subgroup frequencies differed between LCL and DCL, with LCL using higher frequency of IGHV3 and DCL employing higher usage of IGHV1 and IGHV4. Light chain kappa V gene subgroup usage was composed mostly of IGKV1, IGKV1D, IGKV3, and IGKV3D, while lambda V gene subgroup usage was mainly restricted to IGLV1, IGLV2, and IGLV3 (Figure 17B and 17C).

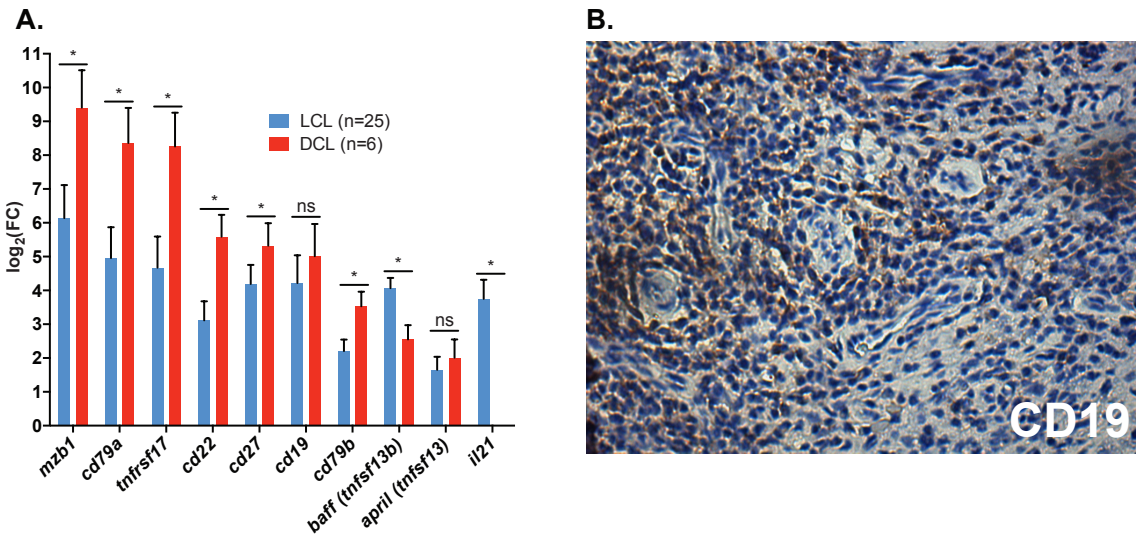

Figure 15. B cell transcripts are significantly upregulated in DCL lesions (A) Bars represent log2 fold-changes of B cell markers (mzb1, cd79a, tnfrsf17, cd22, cd27, cd79b) in LCL (blue) and DCL (red) compared to healthy skin (fold change ≥ 2, $p<0.05$). Significant differences between LCL and DCL are marked (*, fold change ≥ 2, $p<0.05$). **(B)** Immunohistochemistry staining of B cell marker CD19 in DCL lesions.

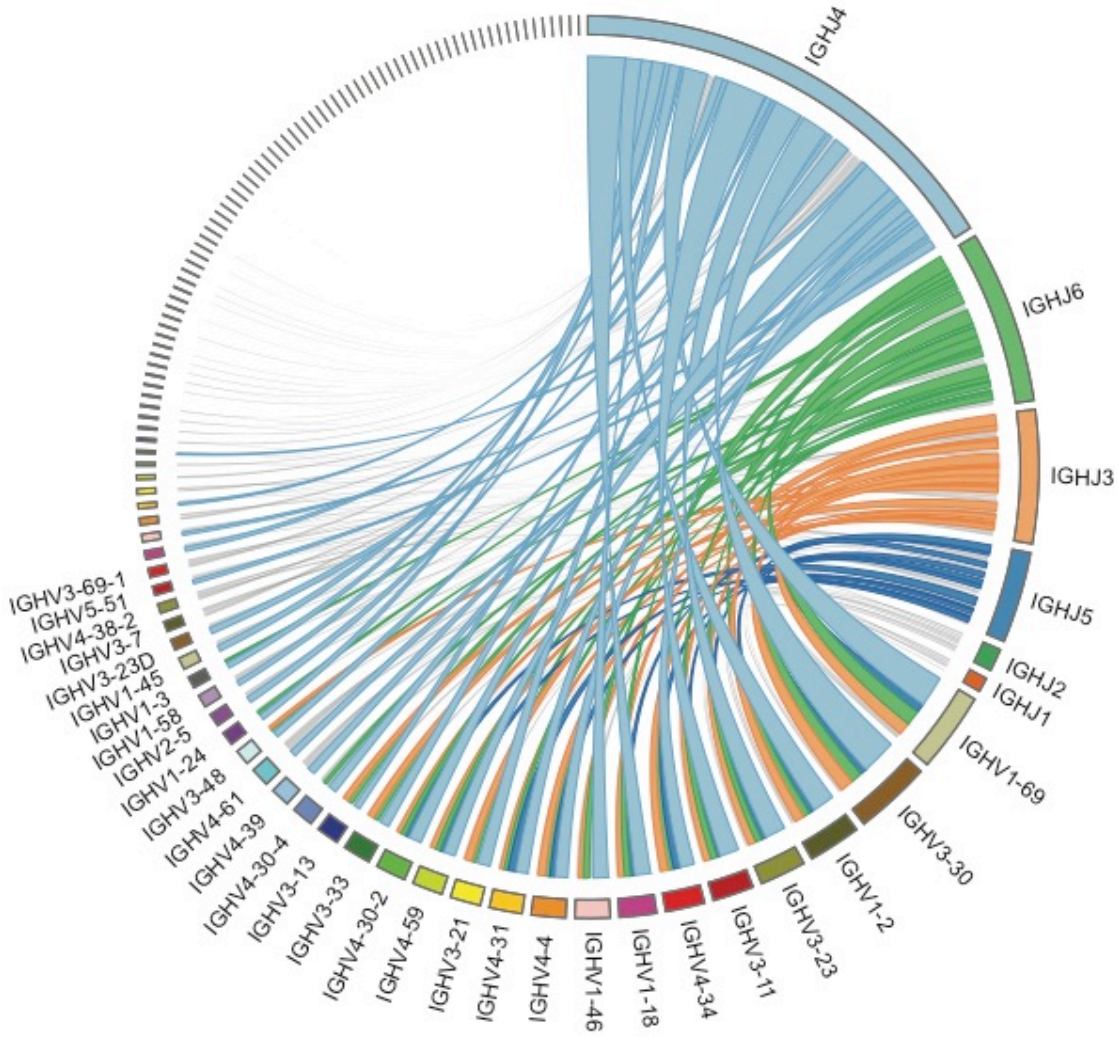

Figure 16. Immunoglobulin repertoires in DCL patients are oligoclonal (1G) A representative chord diagram shows average V and J gene usage (width of gene arc) and combination frequency in DCL patients designated by the width of chords.

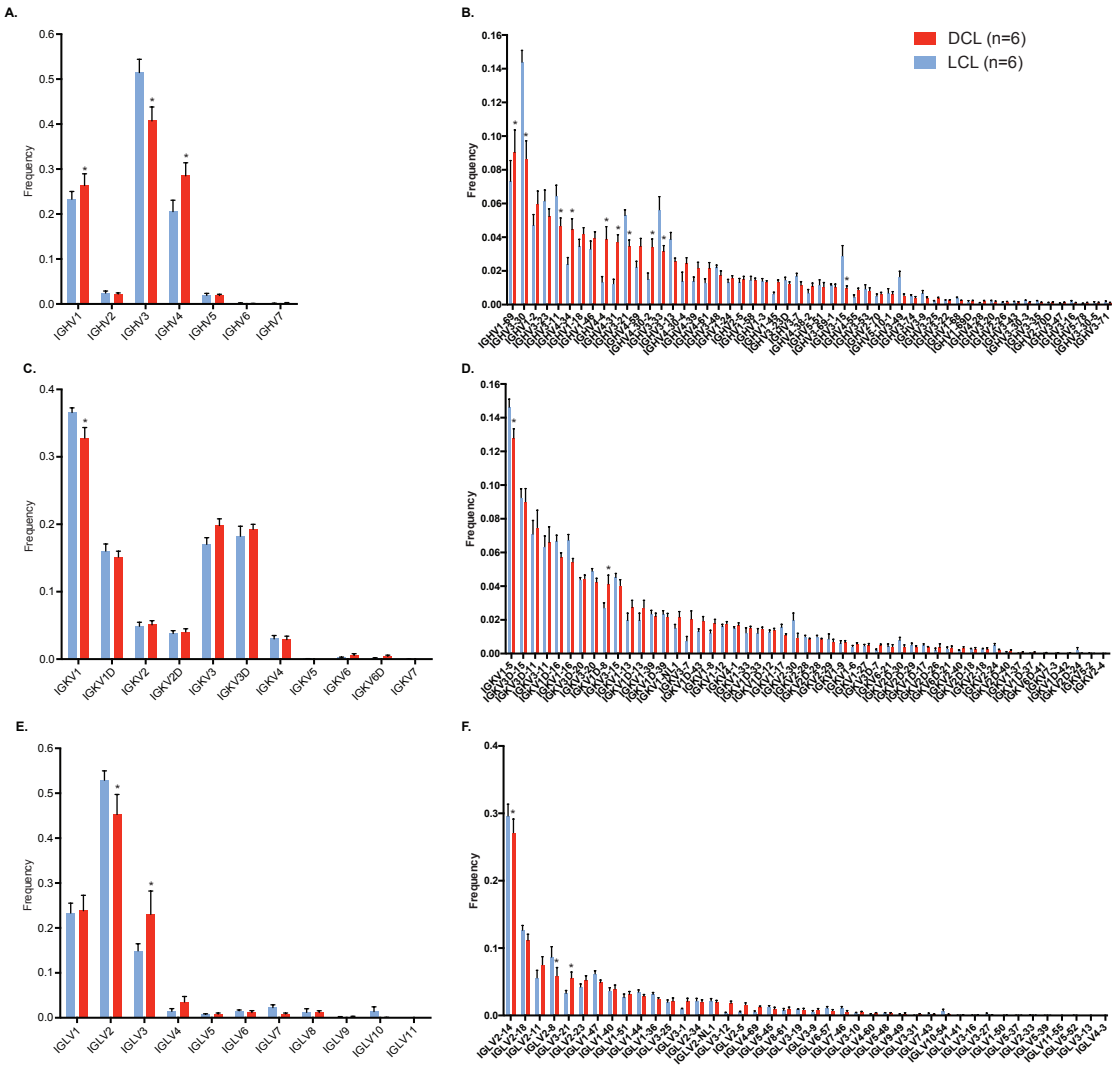

Figure 17. Skewed immunoglobulin V gene and subgroup usage in DCL and LCL lesions. Heavy and light chain V gene subgroup and gene usage frequency shows differences and similarities in LCL (blue bars, n=6) and DCL (red bars, n=6) host immunoglobulin responses. Only 6 of the LCL lesions contained enough immunoglobulin transcripts for a meaningful analysis. **(A, C, E)** Bar graphs show V gene subgroup usage in heavy, kappa, and lambda chains. **(B, D, F)** Bar graphs show V gene usage in heavy, kappa, and lambda chains. Significant differences between LCL and DCL are marked with a * ($p < 0.05$).

Both kappa and lambda subgroup frequencies contained differences between LCL and DCL. Heavy and light chain V gene usage was skewed in both LCL and DCL, as expected. Among heavy chain V genes, more than 90% of transcripts mapped to just 29 genes (34%) (Figure 17D). In the same manner, kappa light chain V gene usage consisted mainly of 24 genes, with IGKV1-5 as the most used kappa V gene (>12%) (Figure 17E). Lastly, lambda light chain V gene usage was limited to 18 genes, all of which made up more than 92% of lambda light chain V gene transcripts, with IGLV2-14 as the most used lambda gene (>27%) (Figure 17F). While most of the V gene usage was comparable between DCL and LCL lesions, nine heavy chain, two kappa light chain, and three lambda light chain V genes exhibited significant differences between the two manifestations of disease (Figure 17, designated *).

Altered cytotoxic T cell responses in DCL lesions. We examined T cell responses in DCL lesions and compared them to healthy controls and lesions from 25 LCL patients previously analyzed (179). DCL and LCL patients expressed similar levels of transcripts for CD4 and CD132 (IL2Rg) (Figure 18A, designated ns), but DCL lesions contained lower transcript levels for all three CD3 chains, CD127 (IL-7r), and zap70 (Figure 18A). DCL also expressed reduced transcripts for the Th1 transcription factor tbet, but similar levels for gata3, foxp3, and rorc (Figure 18A). Cytokine transcripts were also measured in DCL lesions. There was a significant reduction in the Th1-associated transcripts for IFNγ and TNF in DCL lesions, relative to LCL. There was no evidence for a Th2 response in DCL, as transcript levels for IL-4, IL5, and IL-13 were not different from uninfected controls. Surprisingly, IL-10 levels were comparable in both diseases.

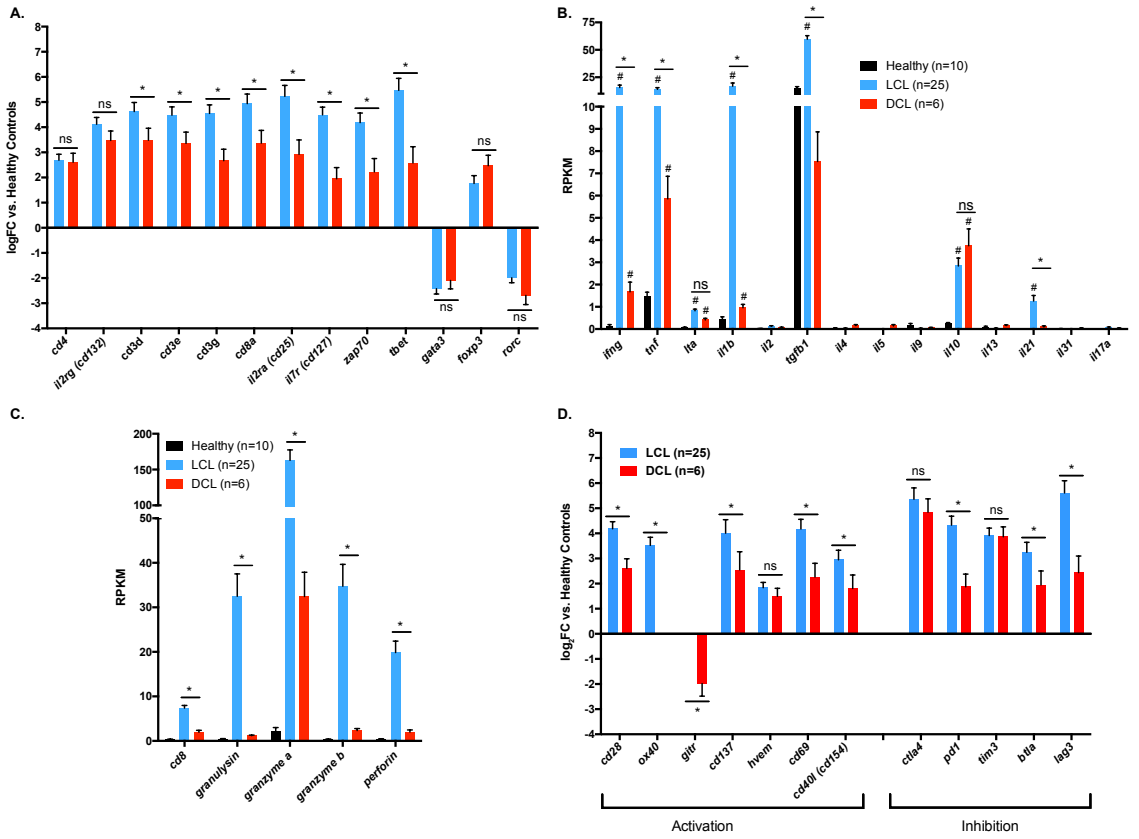

Figure 18. Reduced cytotoxic T cell responses in DCL lesions (A) Bars represent the $\log_2$ fold-change of generic T cell markers and transcription factors in LCL (blue) and DCL (red) patients (mean plus sem, $p < 0.05$). Differences between LCL and DCL are indicated (*p-value < 0.05, ns = not significant). **(B)** Bars show average RPKM values (plus SEM) for healthy (black), LCL (blue), and DCL (red) for various cytokines involved in Th1 (*ifng, tnf, lta, il1b, il2*), Th2 (*tgfb1, il4, il5, il9, il10, il13, il21, il31*), and Th17 (*il17a*) responses. Significant differences versus healthy (#, p-value < 0.05) and between LCL and DCL (*, p-value < 0.05) are indicated. **(C)** Bars show mean RPKM values (plus SEM) for healthy (black), LCL (blue), and DCL (red) for CD8 and cytotoxic T lymphocyte effector molecules. All transcripts in LCL and DCL were significantly upregulated versus healthy. Significant differences between LCL and DCL are indicated (*, p-value < 0.05). **(D)** Bars represent the $\log_2$ fold-change of T cell activation and inhibition markers in LCL (blue) and DCL (red) patients (mean plus sem, $p < 0.05$). Differences between LCL and DCL are indicated (*p-value < 0.05, ns = not significant).

There was a significant reduction in CD8A transcripts in DCL lesions relative to healthy controls and LCL (Figure 18C). Transcripts for cytotoxic effector molecules, including granulysin, granzyme A, granzyme B, and perforin, were also significantly diminished in DCL lesions compared to LCL (Figure 18C).

Various markers of T cell activation, including transcripts for CD28, OX40, GITR, CD137, CD69, and CD40L, were decreased in DCL relative to LCL (Figure 18D). The expression of inhibitory signaling molecules indicative of anergy, including PD-1, BTLA, and LAG3, was also significantly lower in DCL.

Contrasting macrophage activation states in DCL and LCL lesions. Both DCL and LCL lesions have a significant upregulation of pan-macrophage markers compared to healthy skin, and there appears to be no significant difference between the two disease states regarding the presence of macrophages. Comparable expression of genes generally expressed on macrophages, including FCGR1A, FCGR1B, SIGLEC1, CD11b, CD18, CD204, CD209, and CD68, was observed in LCL and DCL with only minor differences between diseases (Figure 19A, designated ns). However, markers of macrophage activation states were significantly different between DCL and LCL.

Data from a separate project in our lab found that LPS-stimulated macrophages (so-called M1) upregulated 2017 genes (data not shown). Of those, 487 genes were expressed significantly higher in LCL compared to DCL (not shown). Figure 19B shows the ten most highly upregulated transcripts in M1 macrophages, nine of which were significantly higher in LCL (blue bars) relative to DCL (red bars). One of the surprising exceptions to this was IL-12β, which is similarly expressed in LCL and DCL lesions (Figure 19B).

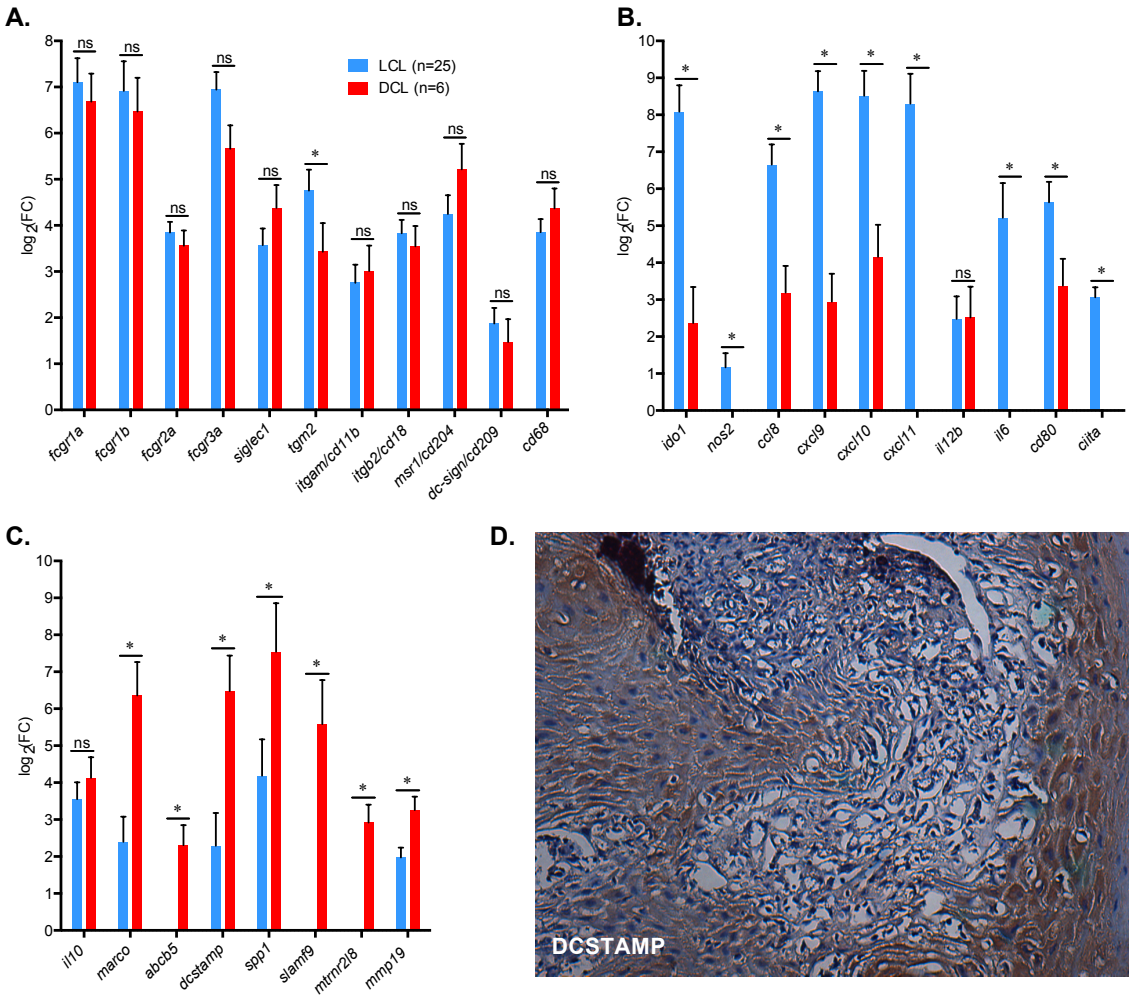

Figure 19. Altered macrophage responses in DCL lesions exhibit regulatory characteristics (A-C) Fold-changes of pan-macrophage markers (A), classically activated macrophage markers (B), and anti-inflammatory macrophage markers (C) in LCL (blue) and DCL (red) compared to healthy skin. Differences between LCL and DCL lesions are shown (ns = not significant, * = significant, fold-change ≥ 2, $p < 0.05$). **(D)** Immunohistochemistry staining of DCSTAMP in DCL lesions.

In a separate project, we demonstrated that human macrophages stimulated with LPS plus immune complexes assume a regulatory phenotype (R-MΦ) (manuscript in preparation). These R-Mϕ differ from LPS stimulation by downregulating inflammatory genes and upregulating anti-inflammatory and growth factor genes. Analysis of data from this project revealed an upregulation of 925 genes and a downregulation of 632 genes in R-MΦ compared to LPS (data not shown). Due to the overwhelming upregulation of immunoglobulin in DCL lesions, we hypothesized that R-MΦ would be present in these lesions.

Among the upregulated genes in R-MΦ, 90 showed significantly higher expression in DCL compared to LCL. DCL and regulatory macrophages similarly upregulated genes that included ABCB5, DCSTAMP, SPP1, SLAMF9, MTRNR2L8, and MMP19 (Figure 19C). A marker of marginal zone (MZ) macrophages (MARCO) was also expressed significantly higher in DCL compared to LCL (Figure 19C). Histology confirmed the presence of DCSTAMP in DCL lesions (Figure 19D). Of note, the anti-inflammatory cytokine IL-10 was unexpectedly equally upregulated in LCL and DCL (Figure 19C). Among the more than 600 downregulated genes in R-MΦ, 148 were downregulated in DCL compared to LCL, indicative of a downregulation of inflammatory responses seen in classical activation.

Effectors of alternative activation (so-called M2a), including IL-4, IL-5, IL-13, were expressed at low or undetectable levels in LCL and DCL lesions (Figure 18B). Markers and chemokines known to identify or influence Th2 or M2a responses were also lowly expressed, including the chemokine and cytokine receptors CCR3, CCR4, CCR8, CXCR4, IFNGR1, IFNGR2, IL4RA, IL17BR, IL1RL1, and TSLPR (Figure 20).

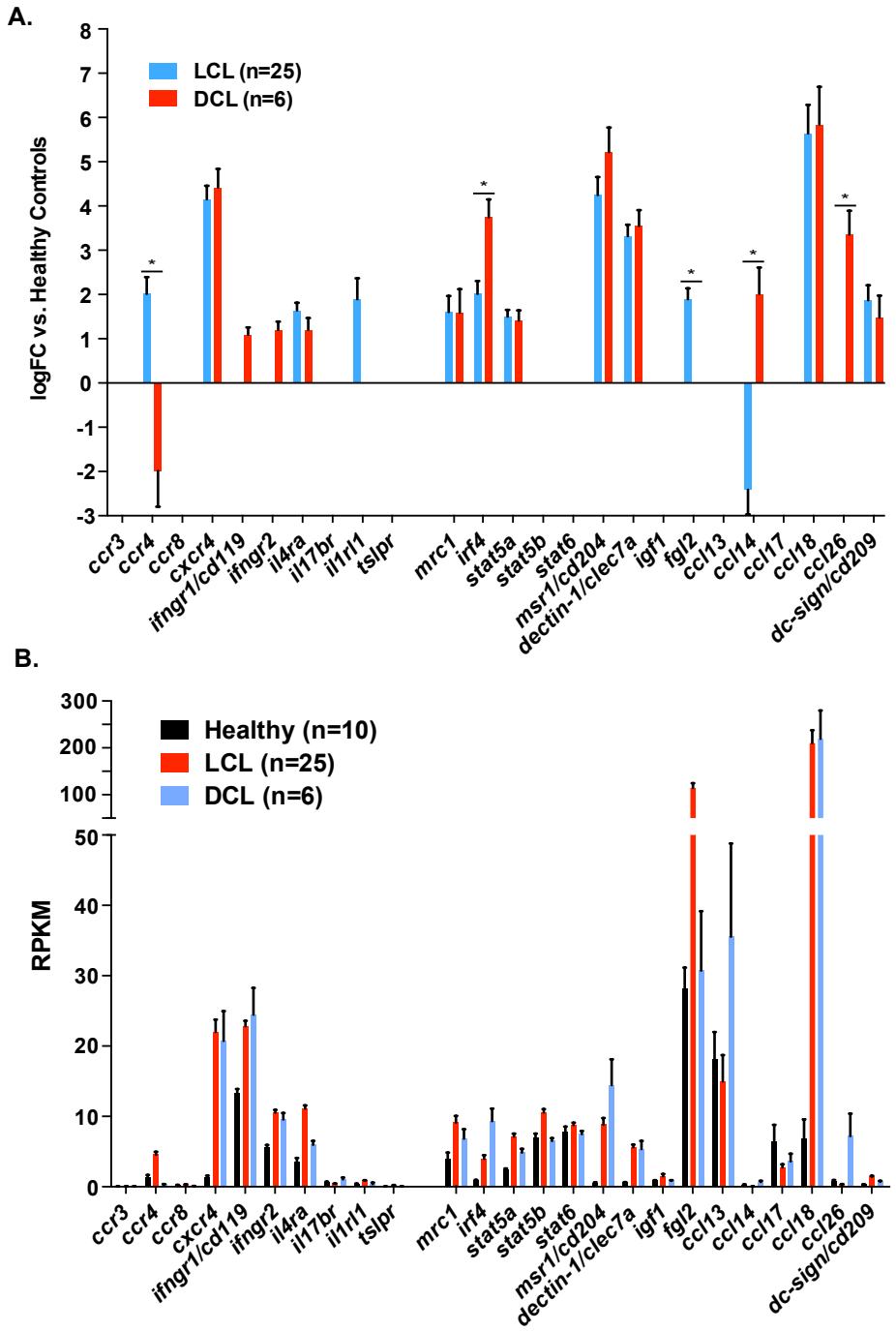

Figure 20. Minimal Th2/M2a responses in LCL and DCL lesions (A) Bars show $\log_2$ fold-changes of various Th2 and M2a markers and effector molecules. Of 26, 14 were upregulated in LCL (blue), 13 in DCL (red), 2 downregulated in LCL, and 2 downregulated in DCL. Only 5 demonstrated significant differences between LCL and DCL (CCR4, IRF4, FGL2, CCL14, CCL26). **(B)** Bars show RPKMs for each of the Th2/M2a-related genes. Only 3 genes exceeded RPKMs of 30.

***L. amazonensis* gene expression in DCL lesions.** Metatranscriptomic analysis revealed that a high percentage (10-30%) of the transcripts in DCL lesions mapped to the *L. amazonensis* genome (Figure 21A, red bars). In contrast, the percentage of reads that mapped to the *L. braziliensis* genome in LCL was below 2% (Figure 21A, blue bars). Parasite transcription in diffuse lesions displayed a high degree of patient-to-patient uniformity (Figure 21B). The top transcripts expressed by parasites in lesions consisted mainly of ribosomal and histone proteins, but did contain some hypothetical proteins and the known virulence factor kinetoplastid membrane protein-11 (Table 7). A deeper look at the top 500 expressed genes (data not shown) revealed 183 hypothetical proteins (>35%) as well as multiple predicted or known peptidases and heat shock proteins.

We reasoned that the deficiency in Th1 immune responses in DCL would result in lesion macrophages that were as susceptible to infection as tissue-cultured macrophages infected *in vitro* in the absence of T cells. We therefore compared the *L. amazonensis* transcripts in diffuse lesions to that of previously analyzed *L. amazonensis* transcripts produced during *in vitro* infection of human macrophages (72 hours). After ranking genes by average RPKM, we observed a general trend of similar parasite gene expression (Figure 21C). Roughly 75% of genes (~6300) were ranked within a margin of 20% of each other when comparing DCL to *in vitro* infection (Figure 21C, shaded region). However, 1904 genes did differ in rank by more than 20%.

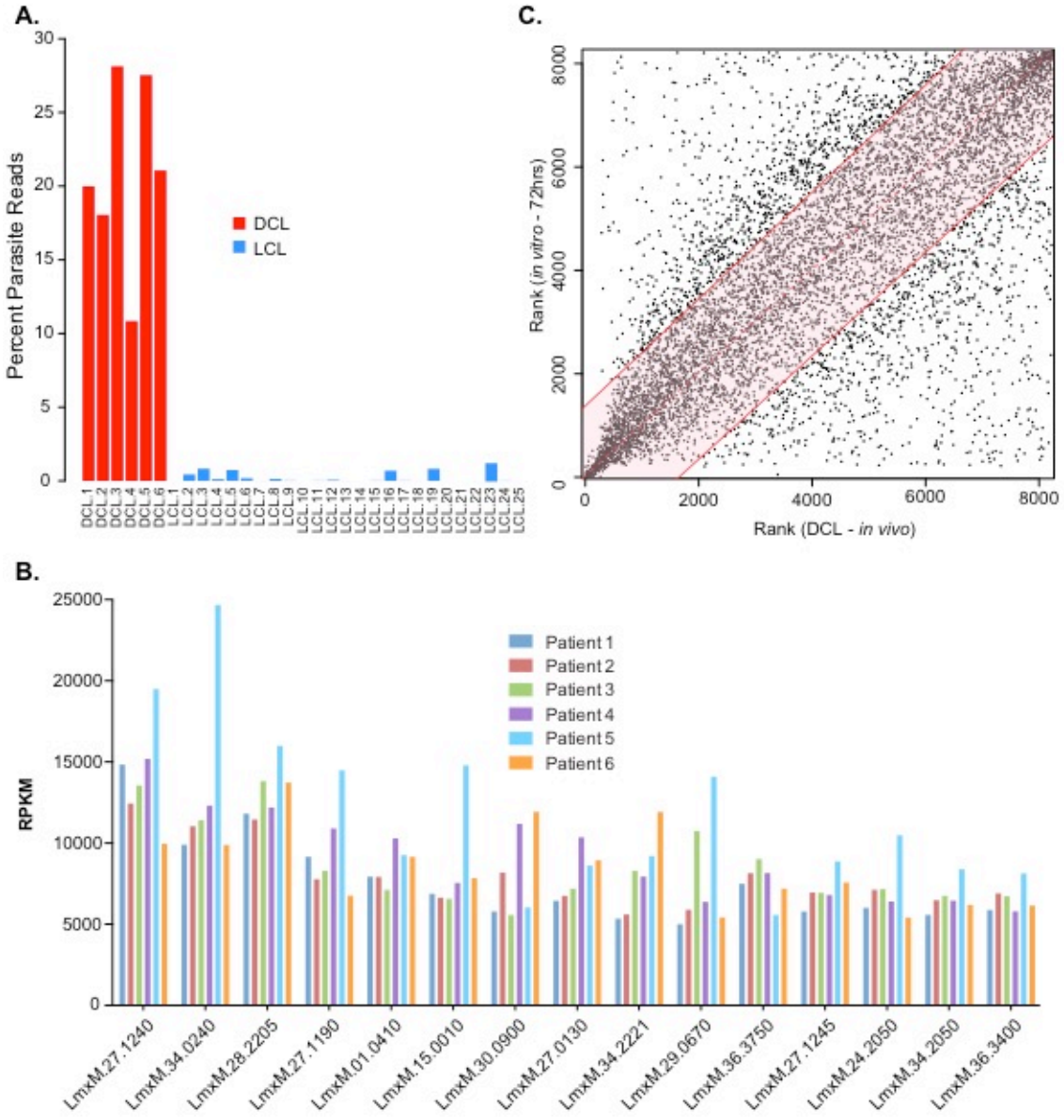

Figure 21. *L. amazonensis* expression in DCL lesions (A) Bars represent the percent of reads that mapped to parasite genomes in DCL (red) and LCL (blue). **(B)** Bars represent RPKMs for the top 15 genes expressed by *L. amazonensis* in 6 DCL patients. (**C)** A scatter plot visualizes the similarity in parasite gene expression between DCL *L. amazonensis* infections (x-axis) and *in vitro L. amazonensis* infection of macrophages (y-axis). Genes were ranked by average RPKM in DCL (n=6) and *in vitro* infection of macrophages at 72 hours (n=3). The shaded region indicates a difference in rank of less than 20%.

Table 7. Top 40 genes by RPKM expressed by *L. amazonensis* in DCL lesions

ID	Description	Average RPKM
LmxM.27.1240	histone H1, putative	14245
LmxM.34.0240	60S ribosomal protein L30	13205
LmxM.28.2205	ribosomal protein S29, putative	13167
LmxM.08_29.2370	60S ribosomal protein L39, putative	9960
LmxM.27.1190	histone H1, putative	9566
LmxM.01.0410	hypothetical protein	8612
LmxM.15.0010	histone H4	8378
LmxM.30.0900	hypothetical protein, conserved	8114
LmxM.27.0130	hypothetical protein, conserved	8054
LmxM.34.2221	kinetoplastid membrane protein-11	8051
LmxM.29.0670	40S ribosomal protein S30, putative	7923
LmxM.36.3750	40S ribosomal protein S27-1, putative	7597
LmxM.24.2050	60S ribosomal protein L26, putative	7103
LmxM.34.2050	60S ribosomal protein L32	6641
LmxM.36.3400	ribosomal protein L29, putative	6599
LmxM.16.1170	60S ribosomal protein L39, putative	6345
LmxM.21.1050	60S ribosomal protein L9, putative	6340
LmxM.13.0570	40S ribosomal protein S12, putative	6211
LmxM.31.2690	ribosomal protein L27, putative	6028
LmxM.36.1925	60S ribosomal protein L37a	5938
LmxM.26.2220	ribosomal protein L38, putative	5930
LmxM.03.0250	ribosomal protein L38, putative	5821
LmxM.09.1340	histone H2B	5772
LmxM.21.1550	40S ribosomal protein S11, putative	5451
LmxM.34.3290	60S ribosomal subunit protein L31, putative	5446
LmxM.34.0600	60S ribosomal protein L18a, putative	5435
LmxM.26.2330	60S ribosomal protein L35, putative	5362
LmxM.34.1910	ribosomal protein L15, putative	5345
LmxM.06.0580	60S ribosomal protein L23a, putative	5254
LmxM.36.2860	40S ribosomal protein S24e	5172
LmxM.36.2870	40S ribosomal protein S24e	5153
LmxM.13.1670	60S ribosomal protein L44, putative	5130
LmxM.08_29.1740	histone H2A, putative	5102
LmxM.34.3780	60S ribosomal protein L27A/L29, putative	5090
LmxM.31.0430	60S ribosomal protein L17, putative	5085
LmxM.17.1220	histone H2B	5058
LmxM.30.1170	hypothetical protein, unknown function	5048
LmxM.36.3770	transcription factor btf3, putative	5018
LmxM.36.3760	60S ribosomal protein L10a, putative	4985
LmxM.36.3270	60S ribosomal protein L22, putative	4932

We further reasoned that the strong Th1 response in LCL would exert immune pressure on *L. braziliensis* parasites in lesions and alter parasite transcriptional responses. We therefore used previously obtained data from our lab (171, 179) and identified 6713 single reciprocal orthologs to compare parasite transcription of *in vivo L. amazonensis* infections in DCL to *in vivo L. braziliensis* infections in LCL and *in vitro L. major* and *L. amazonensis* infections in human-cultivated macrophages (Figure 22). Pearson correlations demonstrated a high degree of similarity between transcripts produced by parasites in DCL and *in vitro* infections in macrophages regardless of species (Figure 22A). The *L. braziliensis* parasite transcriptomes did not correlate at the same level when compared with the rest of the samples. We then normalized gene expression rank in the respective experiments to a scale of 0-1. Using this metric, we extracted 78 genes expressed at a higher level (difference > 0.2) by *L. amazonensis* in DCL, 64 of which are hypothetical proteins (Figure 22B). Lastly, we compared the top 10% of genes (by average RPKM) expressed by the parasite in each experiment, revealing 137 genes commonly expressed at a high level (Figure 22C). Among this subset was 72 hypothetical proteins and 33 proteins with at least one predicted transmembrane region (Table 8). Overlap between these designations was 25 hypothetical proteins with at least one predicted transmembrane region. We also observed multiple peptidases and oxidases that could be important to parasite survival within the host.

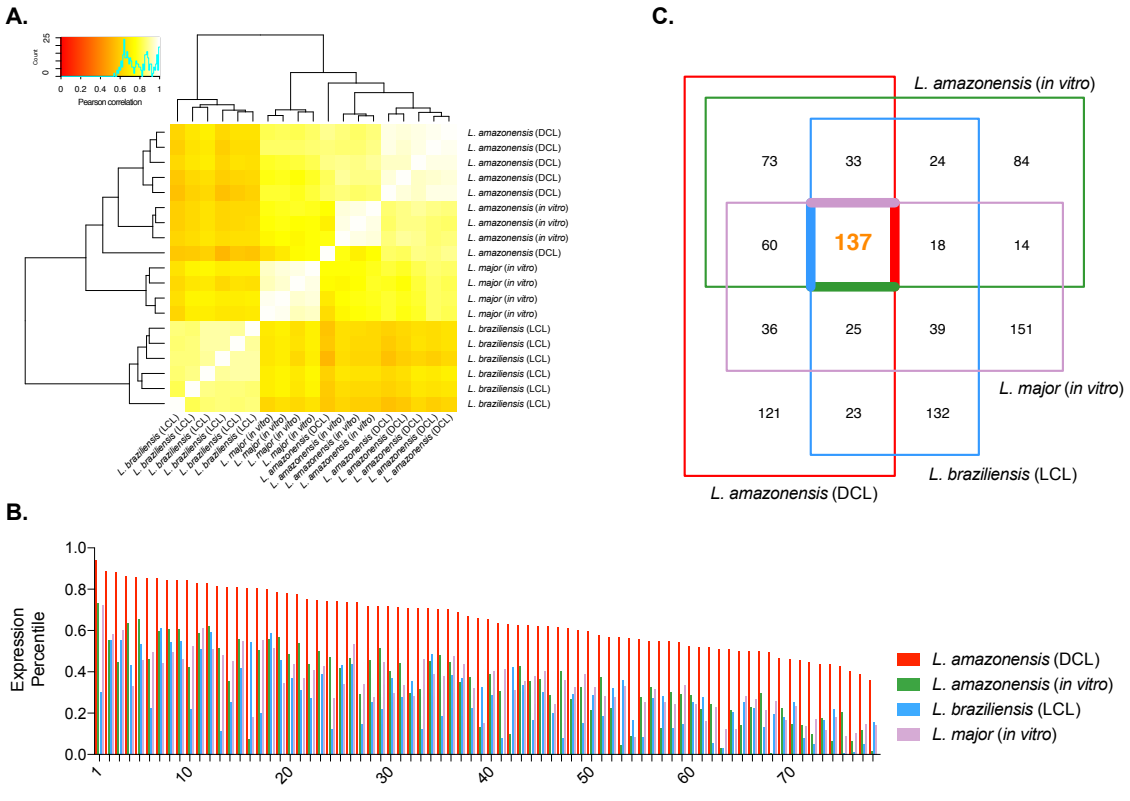

Figure 22. Comparisons of parasite transcriptomes in leishmaniasis and *in vitro* infections. Comparisons were made using single reciprocal orthologous genes between *L. amazonensis* in DCL, *L. amazonensis* during *in vitro* macrophage infection (72hrs), *L. major* during *in vitro* macrophage infection (72hrs), and *L. braziliensis* in LCL **(A)** A heatmap represents the Pearson correlation of expression (RPKM) between samples. Correlations range from 0.54 to 0.98. **(B)** Bars indicate gene rank on a scale of 0-1 in *L. amazonensis* DCL (red), *L. amazonensis in vitro* (green), *L. major in vitro* (purple), and *L. braziliensis* LCL (blue). All 78 genes were expressed at a higher level (>0.2) in DCL compared to the other three infections. **(C)** A Venn diagram of the top 10% of genes expressed (by average RPKM) in *L. amazonensis* in DCL (red box, 508), *L. amazonensis in vitro* (green box, 443), *L. major in vitro* (purple box, 480), and *L. braziliensis* in LCL (blue box, 431). The highlighted 137 genes were commonly expressed within the top 10%.

Table 8. Common highly expressed *Leishmania* genes (top 10%)

TM regions	Description	*L. mexicana* ID
0	60S ribosomal protein L30	LmxM.34.0240
0	40S ribosomal protein S12, putative	LmxM.13.0570
0	hypothetical protein, unknown function	LmxM.30.1170
0	ALBA-domain protein 1	LmxM.13.0450
0	transcription factor btf3, putative	LmxM.36.3770
0	RNA-binding protein 5, putative	LmxM.09.0060
0	hypothetical protein, conserved	LmxM.27.0130
0	hypothetical protein, conserved	LmxM.15.1520
0	hypothetical protein, conserved	LmxM.29.2760
0	nuclear RNA binding domain	LmxM.31.0750
4	hypothetical protein, unknown function	LmxM.08.0640
0	ribosomal protein S6, putative	LmxM.15.1470
4	hypothetical predicted multi-pass transmembrane protein	LmxM.24.2230
0	hypothetical protein, conserved	LmxM.09.0010
0	nucleolar RNA-binding protein, putative	LmxM.07.0990
1	hypothetical protein, conserved	LmxM.17.0340
1	hypothetical protein, conserved	LmxM.27.0110
1	cytochrome c oxidase VIII (COX VIII), putative	LmxM.30.1570
1	hypothetical protein, unknown function	LmxM.27.2150
0	inhibitor of cysteine peptidase	LmxM.24.1770
0	hypothetical protein, conserved	LmxM.29.0770
0	hypothetical protein, conserved	LmxM.03.0960
10	inosine-guanosine transporter	LmxM.36.1940
0	hypothetical protein, conserved	LmxM.01.0300
0	cytochrome c oxidase subunit V, putative	LmxM.26.1710
1	hypothetical protein, conserved	LmxM.04.0630
1	hypothetical protein, conserved	LmxM.17.1280
1	CPC cysteine peptidase, Clan CA, family C1, Cathepsin B-like	LmxM.08_29.0820
0	dynein light chain, flagellar outer arm, putative	LmxM.31.0230
0	hypothetical protein, conserved	LmxM.14.0190
0	hypothetical protein, conserved	LmxM.22.1640
0	cytochrome c oxidase subunit VI, putative	LmxM.21.1710
0	protein disulfide isomerase 2	LmxM.36.6940
1	cytochrome oxidase subunit IX, putative	LmxM.36.6995
0	glutaredoxin-like protein	LmxM.27.0810
0	hypothetical protein, conserved	LmxM.33.4010
0	hypothetical protein, conserved	LmxM.33.0580

0	universal minicircle sequence binding protein, putative	LmxM.36.1640
0	ubiquinol-cytochrome-c reductase-like protein	LmxM.30.2580
1	hypothetical protein, conserved	LmxM.24.1330
0	hypothetical protein, conserved	LmxM.08.1100
0	small GTP-binding protein, putative	LmxM.05.0030
0	sm-f snRNP core complex protein, putative	LmxM.34.4460
0	ADP-ribosylation factor, putative	LmxM.30.2790
0	nuclear protein family a (nop10p), putative	LmxM.36.0340
0	histone H3 variant V	LmxM.19.0630
0	cyclophilin	LmxM.06.0120
0	hypothetical protein, conserved	LmxM.36.0480
0	hypothetical protein, conserved	LmxM.25.0590
0	hypothetical protein, conserved	LmxM.34.0100
1	hypothetical protein, conserved	LmxM.34.0140
1	hypothetical protein, conserved	LmxM.29.2845
0	phosphoprotein lepp12	LmxM.36.5720
0	hypothetical protein, conserved	LmxM.36.0620
1	hypothetical protein, conserved	LmxM.31.3610
0	hypothetical protein, conserved	LmxM.23.0370
1	hypothetical protein, conserved	LmxM.36.1770
0	endoribonuclease L-PSP (pb5), putative	LmxM.23.0200
1	hypothetical protein, unknown function	LmxM.30.1190
0	Ran-binding protein 1, putative	LmxM.13.1480
0	Acyl carrier protein, mitochondrial, putative	LmxM.27.0290
0	hypothetical protein, conserved	LmxM.32.2060
1	protein disulfide isomerase	LmxM.06.1050
1	hypothetical protein, conserved	LmxM.25.2090
0	hypothetical protein, conserved	LmxM.05.0450
0	fructose-1,6-bisphosphate aldolase	LmxM.36.1260
0	kinetoplast-associated protein p18-2, putative	LmxM.31.3770
1	cytochrome oxidase subunit VII	LmxM.25.1130
0	hypothetical protein, conserved	LmxM.34.4640
1	protein transport protein Sec61 gamma subunit, putative	LmxM.25.1015
0	hypothetical protein, conserved	LmxM.21.0040
0	hypothetical protein, conserved	LmxM.31.0165
0	elongation factor-1 gamma	LmxM.09.0970
0	hypothetical protein, conserved	LmxM.22.0270
0	centrin-4, putative	LmxM.22.1410
0	actin	LmxM.04.1230
1	hypothetical protein, conserved	LmxM.25.0660
0	hypothetical protein, conserved	LmxM.17.0850
0	small nuclear ribonucleoprotein, putative	LmxM.31.1070

1	hypothetical protein, conserved	LmxM.34.1210
0	ATP synthase F1 subunit gamma protein, putative	LmxM.21.1770
0	glycine cleavage system H protein, putative	LmxM.34.4720
0	hypothetical protein, conserved	LmxM.05.1000
0	vacuolar ATP synthase subunit, putative	LmxM.12.0520
0	Ras-related protein Rab4, putative	LmxM.31.0490
0	prefoldin subunit, putative	LmxM.05.1200
3	hypothetical protein, conserved	LmxM.31.2995
0	i/6 autoantigen-like protein	LmxM.22.1460
1	ascorbate peroxidase, putative	LmxM.33.0070
0	ubiquitin-conjugating enzyme, putative	LmxM.13.1580
0	small nuclear ribonucleoprotein SmD2	LmxM.32.3190
0	hypothetical protein, conserved	LmxM.17.0890
0	hypothetical protein, conserved	LmxM.22.0680
0	ribonuclease mar1	LmxM.12.0060
0	hypothetical protein, unknown function	LmxM.01.0690
0	hypothetical protein, conserved	LmxM.32.0020
0	hypothetical protein, unknown function	LmxM.34.1370
0	hypothetical protein, conserved	LmxM.31.0630
0	hypothetical protein, conserved	LmxM.33.3910
0	stress-inducible protein STI1 homolog	LmxM.36.0070
0	hypothetical protein, conserved	LmxM.25.0715
1	hypothetical protein, conserved	LmxM.05.1030
0	hypothetical protein, conserved	LmxM.28.2660
4	hypothetical protein, conserved	LmxM.28.1120
0	hypothetical protein, conserved	LmxM.25.1620
0	hypothetical protein, conserved	LmxM.36.3370
0	GTP-binding protein, putative	LmxM.25.1420
0	hypothetical protein, conserved	LmxM.30.1580
0	hypothetical protein, conserved	LmxM.25.0820
2	hypothetical protein, conserved	LmxM.34.1840
0	cytochrome c1, heme protein, mitochondrial, putative	LmxM.07.0060
0	autophagocytosis protein, putative	LmxM.32.0295
0	hypothetical protein, unknown function	LmxM.24.1600
0	profilin, putative	LmxM.31.0520
2	hypothetical protein, conserved	LmxM.30.1120
0	small nuclear ribonucleoprotein polypeptide e, putative	LmxM.29.1205
0	phosphomannomutase, putative	LmxM.36.1960
0	nuclear transport factor 2, putative	LmxM.10.0850
0	ATP synthase, epsilon chain, putative	LmxM.29.3600
0	clathrin coat assembly protein AP17, putative	LmxM.33.2330
0	hypothetical protein, conserved	LmxM.36.6760
0	hypothetical protein, conserved	LmxM.10.1225

0	hypothetical protein, conserved	LmxM.29.0830
0	hypothetical protein, unknown function	LmxM.10.0450
0	nucleolar protein 56, putative	LmxM.10.0210
0	metallo-peptidase, Clan MG, Family M24	LmxM.19.0160
1	hypothetical protein, unknown function	LmxM.29.1390
0	glutamine synthetase, putative	LmxM.06.0370
0	ATG8/AUT7/APG8/PAZ2, putative	LmxM.19.1630
0	prefoldin 5-like protein	LmxM.22.0670
1	hypothetical protein, conserved	LmxM.26.1100
0	hypothetical protein, conserved	LmxM.36.4670
2	hypothetical protein, conserved	LmxM.26.0680
0	eukaryotic translation initiation factor 3 subunit j	LmxM.25.2120
0	hypothetical protein, conserved	LmxM.36.6345
4	hypothetical protein, unknown function	LmxM.25.1880
0	hypothetical protein, conserved	LmxM.30.1620

DISCUSSION

The use of RNA-seq to analyze human skin biopsies from *Leishmania*-infected patients enabled a simultaneous in-depth assessment of the host and parasite transcriptomes. We identified a combination of host responses that correlate with the promotion of disease persistence in DCL lesions. Our observations highlighted a prominent role for B cells in progressive disease. They also pointed to a diminished cytotoxic T cell response and a disease-promoting, rather than restricting, macrophage activation state. We propose that elevated B cell presence and localized antibody production help to initiate a regulatory and anti-inflammatory macrophage activation state leading to exacerbation of infection in the diffuse state (Figure 23).

As previously discussed, infiltration of B cells in leishmaniasis lesions is known and some of their contributions to disease resolution have been reported (105, 113, 114, 187). Our previous work demonstrated correlations between parasite persistence and immunoglobulin production (60, 179). We now characterized the B cell response in human DCL, and demonstrate that immunoglobulins don't simply associate with severe disease, but actually contribute to it. We also uncovered atypical features that could contribute to disease progression. Most strikingly, DCL lesions are dominated by IgG4 (Figure 14), divergent from most other chronic infections (188). The IgG4 isotype does not bind complement or activating FcRs well (189–191). Furthermore, IgG4 binds to the inhibitory FcγRIIB better than other IgG isotypes (189). IgG4 has previously been implicated in other disease states resulting in fibroinflammatory conditions (192). Therefore IgG4 may contribute to the anti-inflammatory and DTH-refractory nature of the disease (23, 193, 194).

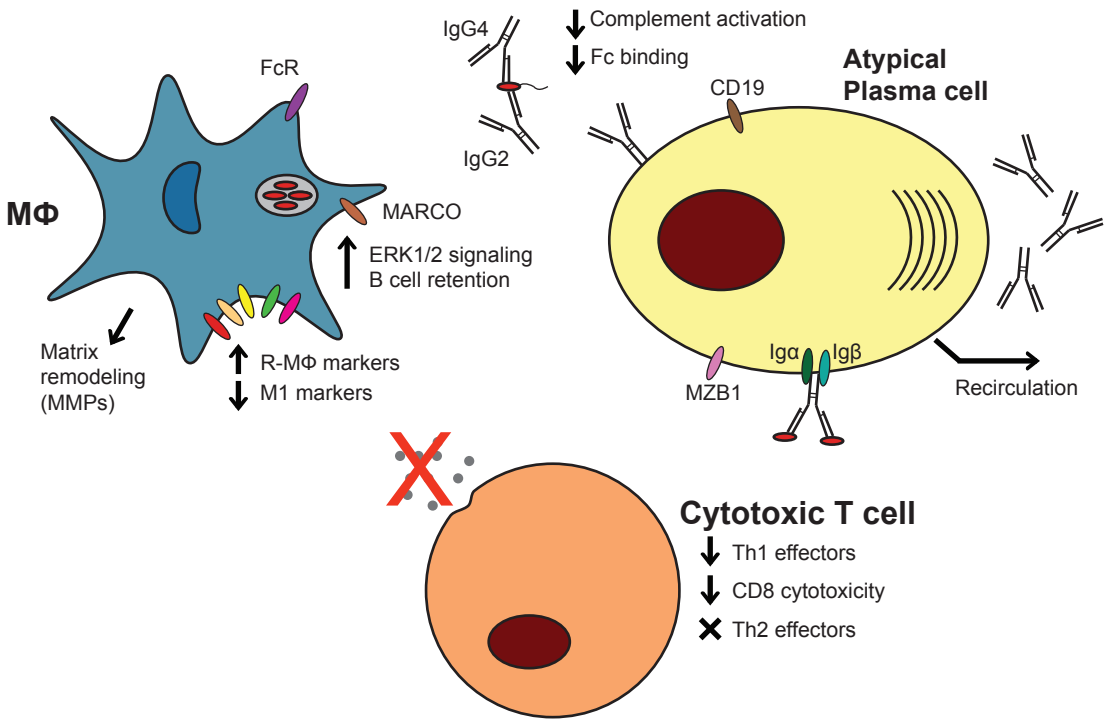

Figure 23. Biased B cell responses and altered macrophage and T cell activation lead to DCL phenotypes. Domination of the immunoglobulin response by IgG4 promote anti-inflammatory phenotypes in infected macrophages and the surrounding microenvironment, promoting parasite survival, extracellular matrix remodeling, and angiogenesis. Regulatory macrophages expressing MARCO receptor augment the anti-inflammatory macrophage response via ERK1/2 signaling and retain plasma B cells. Increased anti-inflammatory factors negate cytotoxic T cell infiltration, activation, and effector functions.

This anomaly in serum IgG production was reported 24 years ago in a small number of patients (195). Here, we demonstrate that the rare IgG4 isotype permeates lesions as well.

Another unexpected feature of B lymphocytes in DCL is that they share markers with MZ B cells. This could explain their retention in lesions and the diffuse nature of the disease. Upregulation of MZB1 in DCL (500-fold) was unexpected in skin and we observed other transcriptional signatures common to MZ B cells in LCL and DCL, including an upregulation of complement receptors (CD1D, CD21, and CD35; data not shown) and CD27 (Figure 15A) and a lack of germinal center markers (BCL6, CD10; data not shown) (196–201). MZ B cells can respond to blood-borne thymus-independent (TI) antigens and help initiate APC uptake of antigen (200), produce excess antibody and cytokines, and act in antigen presentation and tissue repair (196, 202, 203). Schiller et al. discovered these cells in fibrotic skin and lung tissue, exposing their ability to contribute to disease (204). The recirculating tendencies of "memory"-like MZ B cells (197) could explain the phenotype of uncontrolled lesion development in later stages of DCL. It is well known that early immune responses to *Leishmania* sp. in murine infection help define important T cell activation states that eventually lead to control or susceptibility. The same could hold for B cells and an early and sustained atypical B cell response in these patients could contribute to the pathology and progression of this disease

Immunoglobulin sequencing analysis indicating skewed usage of specific V genes in heavy and light chain immunoglobulins (Figure 17). Analysis of V-J combinations in DCL patients supports this theory, revealing a relatively restricted subset of gene usage, indicating the possibility of an oligoclonal response (Figure 16). Further analysis is needed if we are to fully understand the immunoglobulin responses and variable gene

selection processes within diffuse leishmaniasis lesions and the parasite antigens that drive this response.

Along with the presence of atypical and active B cells in DCL lesions, we witnessed a change in the T cell population that could also equally contribute to parasite survival and disease progression. It is widely accepted that in murine models of leishmaniasis, a Th1 response is responsible for protection against *Leishmania major*, while a Th2 response leads to parasite persistence (75, 205). In DCL lesions, we observed an increase in transcripts for CD4 (~6-fold higher than healthy skin), a magnitude similar to that observed in LCL. However, further analysis of Th1 effectors and the transcription factor TBET (Figure 18) demonstrated a diminished Th1 response in DCL relative to LCL. This decreased Th1 response in DCL was not compensated for by an increased Th2 response. Contradictory to previous works (94, 206), neither LCL nor DCL lesions exhibited any signs of a Th2 transcriptional response (Figure 18B, Figure 20). In fact transcripts for the canonical Th2 cytokines, IL-4, and IL-13 were virtually absent in DCL, indicating that the enhanced susceptibility in human DCL is not due to a Th2 immune response.

The role of cytotoxic CD8+ T cells in leishmaniasis remains controversial (72). We observed an increase in CD8 transcripts of nearly 32-fold above uninfected skin in LCL, but in DCL these transcripts were only increased by 8-fold. This relative lack of CD8 transcripts in DCL correlated with a marked decrease in transcripts for perforin, granzymes, and granulysin (Figure 18C). We hypothesize that the paucity of CTLs in DCL may allow for prolonged survival of infected macrophages, thereby promoting parasite survival. This increased survival would be consistent with the high percentage of

transcripts mapping to the parasite genome observed in Figure 21 (207, 208). As for markers of anergy, expression was higher in the LCL compared to DCL environment, but without functional assays, we cannot attribute this to a particular subset of T cells. However, it does suggest that anergy does not contribute to the lack of cytotoxic effector molecules in DCL lesions. Thus, the commonly used designation of anergic DCL may need to be reconsidered.

In our previous work on LCL, we demonstrated host responses indicative of classically-activated macrophages, with substantial upregulation of IDO1, CXCL9, CXCL10, CXCL11, iNOS, IL-6, and TNF (179). We found that classical activation markers were significantly dampened in DCL lesions (Figure 19B). Due to the significant increases in immunoglobulin presence in lesions, we hypothesized that the regulatory macrophage phenotype would more likely exist. Indeed, our data found upregulation of anti-inflammatory and angiogenic gene transcription in DCL lesions (Figure 19C). Expression of MARCO on macrophages could also contribute to parasite persistence through retention of $MZB1^{+}$ B cells (203, 209–211) and enhanced ERK1/2 signaling known to exacerbate disease (212, 213). This heightened presence of the anti-inflammatory nature of regulatory macrophages supports increased parasite survival as intracellular pathogen killing is diminished in this macrophage subset (13).

In-depth views into the parasite transcriptome *in vivo* revealed extensive information and allowed for identification of important parasite genes that could contribute to disease pathology. First and foremost, the uniformity among parasite transcription was quite remarkable (Figure 21) despite the differences in patient age (15-50) and length of infection (14-35 years). By comparing the *in vivo L. amazonensis*

transcriptome to *in vitro* macrophage infection with the same species (Figure 21C), we show that 75% of the genome is expressed at similar levels, while 25% of genes differ in expression between these infections. These differences demonstrate the need for further study of *Leishmania* infections within the lesion microenvironment as *in vitro* studies may not reveal the entire picture.

More importantly, we combined our most recent data from DCL parasites with previous parasite transcriptome datasets to narrow the list of targets for disease causation. On the whole transcriptome scale, we noted that parasites in DCL lesions possess similar gene expression to the senescent and thriving population of parasites in macrophage infections *in vitro* (Figure 22A). We also identified a panel of 137 genes that are highly expressed regardless of disease manifestation and species (Figure 22C). Many of the proteins coded for by these genes have unknown structures and functions (Table 8), indicating the need for continued research and annotation of parasite genomes. These genes could serve as the basis for research in pan-*Leishmania* therapeutics and vaccines.

Previous research has shown that the difference in manifestation of disease is due simply to changes in the host (214). More recent research has implicated specific parasite gene contributions to this phenomena (215–217). We identified *L. amazonensis* genes expressed at a higher level in DCL compared to other infections that could contribute to disease. This list should be a starting point for understanding the host-pathogen interactions and parasite manipulation of host responses.

In conclusion, we used high-throughput sequencing to characterize the host immune response and parasite gene expression in human diffuse cutaneous leishmaniasis lesions. These lesions lack a DTH^{+} response, are generally pain-free, but disfiguring and

spread over most of a patient's body. Our analysis of host transcriptomes demonstrated an expected reduction of inflammatory responses and signaled the existence of regulatory macrophages that are unable to kill parasites. We believe the DCL pathology is a result of improperly biased B cell responses that lead to dampened macrophage inflammation and is coupled with a lack of T cell cytotoxicity. The infiltration of atypical B cells and increased IgG4/IgG2 production demonstrate a possible role in shifting the immune response away from Th1 environments necessary for parasite killing and infection resolution. In macrophages, we observe augmented immunoregulatory and anti-inflammatory responses coupled with angiogenesis, reorganization of extracellular matrix, and flourishing parasite growth. Furthermore, we cannot ignore possible parasite manipulation of the immune response and have identified parasite genes that may contribute to the diffuse nature of the disease. We also identified conserved parasite gene expression across multiple species and conditions. This knowledge is extremely important in understanding pathogen manipulation of the host and developing vaccines and therapeutics for this neglected tropical disease. Further research must be conducted to fully understand these interactions and the detrimental pathologies created.

Chapter 5: Conclusions

This work focused on characterizing the host and parasite transcriptomes in cutaneous leishmaniasis in an effort to further understand the host-pathogen interactions in this disease. We used the platform of RNA-seq to simultaneously analyze human and *Leishmania* transcripts in localized and diffuse manifestations of the disease, comparing and contrasting immune responses and parasite gene expression.

In the first part of this study, we characterized the host transcriptome in localized cutaneous leishmaniasis. Unexpectedly, our analysis discovered host responses diverging based on the presence of actively transcribing parasites. Among the 25 localized cutaneous leishmaniasis patients, we observed three distinct transcriptomic populations based on parasite transcript presence. The differences in parasite reads was unexpected considering a previous study that used RNA-seq to compare *L. braziliensis* LCL and MCL manifestations (218). In that study, Maretti-Mira et al. found the percent of reads that mapped to the parasite genome was less than or equal to 0.25 percent. However, our study contained 25 total samples, five times the number of samples in the previous study.

Using a larger sample set, we found six samples containing parasite transcripts (PT^{Pos}) whose host immune responses differed greatly from 10 samples containing no parasite transcripts (PT^{Neg}). Transcriptomic differences included increased B cell infiltration and transcription of immunoglobulin. This response is paradoxical; increased leukocyte infiltration and activation should help control infection. However, these intracellular pathogens have harnessed the opsonization and subsequent phagocytosis pathway to gain entry into and manipulate their desired host macrophages. These findings suggested that human models mimic our initial findings in murine systems that the

presence of immunoglobulin increases susceptibility to *Leishmania* infections (60). Miles et al. demonstrated that even in mice with a healing Th1 response, irrelevant IgG presence exacerbated disease. It could be that an initial immunoglobulin response to either parasite antigen or sandfly antigen allowed parasite survival in the 6 PT^{Pos} patients. Regardless, we have expanded this observation to human localized cutaneous leishmaniasis.

Markers of inflammation (IFNγ, TNF, GZMB, GLYN) and immune regulation (IL-10, CTLA4, PD-1, LAG3) also correlated well to parasite transcript presence. This displays the balance between inflammatory, inhibitory, and cytotoxic markers within this disease. If parasite persists in the lesion (PT^{Pos}), the immune response is to increase inflammatory cytokines and cytotoxic molecule secretion. These inflammatory cytokines should aid in parasite clearance. However, the increased inhibitory markers demonstrate the counterbalancing effect of IL-10 signaling to infected macrophages and inhibitory CTLA4, PD-1, and LAG3 signaling of T cell activation.

Despite low parasite transcript numbers in 19 of 25 patients, we reported parasite transcriptome information in the 6 PT^{Pos} patients. We observed remarkable uniformity among parasite gene transcription despite varied disease progression (3 early and 3 late). We know that the immune response in these six samples does not vary despite the differences in infection duration and clinical classification. Hence, it is not surprising that the parasite gene expression displays such homogeneity. Combined with data from *in vitro* infections, we noted more than 150 highly expressed parasite genes regardless of species and infection environment. We also were able to identify more than 150 genes that demonstrated a high level of expression unique to *in vivo* infection with *L.*

braziliensis. We controlled for parasite species differences by narrowing the analysis to single reciprocal orthologs based on the TriTrypDB database. While this eliminated some large gene or protein families, our analysis included 6707 genes or roughly 80% of *L. braziliensis* genes.

Expansion of our analyses to include observations in diffuse cutaneous leishmaniasis proved notable as well. Using similar methods, we characterized the host transcriptome in diffuse cutaneous leishmaniasis. Similar to LCL, host responses appear to establish early on during infection and continue unchanged over time. Most notably, we identified increased atypical B cell transcript expression and immunoglobulin isotype switching to IgG4. The upregulation of B cell marker MZB1 was unexpected considering its canonical use as a marker for marginal zone, not peripheral, B cells. The recent discovery by Schiller et al. that revealed increased presence of $MZB1^{+}$ B cells in tissue fibrosis increases our confidence that these cells contribute to DCL disease. The propensity for retention in the skin could contribute to excessive local immunoglobulin production, whereas recirculatory phenotypes could cause diffusion to other skin sites.

Increased overall immunoglobulin production in DCL lesions that contain high numbers of parasites further substantiates our claims that immunoglobulin exacerbates disease. However, it seems that more is at play in diffuse lesions after observing a striking dominance of the rare IgG4 isotype. While other isotypes, such as IgG1 and IgG2, expressed at lower levels may contribute to parasite survival via opsonization and phagocytosis, the IgG4 isotype is known to create anti-inflammatory responses through competitive and inhibitory signaling. We believe the combination of these signals amount to the perfect storm that accounts for such high parasite survival in DCL lesions.

In DCL, lower levels of Th1 effectors IFNγ, TNF, and IL1β did not correlate to higher levels of Th2 effectors or markers. In fact, both LCL and DCL lacked evidence of a Th2 response known for predicting susceptibility and parasite survival in mouse models. Additionally, markers of T cell anergy were not upregulated in DCL compared to LCL. Analysis instead suggested that simply a reduced transcription of Th1 and cytotoxic effector molecules contribute to parasite survival in DCL lesions. The lack of a Th1 dominant response limits the steps necessary for intracellular pathogen killing: macrophage activation and CTL activation.

Further still, macrophage activation states contrasted sharply when comparing LCL and DCL. Markers of M1 "classically activated" macrophages were high in LCL and low in DCL, correlating well with presumed parasite killing. Positive markers of regulatory macrophages were evident in DCL, indicative of anti-inflammatory and angiogenic macrophage responses in a subset known to possess decreased intracellular parasite killing (13). Surprisingly, no evidence of alternatively activated macrophages was observed in LCL or DCL, suggesting that murine models implicating this subset of macrophage activation as contributing to susceptibility may not translate well into human systems.

Analysis of the parasite transcriptome in diffuse lesions displayed a remarkable uniformity, regardless of the wide ranges in patient age and infection duration. This suggests that, similar to host responses, parasites gene expression does not change once infection is established in DCL. It appears that an equilibrium is reached where the host immune response is steady and parasites need not respond to changes in immune pressure.

Comparisons to *in vitro L. amazonensis* demonstrated a similarity in 75% of the transcriptome. Roughly 10% of the difference in expression in ~1900 genes is accounted for by what we believe are genes that contribute to the manifestation of diffuse disease. The rest of the difference demonstrates the potential caveat of macrophage monolayer infections. Despite the lack of immune pressure in DCL disease, there appear to still be aspects of the lesion microenvironment that manifest in differences in parasite gene expression. Additional data from *in vitro L. major* parasite transcriptomes as well as our earlier analysis of the *L. braziliensis* transcriptome revealed a similar expression pattern between DCL and senescent *in vitro* macrophage infections, differing from LCL *L. braziliensis*. We curated lists of parasite genes that may contribute to DCL manifestations and parasite genes commonly expressed at a high level regardless of species, condition, or disease manifestation. Again, we corrected for differences in parasite species by only analyzing ~6700 genes that are single reciprocal orthologs. Despite this caveat, these informative subsets must be integral to *Leishmania* infection and contain potential targets for therapeutics and vaccines.

Chapter 6: Future Directions

Continued research in the area of leishmaniasis based on this work includes future analyses at the RNA and protein levels of the host and parasite. These studies improve our knowledge of the interactions between host and pathogen and uncover contributors to disease manifestation, altered host responses, parasite virulence, and parasite survival. However, limitations based on sample availability, rarity, and special differences existed. Certain additions to the data could strengthen our conclusions.

At the inception of this project, the biopsies acquired did not include healthy skin from the endemic region. The contribution of host genetic background is believed to be minimal considering travelers to endemic regions are also susceptible to infection. However, minimizing variables increases the confidence of conclusions. Our samples did not include paired biopsies from contralateral or "healthy" skin of infected patients. In murine models, previous research has demonstrated the presence of *Leishmania*-specific T cells in contralateral areas of infected mice (169, 219). The leukocytes in non-lesion areas of the skin may not be actively participating in cell-mediated immunity but seem to be poised to do so for the purpose of immune memory. While the addition of these biopsies would differentiate between pathological and nonpathological areas of the skin, our goal was to look at differences between healthy and infected skin as well as any differences within lesions. However, the addition of endemic area healthy and contralateral skin biopsies would give a clearer view of the interactions occurring within lesions.

While our findings on transcriptomic differences in LCL and DCL lesions prove significant, follow-up experiments assessing applicability at the protein level would

certainly strengthen our conclusions. Post-translational manipulations occur and confirmation of protein expression would confirm our hypotheses regarding causative factors within and between each disease. However, sample acquisition is difficult in these endemic areas, limiting follow-up studies. Additionally, the rarity of DCL disease limits study.

Our assessment of two disease manifestations caused by two different parasites begs the question of whether or not the comparison is legitimate. We believe that despite this difference, we are still able to compare host responses that reside at opposite ends of the leishmaniasis disease spectrum. Our discovery notes that myriad factors contribute to the spectral nature of the disease and we have begun to characterize such factors. However, further RNA-seq studies would increase the robustness of our conclusions. Additional biopsies from *L. amazonensis*-infected localized cutaneous leishmaniasis would allow for direct comparisons of *in vitro* macrophage infection alongside *in vivo* LCL and DCL. While this would eliminate the difference in parasite species, we would expect the *L. amazonensis*-infected LCL lesions to exhibit characteristics more similar to DCL than to *L. braziliensis*-infected LCL. We hypothesize this because *L. amazonensis*-infected LCL lesions contain higher levels of parasite than *L. braziliensis* infection due to differences in cellular localization of parasite. Within the macrophage, a phagolysosome can contain multiple *L. amazonensis* parasites, whereas each phagolysosome in *L. braziliensis* infection contains just one parasite. Regardless, this would narrow the lists of genes and pathways responsible in diverging host responses.

In order to further study the differences between *in vitro* macrophage infections and *in vivo* lesions, biopsies of *L. major* infections from lesions could be compared to

already analyzed *in vitro* infections. In the same manner, we could compare *L. braziliensis* macrophage infections *in vitro* to already analyzed lesion data. This would help to test our hypothesis of differing parasite expression in lesion microenvironments (immune pressure) versus *in vitro* macrophage infections. Additional *in vitro* experiments using IFN-γ primed macrophages may show a higher degree of similarity in parasite gene expression to LCL lesions. All of these assessments within each parasite transcriptome would eliminate the caveat of multiple species comparisons and identify parasite genes responding to immune pressure and affecting differing manifestations.

Genomic differences in the host and parasite must also be assessed to ensure that (1) host genomic differences do not contribute to differences in disease manifestation or susceptibility and (2) the *L. amazonensis* parasite that causes LCL and DCL are the same. Analysis of SNPs may be able to confirm or reject the hypothesis regarding host and parasite differences.

Most importantly, the identified highly expressed parasite genes should be screened for contributions to virulence and survival. Because many of these genes code for hypothetical proteins, assays to determine structure, protein-protein interactions, and any contributions to virulence or survival must be completed. With this knowledge, targeted therapies could interfere with specific parasite genes or pathways, opening the door for pan-*Leishmania* therapeutics that could improve patient quality of life. The same data would also unveil new targets for vaccines that could be applied for multiple *Leishmania* species, decreasing medical costs and minimizing prevalence of this neglected tropical disease.

REFERENCES

1. Lemaitre B, Nicolas E, Michaut L, Reichhart JM, Hoffmann JA (1996) The dorsoventral regulatory gene cassette spatzle/Toll/cactus controls the potent antifungal response in *Drosophila* adults. *Cell* 86(6):973–983.
2. Janeway CAJ (1989) Approaching the asymptote? Evolution and revolution in immunology. *Cold Spring Harb Symp Quant Biol* 54 Pt 1:1–13.
3. Bianchi ME (2007) DAMPs, PAMPs and alarmins: all we need to know about danger. *J Leukoc Biol* 81(1):1–5.
4. Adelman K, et al. (2009) Immediate mediators of the inflammatory response are poised for gene activation through RNA polymerase II stalling. *Proc Natl Acad Sci U S A* 106(43):18207–18212.
5. Hamidzadeh K, Christensen SM, Dalby E, Chandrasekaran P, Mosser DM (2017) Macrophages and the Recovery from Acute and Chronic Inflammation. *Annu Rev Physiol* 79:567–592.
6. Sakaki H, Tsukimoto M, Harada H, Moriyama Y, Kojima S (2013) Autocrine regulation of macrophage activation via exocytosis of ATP and activation of P2Y11 receptor. *PLoS One* 8(4):e59778.
7. Kaczmarek E, et al. (1996) Identification and Characterization of CD39/Vascular ATP Diphosphohydrolase. *J Biol Chem* 271(51):33116–33122.
8. Zimmermann H, Braun N (1999) Ecto-nucleotidases--molecular structures, catalytic properties, and functional roles in the nervous system. *Prog Brain Res* 120:371–385.
9. Cohen HB, et al. (2013) TLR stimulation initiates a CD39-based autoregulatory mechanism that limits macrophage inflammatory responses. *Blood* 122(11):1935–1945.
10. Kuroda E, Yamashita U (2003) Mechanisms of Enhanced Macrophage-Mediated Prostaglandin E2 Production and Its Suppressive Role in Th1 Activation in Th2-Dominant BALB/c Mice. *J Immunol* 170(2):757–764.
11. MacKenzie KF, et al. (2013) PGE2 Induces Macrophage IL-10 Production and a Regulatory-like Phenotype via a Protein Kinase A–SIK–CRTC3 Pathway. *J Immunol* 190(2):565–577.
12. Spite M, et al. (2009) Resolvin D2 is a potent regulator of leukocytes and controls microbial sepsis. *Nature* 461(7268):1287–1291.
13. Mosser DM, Edwards JP (2008) Exploring the full spectrum of macrophage activation. *Nat Rev Immunol* 8(12):958–969.
14. Erwig L-P, Henson PM (2007) Immunological Consequences of Apoptotic Cell Phagocytosis. *Am J Pathol* 171(1):2–8.
15. Rhen T, Cidlowski JA (2005) Antiinflammatory Action of Glucocorticoids — New Mechanisms for Old Drugs. *N Engl J Med* 353(16):1711–1723.
16. McKay LI, Cidlowski JA (1999) Molecular Control of Immune/Inflammatory Responses: Interactions Between Nuclear Factor-κB and Steroid Receptor-Signaling Pathways. *Endocr Rev* 20(4):435–459.
17. Cato ACB, Nestl A, Mink S (2002) Rapid Actions of Steroid Receptors in Cellular Signaling Pathways. *Sci Signal* 2002(138):re9-re9.
18. Scheinman RI, Cogswell PC, Lofquist AK, Baldwin AS (1995) Role of Transcriptional Activation of IκBα in Mediation of Immunosuppression by

Glucocorticoids. *Science (80-)* 270(5234):283–286.
19. Lemke G (2013) Biology of the TAM Receptors. *Cold Spring Harb Perspect Biol* 5(11):a009076.
20. Bhardwaj S, Srivastava N, Sudan R, Saha B (2010) *Leishmania* Interferes with Host Cell Signaling to Devise a Survival Strategy. *J Biomed Biotechnol* 2010:109189.
21. Hickman SP, Chan J, Salgame P (2002) *Mycobacterium tuberculosis* Induces Differential Cytokine Production from Dendritic Cells and Macrophages with Divergent Effects on Naive T Cell Polarization. *J Immunol* 168(9):4636–4642.
22. Kim SO, Sheikh HI, Ha S-D, Martins A, Reid G (2006) G-CSF-mediated inhibition of JNK is a key mechanism for *Lactobacillus rhamnosus*-induced suppression of TNF production in macrophages. *Cell Microbiol* 8(12):1958–1971.
23. Tao MH, Smith RI, Morrison SL (1993) Structural features of human immunoglobulin G that determine isotype-specific differences in complement activation. *J Exp Med* 178(2):661 LP-667.
24. Finlay BB, McFadden G (2006) Anti-Immunology: Evasion of the Host Immune System by Bacterial and Viral Pathogens. *Cell* 124(4):767–782.
25. Kahler CM, Stephens DS (1998) Genetic Basis for Biosynthesis, Structure, and Function of Meningococcal Lipooligosaccharide (Endotoxin). *Crit Rev Microbiol* 24(4):281–334.
26. Pinger J, Chowdhury S, Papavasiliou FN (2017) Variant surface glycoprotein density defines an immune evasion threshold for African trypanosomes undergoing antigenic variation. *Nat Commun* 8(1):828.
27. Hewitson JP, Grainger JR, Maizels RM (2009) Helminth immunoregulation: The role of parasite secreted proteins in modulating host immunity. *Mol Biochem Parasitol* 167(1):1–11.
28. Gebert B, Fischer W, Weiss E, Hoffmann R, Haas R (2003) *Helicobacter pylori* Vacuolating Cytotoxin Inhibits T Lymphocyte Activation. *Science (80-)* 301(5636):1099 LP-1102.
29. Boulton IC, Gray-Owen SD (2002) Neisserial binding to CEACAM1 arrests the activation and proliferation of CD4+ T lymphocytes. *Nat Immunol* 3:229.
30. Ahr B, Robert-Hebmann V, Devaux C, Biard-Piechaczyk M (2004) Apoptosis of uninfected cells induced by HIV envelope glycoproteins. *Retrovirology* 1(1):12.
31. Badr G, et al. (2005) HIV Type 1 Glycoprotein 120 Inhibits Human B Cell Chemotaxis to CXC Chemokine Ligand (CXCL) 12, CC Chemokine Ligand (CCL)20, and CCL21. *J Immunol* 175(1):302 LP-310.
32. Perfettini J-L, et al. (2005) Mechanisms of apoptosis induction by the HIV-1 envelope. *Cell Death Differ* 12:916.
33. Heath WR, Carbone FR (2013) The skin-resident and migratory immune system in steady state and memory: innate lymphocytes, dendritic cells and T cells. *Nat Immunol* 14:978.
34. Nestle FO, Di Meglio P, Qin J-Z, Nickoloff BJ (2009) Skin immune sentinels in health and disease. *Nat Rev Immunol* 9:679.
35. Ouchi T, et al. (2011) Langerhans cell antigen capture through tight junctions confers preemptive immunity in experimental staphylococcal scalded skin syndrome. *J Exp Med* 208(13):2607 LP-2613.

36. Kautz-Neu K, et al. (2011) Langerhans cells are negative regulators of the anti-Leishmania response. *J Exp Med* 208(5):885 LP-891.
37. Seneschal J, Clark RA, Gehad A, Baecher-Allan CM, Kupper TS (2018) Human Epidermal Langerhans Cells Maintain Immune Homeostasis in Skin by Activating Skin Resident Regulatory T Cells. *Immunity* 36(5):873–884.
38. Uwe R, Anja M, Christina S, Heinrich K (2004) CD8α- and Langerin-negative dendritic cells, but not Langerhans cells, act as principal antigen-presenting cells in leishmaniasis. *Eur J Immunol* 34(6):1542–1550.
39. Kim BS, et al. (2013) TSLP Elicits IL-33–Independent Innate Lymphoid Cell Responses to Promote Skin Inflammation. *Sci Transl Med* 5(170):170ra16 LP-170ra16.
40. Toulon A, et al. (2009) A role for human skin–resident T cells in wound healing. *J Exp Med* 206(4):743 LP-750.
41. Gurtner GC, Werner S, Barrandon Y, Longaker MT (2008) Wound repair and regeneration. *Nature* 453:314.
42. Zielins ER, et al. (2014) Wound healing: an update. *Regen Med* 9(6):817–830.
43. Baum CL, Arpey CJ (2005) Normal cutaneous wound healing: clinical correlation with cellular and molecular events. *Dermatol Surg* 31(6):674–86; discussion 686.
44. Wilgus TA, Roy S, McDaniel JC (2013) Neutrophils and Wound Repair: Positive Actions and Negative Reactions. *Adv Wound Care* 2(7):379–388.
45. Takeo M, Lee W, Ito M (2015) Wound Healing and Skin Regeneration. *Cold Spring Harb Perspect Med* 5(1):a023267.
46. Dang CM, et al. (2003) Scarless Fetal Wounds Are Associated with an Increased Matrix Metalloproteinase–to–Tissue-Derived Inhibitor of Metalloproteinase Ratio. *Plast Reconstr Surg* 111(7).
47. Bao P, et al. (2018) The Role of Vascular Endothelial Growth Factor in Wound Healing. *J Surg Res* 153(2):347–358.
48. Novais FO, et al. (2015) Genomic Profiling of Human *Leishmania braziliensis* Lesions Identifies Transcriptional Modules Associated with Cutaneous Immunopathology. *J Invest Dermatol* 135(1):94–101.
49. Aderem A, Underhill DM (1999) Mechanisms Of Phagocytosis In Macrophages. *Annu Rev Immunol* 17(1):593–623.
50. Jayakumar A, Donovan MJ, Tripathi V, Ramalho-Ortigao M, McDowell MA (2008) *Leishmania major* Infection Activates NF-κB and Interferon Regulatory Factors 1 and 8 in Human Dendritic Cells. *Infect Immun* 76(5):2138–2148.
51. Weiss G, Schaible UE (2015) Macrophage defense mechanisms against intracellular bacteria. *Immunol Rev* 264(1):182–203.
52. Nathan C, Shiloh MU (2000) Reactive oxygen and nitrogen intermediates in the relationship between mammalian hosts and microbial pathogens. *Proc Natl Acad Sci U S A* 97(16):8841–8848.
53. Fang FC (2004) Antimicrobial reactive oxygen and nitrogen species: concepts and controversies. *Nat Rev Microbiol* 2:820.
54. Matzaraki V, Kumar V, Wijmenga C, Zhernakova A (2017) The MHC locus and genetic susceptibility to autoimmune and infectious diseases. *Genome Biol* 18:76.
55. Fiorentino DF, Zlotnik A, Mosmann TR, Howard M, O'Garra A (1991) IL-10 inhibits cytokine production by activated macrophages. *J Immunol* 147(11):3815–

3822.
56. Engelhardt KR, Grimbacher B (2014) IL-10 in Humans: Lessons from the Gut, IL-10/IL-10 Receptor Deficiencies, and IL-10 Polymorphisms. In: Fillatreau S., O'Garra A. (eds) Interleukin-10 in Health and Disease. Current Topics in Microbiology and Immunology, vol 380. Springer, Berlin, Heidelberg
57. Mosser DM, Zhang X (2008) Interleukin-10: new perspectives on an old cytokine. *Immunol Rev* 226:205–218.
58. Sutterwala FS, Noel GJ, Clynes R, Mosser DM (1997) Selective Suppression of Interleukin-12 Induction after Macrophage Receptor Ligation. *J Exp Med* 185(11):1977–1985.
59. Fleming BD, et al. (2015) The generation of macrophages with anti-inflammatory activity in the absence of STAT6 signaling. *J Leukoc Biol* 98(3):395–407.
60. Miles SA, Conrad SM, Alves RG, Jeronimo SMB, Mosser DM (2005) A role for IgG immune complexes during infection with the intracellular pathogen *Leishmania*. *J Exp Med* 201(5):747–754.
61. Massagué J (2012) TGFβ signalling in context. *Nat Rev Mol Cell Biol* 13(10):616–630.
62. Fadok VA, et al. (1998) Macrophages that have ingested apoptotic cells in vitro inhibit proinflammatory cytokine production through autocrine/paracrine mechanisms involving TGF-beta, PGE2, and PAF. *J Clin Invest* 101(4):890–898.
63. Kuruvilla AP, et al. (1991) Protective effect of transforming growth factor beta 1 on experimental autoimmune diseases in mice. *Proc Natl Acad Sci* 88(7):2918–2921.
64. Racke MK, et al. (1991) Prevention and treatment of chronic relapsing experimental allergic encephalomyelitis by transforming growth factor-beta 1. *J Immunol* 146(9):3012–3017.
65. Willis BC, Borok Z (2007) TGF-β-induced EMT: mechanisms and implications for fibrotic lung disease. *Am J Physiol - Lung Cell Mol Physiol* 293(3):L525–L534.
66. Mills CD (2012) M1 and M2 Macrophages: Oracles of Health and Disease. *Crit Rev Immunol* 32(6):463–488.
67. Gordon S (2003) Alternative activation of macrophages. *Nat Rev Immunol* 3:23.
68. Loke P, et al. (2002) IL-4 dependent alternatively-activated macrophages have a distinctive in vivo gene expression phenotype. *BMC Immunol* 3:7.
69. Mantovani A, et al. (2004) The chemokine system in diverse forms of macrophage activation and polarization. *Trends Immunol* 25(12):677–686.
70. Martinez FO, Gordon S (2014) The M1 and M2 paradigm of macrophage activation: time for reassessment. *F1000Prime Rep* 6:13.
71. Martinez FO, et al. (2013) Genetic programs expressed in resting and IL-4 alternatively activated mouse and human macrophages: similarities and differences. *Blood* 121(9):57-69.
72. Scott P, Novais FO (2016) Cutaneous leishmaniasis: immune responses in protection and pathogenesis. *Nat Rev Immunol* 16:581.
73. WHO | Global leishmaniasis update, 2006–2015: a turning point in leishmaniasis surveillance (2017) *WHO*. Available at: http://www.who.int/leishmaniasis/resources/who_wer9238/en/#.WpSC_RPKEGM

.mendeley [Accessed February 26, 2018].
74. Scorza MB, Carvalho ME, Wilson EM (2017) Cutaneous Manifestations of Human and Murine Leishmaniasis. *Int J Mol Sci* 18(6).
75. Scott P, Natovitz P, Coffman RL, Pearce E, Sher A (1988) Immunoregulation of cutaneous leishmaniasis. T cell lines that transfer protective immunity or exacerbation belong to different T helper subsets and respond to distinct parasite antigens. *J Exp Med* 168(5):1675–84.
76. Heinzel FP, Sadick MD, Mutha SS, Locksley RM (1991) Production of interferon gamma, interleukin 2, interleukin 4, and interleukin 10 by CD4+ lymphocytes in vivo during healing and progressive murine leishmaniasis. *Proc Natl Acad Sci U S A* 88(16):7011–7015.
77. Sypek J, et al. (1993) Resolution of cutaneous leishmaniasis: interleukin 12 initiates a protective T helper type 1 immune response. *J Exp Med* 177(6):1797–1802.
78. Heinzel F, Schoenhaut D, Rerko R, Rosser L, Gately M (1993) Recombinant interleukin 12 cures mice infected with *Leishmania major*. *J Exp Med* 177(5):1505–1509.
79. Bogdan C, Moll H, Solbach W, Röllinghoff M (1990) Tumor necrosis factor-α in combination with interferon-γ, but not with interleukin 4 activates murine macrophages for elimination of *Leishmania major* amastigotes. *Eur J Immunol* 20(5):1131–1135.
80. Chatelain R, Varkila K, Coffman RL (1992) IL-4 induces a Th2 response in *Leishmania major*-infected mice. *J Immunol* 148(4):1182-1187.
81. Kane MM, Mosser DM (2001) The role of IL-10 in promoting disease progression in leishmaniasis. *J Immunol* 166(2):1141–1147.
82. Murphy ML, Wille U, Villegas EN, Hunter CA, Farrell JP (2001) IL-10 mediates susceptibility to *Leishmania donovani* infection. *Eur J Immunol* 31(10):2848–2856.
83. Padigel UM, Alexander J, Farrell JP (2003) The Role of Interleukin-10 in Susceptibility of BALB/c Mice to Infection with *Leishmania mexicana* and *Leishmania amazonensis*. *J Immunol* 171(7):3705-3710.
84. Scott P, Eaton A, Gause WC, di Zhou X, Hondowicz B (1996) Early IL-4 Production Does Not Predict Susceptibility to *Leishmania major*. *Exp Parasitol* 84(2):178–187.
85. Li J, Scott P, Farrell JP (1996) In vivo alterations in cytokine production following interleukin-12 (IL-12) and anti-IL-4 antibody treatment of CB6F1 mice with chronic cutaneous leishmaniasis. *Infect Immun* 64(12):5248–5254.
86. Biedermann T, et al. (2001) IL-4 instructs TH1 responses and resistance to *Leishmania major* in susceptible BALB/c mice. *Nat Immunol* 2(11):1054–1060.
87. Cáceres-Dittmar G, et al. (1993) Determination of the cytokine profile in American cutaneous leishmaniasis using the polymerase chain reaction. *Clin Exp Immunol* 91(3):500–505.
88. Pirmez C, et al. (1993) Cytokine patterns in the pathogenesis of human leishmaniasis. *J Clin Invest* 91(4):1390–1395.
89. Santos C da S, et al. (2013) CD8(+) Granzyme B(+)–Mediated Tissue Injury vs. CD4(+)IFNγ(+)–Mediated Parasite Killing in Human Cutaneous Leishmaniasis. *J*

Invest Dermatol 133(6):1533–1540.
90. Bacellar O, et al. (2002) Up-Regulation of Th1-Type Responses in Mucosal Leishmaniasis Patients. *Infect Immun* 70(12):6734–6740.
91. Melby PC, et al. (1994) Increased expression of proinflammatory cytokines in chronic lesions of human cutaneous leishmaniasis. *Infect Immun* 62(3):837–842.
92. Keyhani A, Riazi-Rad F, Pakzad SR, Ajdary S (2014) Human polymorphonuclear leukocytes produce cytokines in response to *Leishmania major* promastigotes. *Apmis* 122(9):891–898.
93. Kumar R, Bumb RA, Salotra P (2010) Evaluation of localized and systemic immune responses in cutaneous leishmaniasis caused by *Leishmania tropica*: Interleukin-8, monocyte chemotactic protein-1 and nitric oxide are major regulatory factors. *Immunology* 130(2):193–201.
94. Tapia FJ, Caceres-Dittmar G, Sanchez MA, Fernandez AE, Convit J (1993) The cutaneous lesion in American leishmaniasis: Leukocyte subsets, cellular interaction and cytokine production. *Biol Res* 26(1–2):239–247.
95. Costa-Silva MF, et al. (2014) Gene expression profile of cytokines and chemokines in skin lesions from Brazilian Indians with localized cutaneous leishmaniasis. *Mol Immunol* 57(2):74–85.
96. Bomfim G, et al. (1996) Variation of Cytokine Patterns Related to Therapeutic Response in Diffuse Cutaneous Leishmaniasis. *Exp Parasitol* 84(2):188–194.
97. Valencia-Pacheco G, et al. (2014) In situ cytokines (IL-4, IL-10, IL-12, IFN-γ) and chemokines (MCP-1, MIP-1α) gene expression in human *Leishmania (Leishmania) mexicana* infection. *Cytokine* 69(1):56–61.
98. Manamperi NH, et al. (2017) In situ immunopathological changes in cutaneous leishmaniasis due to *Leishmania donovani*. *Parasite Immunol* 39(3).
99. Kammoun-Rebai W, et al. (2016) Protein biomarkers discriminate *Leishmania major*-infected and non-infected individuals in areas endemic for cutaneous leishmaniasis. *BMC Infect Dis* 16:138.
100. Rocha PN, et al. (1999) Down-Regulation of Th1 Type of Response in Early Human American Cutaneous Leishmaniasis. *J Infect Dis* 180(5):1731–1734.
101. Hejazi SH, Hoseini SG, Javanmard SH, Zarkesh SH, Khamesipour A (2012) Interleukin-10 and Transforming Growth Factor-β in Early and Late Lesions of Patients with *Leishmania major* Induced Cutaneous Leishmaniasis. *Iran J Parasitol* 7(3):16–23.
102. Louzir H, et al. (1998) Immunologic determinants of disease evolution in localized cutaneous leishmaniasis due to *Leishmania major*. *J Infect Dis* 177(6):1687–1695.
103. Cardoso TM, et al. (2015) Protective and Pathological Functions of CD8(+) T Cells in *Leishmania braziliensis* Infection. *Infect Immun* 83(3):898–906.
104. Da-Cruz AM, Conceição-Silva F, Bertho AL, Coutinho SG (1994) *Leishmania*-reactive CD4+ and CD8+ T cells associated with cure of human cutaneous leishmaniasis. *Infect Immun* 62(6):2614–2618.
105. Esterre P, Dedet JP, Frenay C, Chevallier M, Grimaud JA (1992) Cell populations in the lesion of human cutaneous leishmaniasis: a light microscopical, immunohistochemical and ultrastructural study. *Virchows Arch A Pathol Anat Histopathol* 421(3):239–247.
106. Laskay T, van Zandbergen G, Solbach W (2003) Neutrophil granulocytes – Trojan

horses for *Leishmania major* and other intracellular microbes? *Trends Microbiol* 11(5):210–214.
107. Novais FO, et al. (2013) Cytotoxic T Cells Mediate Pathology and Metastasis in Cutaneous Leishmaniasis. *PLoS Pathog* 9(7):e1003504.
108. Antonelli LR V, et al. (2005) Activated inflammatory T cells correlate with lesion size in human cutaneous leishmaniasis. *Immunol Lett* 101(2):226–230.
109. Costa DL, et al. (2015) Tr-1–Like CD4(+)CD25(−)CD127(−/low)FOXP3(−) Cells Are the Main Source of Interleukin 10 in Patients With Cutaneous Leishmaniasis Due to *Leishmania braziliensis*. *J Infect Dis* 211(5):708–718.
110. Campanelli AP, et al. (2006) CD4+CD25+ T Cells in Skin Lesions of Patients with Cutaneous Leishmaniasis Exhibit Phenotypic and Functional Characteristics of Natural Regulatory T Cells. *J Infect Dis* 193(9):1313–1322.
111. Bogdan C (2012) Natural killer cells in experimental and human leishmaniasis. *Front Cell Infect Microbiol* 2:69.
112. Ehrchen JM, et al. (2010) Keratinocytes Determine Th1 Immunity during Early Experimental Leishmaniasis. *PLoS Pathog* 6(4):e1000871.
113. Wanasen N, Xin L, Soong L (2008) Pathogenic role of B cells and antibodies in murine *Leishmania amazonensis* infection. *Int J Parasitol* 38(3–4):417–429.
114. Gaafar A, et al. (1999) Characterization of the Local and Systemic Immune Responses in Patients with Cutaneous Leishmaniasis Due to *Leishmania major*. *Clin Immunol* 91(3):314–320.
115. Guy RA, Belosevic M (1993) Comparison of receptors required for entry of *Leishmania major* amastigotes into macrophages. *Infect Immun* 61(4):1553–1558.
116. Sutterwala FS, Noel GJ, Salgame P, Mosser DM (1998) Reversal of Proinflammatory Responses by Ligating the Macrophage Fcγ Receptor Type I . *J Exp Med* 188(1):217–222.
117. Chu N, Thomas BN, Patel SR, Buxbaum LU (2010) IgG1 Is Pathogenic in *Leishmania mexicana* Infection. *J Immunol* 185(11):6939-6946.
118. Kima PE, et al. (2000) Internalization of *Leishmania mexicana* Complex Amastigotes via the Fc Receptor Is Required to Sustain Infection in Murine Cutaneous Leishmaniasis. *J Exp Med* 191(6):1063-1068.
119. Buxbaum LU, Scott P (2005) Interleukin 10- and Fcγ Receptor-Deficient Mice Resolve *Leishmania mexicana* Lesions . *Infect Immun* 73(4):2101–2108.
120. Thomas BN, Buxbaum LU (2008) FcγRIII Mediates Immunoglobulin G-Induced Interleukin-10 and Is Required for Chronic *Leishmania mexicana* Lesions. *Infect Immun* 76(2):623–631.
121. Silveira FT, Lainson R, Corbett CEP (2004) Clinical and immunopathological spectrum of American cutaneous leishmaniasis with special reference to the disease in Amazonian Brazil: a review. *Memórias do Inst Oswaldo Cruz* 99:239–251.
122. Chagas E, Corrêa C, Silveira F (1999) valiação da resposta imune humoral através do teste de imunofluorescência indireta na leishmaniose cutânea causada por *Leishmania (L.) amazonensis* na região Amazônica do Brasil. *Rev Soc Bras Med Trop* 32:26.
123. Chagas E, Ishikawa E, Silveira F (2001) Humoral response (IgG) in the borderline disseminated cutaneous leishmaniasis (BDCL) caused by *Leishmania (L.)*

amazonensis in Pará State, Brazil. *WOLRDleish 2, Crete, Greece* P226:118.
124. Casadevall A, Pirofski L (2012) Immunoglobulins In Defense, Pathogenesis And Therapy Of Fungal Diseases. *Cell Host Microbe* 11(5):447–456.
125. de Souza Testasicca MC, et al. (2014) Antibody responses induced by Leish-Tec®, an A2-based vaccine for visceral leishmaniasis, in a heterogeneous canine population. *Vet Parasitol* 204(3):169–176.
126. Moreno J, et al. (2012) Use of a LiESP/QA-21 Vaccine (CaniLeish) Stimulates an Appropriate Th1-Dominated Cell-Mediated Immune Response in Dogs. *PLoS Negl Trop Dis* 6(6):e1683.
127. Fernandes AP, Coelho EAF, Machado-Coelho GLL, Grimaldi G, Gazzinelli RT (2012) Making an anti-amastigote vaccine for visceral leishmaniasis: rational, update and perspectives. *Curr Opin Microbiol* 15(4):476–485.
128. Fernandes AP, et al. (2008) Protective immunity against challenge with *Leishmania (Leishmania) chagasi* in beagle dogs vaccinated with recombinant A2 protein. *Vaccine* 26(46):5888–5895.
129. Brittingham A, et al. (1995) Role of the Leishmania surface protease gp63 in complement fixation, cell adhesion, and resistance to complement-mediated lysis. *J Immunol* 155(6):3102 LP-3111.
130. Mosser DM, Edelson PJ (1985) The mouse macrophage receptor for C3bi (CR3) is a major mechanism in the phagocytosis of *Leishmania* promastigotes. *J Immunol* 135(4):2785 LP-2789.
131. Kane MM, Mosser DM (2000) *Leishmania* parasites and their ploys to disrupt macrophage activation. *Curr Opin Hematol* 7(1).
132. Olivier M, Gregory DJ, Forget G (2005) Subversion Mechanisms by Which *Leishmania* Parasites Can Escape the Host Immune Response: a Signaling Point of View. *Clin Microbiol Rev* 18(2):293–305.
133. Muleme HM, et al. (2009) Infection with arginase deficient *Leishmania major* reveals a parasite number-dependent and cytokine-independent regulation of host cellular arginase activity and disease pathogenesis. *J Immunol* 183(12):8068–8076.
134. Shio MT, Olivier M (2010) Editorial: *Leishmania* survival mechanisms: the role of host phosphatases. *J Leukoc Biol* 88(1):1–3.
135. Gupta G, Oghumu S, Satoskar AR (2014) Mechanisms of Immune Evasion in Leishmaniasis. *Adv Appl Microbiol* 82:1–23.
136. Olivier M, Atayde VD, Isnard A, Hassani K, Shio MT (2012) Leishmania virulence factors: focus on the metalloprotease GP63. *Microbes Infect* 14(15):1377–1389.
137. Abu-Dayyeh I, Hassani K, Westra ER, Mottram JC, Olivier M (2010) Comparative Study of the Ability of *Leishmania mexicana* Promastigotes and Amastigotes To Alter Macrophage Signaling and Functions. *Infect Immun* 78(6):2438–2445.
138. Gregory DJ, Godbout M, Contreras I, Forget G, Olivier M (2008) A novel form of NF-κB is induced by *Leishmania* infection: Involvement in macrophage gene expression. *Eur J Immunol* 38(4):1071–1081.
139. Contreras I, et al. (2010) *Leishmania*-Induced Inactivation of the Macrophage Transcription Factor AP-1 Is Mediated by the Parasite Metalloprotease GP63. *PLOS Pathog* 6(10):e1001148.

140. Jaramillo M, et al. (2018) *Leishmania* Repression of Host Translation through mTOR Cleavage Is Required for Parasite Survival and Infection. *Cell Host Microbe* 9(4):331–341.
141. Holm Å, Tejle K, Magnusson K-E, Descoteaux A, Rasmusson B (2001) *Leishmania donovani* lipophosphoglycan causes periphagosomal actin accumulation: correlation with impaired translocation of PKCα and defective phagosome maturation. *Cell Microbiol* 3(7):439–447.
142. Vinet AF, Fukuda M, Turco SJ, Descoteaux A (2009) The *Leishmania donovani* Lipophosphoglycan Excludes the Vesicular Proton-ATPase from Phagosomes by Impairing the Recruitment of Synaptotagmin V. *PLOS Pathog* 5(10):e1000628.
143. Chan J, et al. (1989) Microbial glycolipids: possible virulence factors that scavenge oxygen radicals. *Proc Natl Acad Sci USA* 86(7):2453–2457.
144. Lo SK, et al. (1998) Leishmania lipophosphoglycan reduces monocyte transendothelial migration: modulation of cell adhesion molecules, intercellular junctional proteins, and chemoattractants. *J Immunol* 160(4):1857–1865.
145. Jacques I, Andrews NW, Huynh C (2010) Functional characterization of LIT1, the *Leishmania amazonensis* ferrous iron transporter. *Mol Biochem Parasitol* 170(1):28.
146. Wang Z, Gerstein M, Snyder M (2009) RNA-Seq: A revolutionary tool for transcriptomics. *Nat Rev Genet* 10(1):57–63.
147. Cloonan N, et al. (2008) Stem cell transcriptome profiling via massive-scale mRNA sequencing. *Nat Methods* 5:613.
148. Bolger AM, Lohse M, Usadel B (2014) Trimmomatic: a flexible trimmer for Illumina sequence data. *Bioinformatics* 30(15):2114–2120.
149. Trapnell C, Pachter L, Salzberg SL (2009) TopHat: discovering splice junctions with RNA-Seq. *Bioinformatics* 25(9):1105–1111.
150. Anders S, Pyl PT, Huber W (2015) HTSeq—a Python framework to work with high-throughput sequencing data. *Bioinformatics* 31(2):166–169.
151. Anders S, et al. (2013) Count-based differential expression analysis of RNA sequencing data using R and Bioconductor. *Nat Protocols* 8(9):1765–1786.
152. Bolstad BM, Irizarry RA, Åstrand M, Speed TP (2003) A comparison of normalization methods for high density oligonucleotide array data based on variance and bias. *Bioinformatics* 19(2):185–193.
153. Smyth GK (2004) Linear Models and Empirical Bayes Methods for Assessing Differential Expression in Microarray Experiments. *Stat Appl Genet Mol Biol* 3:1.
154. Law CW, Chen Y, Shi W, Smyth GK (2014) voom: precision weights unlock linear model analysis tools for RNA-seq read counts. *Genome Biol* 15(2):R29.
155. Bolotin DA, et al. (2015) MiXCR: software for comprehensive adaptive immunity profiling. *Nat Methods* 12:380.
156. Vander Heiden JA, et al. (2014) pRESTO: a toolkit for processing high-throughput sequencing raw reads of lymphocyte receptor repertoires. *Bioinformatics* 30(13):1930–1932.
157. Alamyar E, Duroux P, Lefranc M-P, Giudicelli V (2012) IMGT® Tools for the Nucleotide Analysis of Immunoglobulin (IG) and T Cell Receptor (TR) V-(D)-J Repertoires, Polymorphisms, and IG Mutations: IMGT/V-QUEST and IMGT/HighV-QUEST for NGS. In: Immunogenetics: Methods and Applications

in Clinical Practice. eds Christiansen FT, Tait BD (Humana Press, Totowa, NJ), pp 569–604.
158. Li S, et al. (2013) IMGT/HighV QUEST paradigm for T cell receptor IMGT clonotype diversity and next generation repertoire immunoprofiling. *Nat Commun* 4:2333.
159. Bischof J, Ibrahim SM (2016) bcRep: R Package for Comprehensive Analysis of B Cell Receptor Repertoire Data. *PLoS One* 11(8):e0161569.
160. Das S, et al. (2014) Lipid Isolated from a *Leishmania donovani* Strain Reduces Escherichia coli Induced Sepsis in Mice through Inhibition of Inflammatory Responses. *Mediators Inflamm* 2014:409694.
161. Castellucci LC, et al. (2014) Host genetic factors in American cutaneous leishmaniasis: a critical appraisal of studies conducted in an endemic area of Brazil. *Mem Inst Oswaldo Cruz* 109(3):279–288.
162. Giudice A, et al. (2012) Macrophages participate in host protection and the disease pathology associated with *Leishmania braziliensis* infection. *BMC Infect Dis* 12:75.
163. Novais FO, et al. (2009) Neutrophils and macrophages cooperate in host resistance against *Leishmania braziliensis* infection. *J Immunol* 183(12):8088–8098.
164. Ronet C, et al. (2010) Regulatory B cells shape the development of Th2 immune responses in BALB/c mice infected with *Leishmania major* through IL-10 production. *J Immunol* 184(2):886–894.
165. Conrad SM, Strauss-Ayali D, Field AE, Mack M, Mosser DM (2007) *Leishmania*-derived murine monocyte chemoattractant protein 1 enhances the recruitment of a restrictive population of CC chemokine receptor 2-positive macrophages. *Infect Immun* 75(2):653–665.
166. Goncalves R, Zhang X, Cohen H, Debrabant A, Mosser DM (2011) Platelet activation attracts a subpopulation of effector monocytes to sites of *Leishmania major* infection. *J Exp Med* 208(6):1253–1265.
167. ElHassan AM, Gaafar A, Theander TG (1995) Antigen-presenting cells in human cutaneous leishmaniasis due to *Leishmania major*. *Clin Exp Immunol* 99(3):445–453.
168. Diaz NL, et al. (2002) Intermediate or chronic cutaneous leishmaniasis: leukocyte immunophenotypes and cytokine characterisation of the lesion. *Exp Dermatol* 11(1):34–41.
169. Glennie ND, et al. (2015) Skin-resident memory CD4+ T cells enhance protection against *Leishmania major* infection. *J Exp Med* 212(9):1405–1414.
170. Naik S, et al. (2012) Compartmentalized Control of Skin Immunity by Resident Commensals. *Science* 337(6098):1115–1119.
171. Fernandes MC, et al. (2016) Dual Transcriptome Profiling of *Leishmania*-Infected Human Macrophages Reveals Distinct Reprogramming Signatures. *mBio* 7(3).
172. Lessa MM, et al. (2007) Mucosal leishmaniasis: epidemiological and clinical aspects. *Braz J Otorhinolaryngol* 73(6):843–847.
173. de Oliveira CI, Brodskyn CI (2012) The immunobiology of *Leishmania braziliensis* infection. *Front Immunol* 3:145.
174. Gollob KJ, Viana AG, Dutra WO (2014) Immunoregulation in Human American Leishmaniasis: Balancing Pathology and Protection. *Parasite Immunol* 36(8):367–

376.
175. Belkaid Y, et al. (2001) The Role of Interleukin (IL)-10 in the Persistence of *Leishmania major* in the Skin after Healing and the Therapeutic Potential of Anti–IL-10 Receptor Antibody for Sterile Cure. *J Exp Med* 194(10):1497–1506.
176. Murray HW, Berman JD, Davies CR, Saravia NG (2005) Advances in leishmaniasis. *Lancet* 366(9496):1561–1577.
177. Hurdayal R, Brombacher F (2017) Interleukin-4 receptor alpha: From innate to adaptive immunity in murine models of cutaneous leishmaniasis. *Front Immunol* 8(NOV).
178. Saha A, et al. (2014) Prostaglandin E2 Negatively Regulates the Production of Inflammatory Cytokines/Chemokines and IL-17 in Visceral Leishmaniasis. *J Immunol* 193(5):2330–2339.
179. Christensen SM, et al. (2016) Meta-transcriptome Profiling of the Human-*Leishmania braziliensis* Cutaneous Lesion. *PLoS Negl Trop Dis*. 10(9): e0004992.
180. Convit J, Lapenta P (1946) Sobre un caso de leishmaniose tegumentaria de forma disseminada. *Rev la Policlin* 18:153–158.
181. Lainson R (1983) The American leishmaniases: some observations on their ecology and epidemiology. *Trans R Soc Trop Med Hyg* 77(5):569–596.
182. Bittencourt A, Guimarães N (1968) Imunopatologia da leishmaniose tegumentar difusa. *Med Cutan Ibero Lat Am* 2:395–402.
183. Bittencourt AL, Barral A (1991) Evaluation of the histopathological classifications of American cutaneous and mucocutaneous leishmaniasis . *Memórias do Inst Oswaldo Cruz* 86:51–56.
184. Silveira FT, Moraes MAP, Lainson R, Shaw JJ (1990) Leishmaniose cutânea experimental. III- Aspectos histopatológicos do comportamento evolutivo da lesão cutânea produzida em Cebus apella (Primates: Cebidae) por *Leishmania (Viannia) lainsoni, L. (V.) braziliensis e L. (Leishmania) amazonensis*. *Rev do Inst Med Trop São Paulo* 32:387–394.
185. Moraes MAP, Silveira FT (1994) Histopatologia da forma localizada de leishmaniose cutânea por *Leishmania (Leishmania) amazonensis*. *Rev do Inst Med Trop São Paulo* 36:459–463.
186. Silveira FT, Lainson R, Gomes CMC, Laurenti MD, Corbett CEP (2008) Reviewing the role of the dendritic Langerhans cells in the immunopathogenesis of American cutaneous leishmaniasis. *Trans R Soc Trop Med Hyg* 102(11):1075–1080.
187. Rodriguez-Pinto D, Saravia NG, McMahon-Pratt D (2014) CD4 T cell activation by B cells in human *Leishmania (Viannia)* infection. *BMC Infect Dis* 14:108.
188. de Jong BG, et al. (2017) Human IgG2- and IgG4-expressing memory B cells display enhanced molecular and phenotypic signs of maturity and accumulate with age. *Immunol Cell Biol* 95:744.
189. Bruhns P (2012) Properties of mouse and human IgG receptors and their contribution to disease models. *Blood* 119(24):5640 LP-5649.
190. Collins AM, Jackson KJL (2013) A temporal model of human IgE and IgG antibody function. *Front Immunol* 4(AUG):1–6.
191. Vidarsson G, Dekkers G, Rispens T (2014) IgG Subclasses and Allotypes: From Structure to Effector Functions. *Front Immunol* 5:520.

192. Lang D, Zwerina J, Pieringer H (2016) IgG4-related disease: current challenges and future prospects. *Ther Clin Risk Manag* 12:189–199.
193. Haldar D, Hirschfield GM (2017) Deciphering the biology of IgG4-related disease: specific antigens and disease? *Gut*. Published Online First: 03 November 2017. doi: 10.1136/gutjnl-2017-314861
194. van der Neut Kolfschoten M, et al. (2007) Anti-Inflammatory Activity of Human IgG4 Antibodies by Dynamic Fab Arm Exchange. *Science (80-)* 317(5844):1554-1557.
195. Ulrich M, Rodriguez V, Centeno M, Convit J (1995) Differing antibody IgG isotypes in the polar forms of leprosy and cutaneous leishmaniasis characterized by antigen-specific T cell anergy. *Clin Exp Immunol* 100(1):54–8.
196. Zouali M, Richard Y (2011) Marginal Zone B-Cells, a Gatekeeper of Innate Immunity. *Front Immunol* 2:63.
197. Weller S, et al. (2004) Human blood IgM "memory" B cells are circulating splenic marginal zone B cells harboring a prediversified immunoglobulin repertoire. *Blood* 104(12):3647–3654.
198. Dunn-Walters DK, Isaacson PG, Spencer J (1995) Analysis of mutations in immunoglobulin heavy chain variable region genes of microdissected marginal zone (MGZ) B cells suggests that the MGZ of human spleen is a reservoir of memory B cells. *J Exp Med* 182(2):559–66.
199. Tangye SG, Liu Y-J, Aversa G, Phillips JH, de Vries JE (1998) Identification of Functional Human Splenic Memory B Cells by Expression of CD148 and CD27. *J Exp Med* 188(9):1691–1703.
200. Weill J-C, Weller S, Reynaud C-A (2009) Human marginal zone B cells. *Annu Rev Immunol* 27:267–285.
201. Weller S, et al. (2008) Somatic diversification in the absence of antigen-driven responses is the hallmark of the IgM(+)IgD(+)CD27(+) B cell repertoire in infants. *J Exp Med* 205(6):1331–1342.
202. Zouali M (2008) B lymphocytes--chief players and therapeutic targets in autoimmune diseases. *Front Biosci* 13:4852–4861.
203. Attanavanich K, Kearney JF (2004) Marginal Zone, but Not Follicular B Cells, Are Potent Activators of Naive CD4 T Cells. *J Immunol* 172(2):803-811.
204. Schiller HB, et al. (2017) Deep Proteome Profiling Reveals Common Prevalence of MZB1-Positive Plasma B Cells in Human Lung and Skin Fibrosis. *Am J Respir Crit Care Med* 196(10):1298–1310.
205. Heinzel FP, Sadick MD, Holaday BJ, Coffman RL, Locksley RM (1989) Reciprocal expression of interferon gamma or interleukin 4 during the resolution or progression of murine leishmaniasis. Evidence for expansion of distinct helper T cell subsets. *J Exp Med* 169(1):59–72.
206. Cáceres-Dittmar G, et al. (1993) Determination of the cytokine profile in American cutaneous leishmaniasis using the polymerase chain reaction. *Clin Exp Immunol* 91(3):500–505.
207. Walch M, et al. (2014) Cytotoxic cells kill intracellular bacteria through Granulysin-mediated delivery of Granzymes. *Cell* 157(6):1309–1323.
208. Dotiwala F, et al. (2016) Killer lymphocytes use granulysin, perforin and granzymes to kill intracellular parasites. *Nat Med* 22(2):210–216.

209. Kellermayer Z, et al. (2014) Marginal Zone Macrophage Receptor MARCO Is Trapped in Conduits Formed by Follicular Dendritic Cells in the Spleen. *J Histochem Cytochem* 62(6):436–449.
210. Balázs M, Martin F, Zhou T, Kearney JF (2002) Blood Dendritic Cells Interact with Splenic Marginal Zone B Cells to Initiate T-Independent Immune Responses. *Immunity* 17(3):341–352.
211. Jones C, Virji M, Crocker PR (2003) Recognition of sialylated meningococcal lipopolysaccharide by siglecs expressed on myeloid cells leads to enhanced bacterial uptake. *Mol Microbiol* 49(5):1213–1225.
212. Yang Z, Mosser DM, Zhang X (2007) Activation of the MAPK, ERK, following *Leishmania amazonensis* Infection of Macrophages. *J Immunol* 178(2):1077–1085.
213. Feng G-J, et al. (1999) Extracellular Signal-Related Kinase (ERK) and p38 Mitogen-Activated Protein (MAP) Kinases Differentially Regulate the Lipopolysaccharide-Mediated Induction of Inducible Nitric Oxide Synthase and IL-12 in Macrophages: Leishmania phosphoglycans subvert macrophage IL-12 production by targeting ERK MAP kinase. *J Immunol* 163(12):6403-6412.
214. Convit J, Pinardi ME, Rondon AJ (1972) Diffuse cutaneous leishmaniasis: a disease due to an immunological defect of the host. *Trans R Soc Trop Med Hyg* 66(4):603–610.
215. Casgrain P-A, et al. (2016) Cysteine Peptidase B Regulates *Leishmania mexicana* Virulence through the Modulation of GP63 Expression. *PLoS Pathog* 12(5):e1005658.
216. Campos-Salinas J, et al. (2013) LABCG2, a new ABC transporter implicated in phosphatidylserine exposure, is involved in the infectivity and pathogenicity of *Leishmania*. *PLoS Negl Trop Dis* 7(4):e2179.
217. Teixeira PC, et al. (2015) Regulation of *Leishmania (L.) amazonensis* protein expression by host T cell dependent responses: differential expression of oligopeptidase B, tryparedoxin peroxidase and HSP70 isoforms in amastigotes isolated from BALB/c and BALB/c nude mice. *PLoS Negl Trop Dis* 9(2):e0003411.
218. Maretti-Mira AC, et al. (2012) Transcriptome Patterns from Primary Cutaneous *Leishmania braziliensis* Infections Associate with Eventual Development of Mucosal Disease in Humans. *PLoS Negl Trop Dis* 6(9):e1816.
219. Peters NC, et al. (2014) Chronic Parasitic Infection Maintains High Frequencies of Short-Lived Ly6C(+)CD4(+) Effector T Cells That Are Required for Protection against Re-infection. *PLoS Pathog* 10(12):e1004538.

UNIVERSITY OF MARYLAND
BIOLOGICAL SCIENCES GRADUATE PROGRAM

2101 Bioscience Research Building
College Park, Maryland 20742-4415
301.405.6905/6991 TEL, 301.314.9921 FAX

Dr. Steve Fetter
Interim Dean and Associate Provost for Academic Affairs
The Graduate School
2123 Lee Building
University of Maryland
College Park, MD 20742

Dear Dean Fetter,

This letter is written to signify that the dissertation committee, committee chair, and the graduate director have all approved the use of previously published co-authored work in the final dissertation of Stephen M. Christensen, Biological Sciences, UID 113134531.

Citations for the published work(s):

1. Christensen SM, Dillon LAL, Carvalho LP, Passos S, Novais FO, Hughitt VK, Beiting DP, Carvalho EM, Scott P, El-Sayed NM, Mosser, DM. Meta-transcriptome Profiling of the Human-Leishmania braziliensis Cutaneous Lesion. PLoS Negl Trop Dis. 2016.

2. Hamidzadeh K, Christensen SM, Dalby E, Chandrasekaran P, Mosser DM. Macrophages and the Recovery From Acute and Chronic Inflammation. Annu Rev Physiol. 2017.

In accordance with the Graduate School's policy the dissertation committee has determined that they made substantial contributions to the included work.

Per Graduate School policy the dissertation foreword will identify the scope and nature of the student's contributions to the jointly authored work included in the dissertation and a copy of this letter will be submitted with the dissertation.

Sincerely,

David Mosser, Dissertation Committee Chair,
Professor, Cell Biology and Molecular Genetics

Dr. Charles Delwiche,
Associate Director, Biological Sciences Graduate Program